

VIBRATION-BASED MONITORING AND DAMAGE DETECTION OF STRUCTURES USING WIRELESS SENSORS

Srishti Banerji

A Thesis

in

The Department

of

Building, Civil and Environmental Engineering

Presented in Partial Fulfilment of the Requirements
For the Degree of Applied Science (Civil Engineering) at
Concordia University

Montreal, Quebec, Canada

August 2016

©Srishti Banerji, 2016

CONCORDIA UNIVERSITY
School of Graduate Studies

This is to certify that the thesis prepared

By: Srishti Banerji

Entitled: Vibration-Based Monitoring and Damage Detection of Structures Using
Wireless Sensors

and submitted in partial fulfillment of the requirements for the degree of

MASc Civil Engineering

complies with the regulations of the University and meets the accepted standards with respect to originality and quality.

Signed by the final examining committee:

Dr. Lucia Tirca Chair

Dr. Osama Moselhi Examiner

Dr. Amr Youssef Examiner

Dr. Ashutosh Bagchi Supervisor

Approved by _____

Chair of Department or Graduate Program Director

Dean of Faculty

Date _____

ABSTRACT

VIBRATION-BASED MONITORING AND DAMAGE DETECTION OF STRUCTURES USING WIRELESS SENSORS

MASc Thesis

Srishti Banerji

Structural Health Monitoring (SHM) implies monitoring the performance of structures using sensors to get an advance warning of the loss of structural capacity or potential collapse. Wireless-sensor based monitoring system is found to be advantageous over traditional wire-based system because of their ease of implementation, cost, flexibility and maintenance. However, power supply is an important concern for wireless sensors used in monitoring of civil engineering structures. While there are different efficient power usage methods and power supply solutions available for wireless sensors, their applications to SHM systems for civil infrastructure are not standardized. Energy harvesting by means of converting energy from the surrounding environment provides a desirable solution to address the issue of finite power source for wireless sensors. There are several sources of renewable energy that can be harnessed to generate electrical energy for the sensors. Use of energy harvesters for SHM applications are advancing these days. This research proposes the utilization of energy harvesters as damage detectors in addition to supplying power to the wireless nodes. This will ensure higher accuracy in the damage detection and capture sensor faults as well. This proposed concept is evaluated using pre-stressed concrete box bridge and steel truss bridge models in this thesis. This is a step towards increasing reliability of data acquisition. Instrumented structures are monitored by

analyzing the responses recorded by deployed sensors in the form of signals. Processing these signals accurately is another important aspect of SHM to diagnose anomalies in structural behavior. The vibration signature of a structure changes with damage. In order to detect damage effectively, preservation of non-linear and non-stationary features of real structural responses is important. Decomposition of the signals into Intrinsic Mode Functions (IMF) by Empirical Mode Decomposition (EMD) and application of Hilbert-Huang Transform (HHT) addresses the time-varying instantaneous properties of the structural response. The energy distribution among different vibration modes of the intact and damaged structure depicted by Marginal Hilbert Spectrum (MHS) can detect location and severity of the damage. This research investigates this damage detection method by experimental modal testing of a steel frame structure and numerical simulation testing of a steel beam. The performance of Damage Indices (DI) from the energy distribution curves of the undamaged and damaged structure are assessed. It is found that MHS can effectively identify the presence and location of damage in the structure using its vibration response at undamaged and damaged conditions.

ACKNOWLEDGEMENTS

I would like to express my deepest gratitude to my supervisor, Dr. Ashutosh Bagchi for his inspiring guidance and constant encouragement throughout my graduate studies. He has continuously supported me for my academic growth and I thank him wholeheartedly for providing me this opportunity to pursue my research.

I want to sincerely thank Dr. Sheldon Williamson for his motivation to pursue my studies at Concordia University.

I would like extend my gratitude to the faculty members and staff of Concordia University with special mentions to Dr. Amin Hammad, Dr. Lan Lin, Dr. Khaled Galal and Dr. Pragasen Pillay their exceptional support during the last two years. I also want to thank Mr.Roberto Avila Perez for his valuable assistance in my structural lab work.

I am grateful to IC-IMPACTS for their funding support and enriching collaboration, especially to Helena Fehr and Angie Reed for their helpful contributions. Thanks are also due for Dr. S.K. Panigrahi at the Central Building Research Institute, Roorkee, India for providing a set of data required for this research. I am also thankful to Dr. R. M. Ghazi at MIT for discussion and suggestions. I also thank the Natural Sciences and Engineering Research Council of Canada (NSERC) for supporting a part of the research and Sensequake Inc. for collaboration.

My profound gratitude to my family and special thanks to my friends and colleagues Fuhar Dixit, Mrinmoy Nath, Sudharshan Karthik, Angshuman Deb, Timir Baran Roy, Shervin Khazaeli, Ardalan Sabameher, Chae Woon Lim and Amit Chandra for their support.

To my parents, I dedicate this thesis.

TABLE OF CONTENTS

ACKNOWLEDGEMENTS	v
TABLE OF CONTENTS.....	vii
LIST OF FIGURES	x
LIST OF TABLES	xiv
LIST OF ABBREVIATIONS.....	xv
CHAPTER 1: INTRODUCTION	1
1.1. General background.....	1
1.2. Research objectives	2
1.3. Thesis organization.....	4
CHAPTER 2: LITERATURE REVIEW	5
2.1. Introduction	5
2.2. Structural Health Monitoring (SHM).....	7
2.3. Wireless monitoring of structures.....	8
2.4. Power supply of wireless sensors	13
2.4.1. Solar energy:	14
2.4.2. Piezoelectric Transducers:.....	15
2.4.3. Electromagnetic Induction:	16
2.4.4. Thermal energy:	17

2.5. Analysis of vibration data.....	17
2.6. Summary.....	26
CHAPTER 3: METHODOLOGY	28
3.1. Introduction	28
3.2. Damage detection by energy harvesters	29
3.2.1. Pre-Stressed Concrete Box (PSCB) Bridge	31
3.2.2. Wireless monitoring of PSCB Bridge	32
3.2.3. Energy harvester design	32
3.2.4. PSCB Bridge model	34
3.2.5. Truss Bridge model	35
3.2.6. Harvester simulations.....	37
3.2.7. Damage detection method.....	39
3.3. Damage detection by MHS.....	43
3.3.1. Beam structure.....	48
3.3.2. Bookshelf structure experiment	50
3.4. Summary.....	56
CHAPTER 4: DAMAGE DETECTION BY ENERGY HARVESTERS.....	58
4.1. Introduction	58
4.2. Electromagnetic energy harvesters.....	59
4.3. PSCB Bridge model and harvester deployment	62

4.4. Truss Bridge model and harvester deployment	63
4.5. Vibration responses and harvested energy	65
4.6. Results	68
4.7. Discussion.....	73
4.8. Summary.....	79
CHAPTER 5: DAMAGE DETECTION BY MARGINAL HILBERT SPECTRUM	
METHOD	81
5.1. Introduction	81
5.2. Description of the structures and data acquisition.....	84
5.3. Structural response data.....	88
5.4. HHT and MHS plots.....	91
5.5. Damage Detection	98
5.6. Discussion.....	116
5.7. Summary.....	119
CHAPTER 6: SUMMARY, CONCLUSIONS AND FUTURE WORK.....	120
6.1. Summary.....	120
6.2 Conclusions	122
6.3. Future Work.....	125
REFERENCES.....	126
APPENDIX: LIST OF PUBLICATIONS	134

LIST OF FIGURES

Figure 2. 1: Layout of nodes on the Golden Gate Bridge (Kim et al. 2007)	10
Figure 2. 2: Layout of WSN on the New Carquinez Bridge (Kurata et al. 2013)	11
Figure 2. 3: Structural plan of National Stadium, China (Shen et al. 2013).....	12
Figure 2. 4: Multi type WSN for National Stadium, China (Shen et al. 2013).....	13
Figure 3. 1: Overview of damage detection methods in thesis	28
Figure 3.2: Flowchart of damage detection method by energy harvesters	30
Figure 3.3: PSCB bridge details: (a) photograph of the bridge; (b) longitudinal elevation	31
Figure 3.4: Sensor locations on PSCB bridge.....	32
Figure 3.5: a) Schematic diagram; b) picture of linear generator	33
Figure 3.6: FFT results of all 30 wireless accelerometers on PSCB bridge	35
Figure 3.7: Nieporęt truss bridge, Poland (Kolakowski et al. 2011)	36
Figure 3.8: Structural configuration of Nieporęt truss bridge, Poland (Favai et al. 2014)	37
Figure 3.9: Transient vibration process	39
Figure 3.10: White Gaussian Noise applied as ambient vibration.....	40
Figure 3.11: Plot of signal $x(t)$	44
Figure 3.12: IMFs of signal $x(t)$	45
Figure 3.13: Hilbert-Huang Transform (HHT) plot of signal $x(t)$	45
Figure 3.14: a) MHS; b) FFT of signal $x(t)$	46
Figure 3.15: Simply supported beam section details	48
Figure 3.16: SAP 2000 model of simply supported beam	49
Figure 3.17: Sensor and damage locations on simply supported beam	50

Figure 3.18: Bookshelf frame structure picture	51
Figure 3.19: USB base station	52
Figure 3.20: SAP 2000 model of three story steel frame.....	53
Figure 3.21: Top level damage scenario by loosening bolts.....	53
Figure 4. 1: Simulink model in MATLAB of acceleration to energy harvested data.....	60
Figure 4. 2: SAP 2000 model of PSCB bridge	62
Figure 4. 3: a) Harvester and sensor locations; b) Harvester and damage locations	63
Figure 4. 4: SAP 2000 model of steel truss bridge	64
Figure 4. 5: Energy harvester locations on steel truss bridge	64
Figure 4. 6: Damage locations on steel truss bridge	65
Figure 4. 7: Acceleration response to WGN for PSCB energy harvester 3	66
Figure 4. 8: Harvested energy for PSCB energy harvester 3	67
Figure 4. 9: Acceleration response to WGN for truss bridge energy harvester 5	67
Figure 4. 10: Harvested energy for truss bridge energy harvester 5	68
Figure 4. 11: Energy harvesters and damage scenario locations for PSCB	68
Figure 4. 12: Energy harvesters and damage scenario locations for truss bridge.....	69
Figure 4. 13: Damage Metric 1 results for all damage scenarios of PSCB	70
Figure 4. 14: Damage Metric 2 results for all damage scenarios of PSCB	70
Figure 4. 15: Damage Metric 1 results for all damage scenarios of truss bridge	71
Figure 4. 16: Damage Metric 2 results for all damage scenarios of truss bridge	72
Figure 4. 17: Variation of a) Damage Metric 1; b) Damage Metric 2 under all the damage scenarios for PSCB	75
Figure 4. 18: Bending mode 1 of PSCB bridge in SAP 2000.....	77

Figure 4. 19: Variation of a) Damage Metric 1; b) Damage Metric 2 under all the damage scenarios for truss bridge	78
Figure 5. 1: Damage detection flow chart by Marginal Hilbert Spectrum (MHS).....	83
Figure 5. 2: First three mode shapes of the simply supported beam in SAP 2000	85
Figure 5. 3: Wireless accelerometer a) turned off; b) data transmission mode	86
Figure 5. 4: First three mode shapes of the frame in SAP 2000	87
Figure 5. 5: Frequency Domain Decomposition (FDD) results in MATLAB.....	88
Figure 5. 6: Acceleration response of Node 1 on simply supported beam	89
Figure 5. 7: Acceleration response of top floor sensor	90
Figure 5. 8: Five IMFs of the Node 1 (30cm from left) sensor data for intact structure ..	92
Figure 5. 9: Five IMFs of the top floor sensor data for intact structure.....	92
Figure 5. 10: Energy distribution with IMFs for Node 1 intact simply supported structure	93
Figure 5. 11: Energy distribution with IMFs for first floor bookshelf intact structure.....	93
Figure 5. 12: HHT plot for first floor intact bookshelf structure	94
Figure 5. 13: HHT plot for Node 1 (30cm) on simply supported beam	94
Figure 5. 14: MHS plot for Node 1 intact structure	95
Figure 5. 15: MHS plot for first floor intact structure	96
Figure 5. 16: Normalized MHS plot for Node 1 intact structure	96
Figure 5. 17: Normalized MHS plot for first floor intact structure	97
Figure 5. 18: Normalized Cumulative MHS (NCMHS) plot for Node 1 intact beam.....	97
Figure 5. 19: Normalized Cumulative MHS (NCMHS) plot for first floor intact structure	98

Figure 5. 20: Normalized energy vs IMF number curves for damage near Node 3	99
Figure 5. 22: Damage indices plots for damage near node 3 of the beam	100
Figure 5. 21: Normalized energy vs IMF number curves for damage in top floor of bookshelf frame structure	100
Figure 5. 23: Damage indices plots for damage in top floor of bookshelf	101
Figure 5. 24: NMHS plots for 3 sensors for damage near node 3 in the beam.....	102
Figure 5. 25: NMHS plots for 3 sensors for damage in top floor of bookshelf structure	103
Figure 5. 26: Damage index 3 plot for damage near node 3	104
Figure 5. 27: Damage index 3 plot for damage in top floor	104
Figure 5. 28: NCMHS plots for 3 sensors for damage scenario 1 of beam	105
Figure 5. 29: NCMHS plots for 3 sensors for damage in top floor	106
Figure 5. 30: Damage index 4 plot for damage in top floor	107
Figure 5. 31: Damage index 4 plot for beam damage scenario 1	107
Figure 5. 32: Normalized energy vs IMF number curves for damage in middle floor...	108
Figure 5. 33: Normalized energy vs IMF number curves for beam damage scenario 2.	109
Figure 5. 34: Damage indices plots for damage in middle floor	109
Figure 5. 35: Damage index plots for damage near node 2 in the beam.....	110
Figure 5. 36: NMHS plots for 3 sensors for damage scenario 2 in beam	111
Figure 5. 37: NMHS plots for 3 sensors for damage in middle floor	112
Figure 5. 38: Damage index 3 plot for both structures	113
Figure 5. 39: NCMHS plots for 3 sensors for damage scenario 2 in beam	114
Figure 5. 40: NCMHS plots for 3 sensors for damage in middle floor of frame.....	115
Figure 5. 41: Damage index 4 plots for the frame and beam.....	116

LIST OF TABLES

Table 2. 1: Overview of energy harvesting systems for SHM applications	18
Table 3. 1: Parameters of linear generator	38
Table 3. 2: PSCB bridge damage cases	41
Table 3. 3: Steel truss bridge damage cases.....	42
Table 3. 4: Properties of the simply supported beam section	49
Table 3. 5: Bookshelf frame structure dimensions	51
Table 4. 1: Simulink generator model parameters	61
Table 4. 2: Comparison of damage metric results for PSCB	74
Table 4. 3: Comparison of damage metric results for truss bridge.....	74
Table 5. 1: Experimental data verification for frame.....	87
Table 5. 2: Experimental data verification for frame.....	117
Table 5. 3: Experimental data verification for simply supported beam.....	117

LIST OF ABBREVIATIONS

SHM	Structural Health Monitoring
WSN	Wireless Sensor Network
HHT	Hilbert Huang Transform
HSA	Hilbert Spectral Analysis
MHS	Marginal Hilbert Spectrum
VBDI	Vibration Based Damage Identification
GGB	Golden Gate Bridge
PVDF	Piezo-polymer Poly Vinyl Dene Fluoride
PZT	Piezo-ceramic lead Zirconate Titanate
TEG	Thermo Electric generators
MEMS	Micro Electro Mechanical Systems
STFT	Short-Time Fourier Transform
WVT	Wigner–Ville Transform
EMD	Empirical Mode Decomposition
IMF	Intrinsic Mode Functions
PSCB	Pre-Stressed Concrete Box
FFT	Fast Fourier Transform

WGN	White Gaussian Noise
DI	Damage Index
NCMHS	Normalized Cumulative Marginal Hilbert Spectrum
FDD	Frequency Domain Decomposition

CHAPTER 1: INTRODUCTION

1.1. General background

In the current scenario of development, new structures with innovative materials and designs are built widely across the world such as the second tallest building in the world, Shanghai World Financial Center with a height of 492 metres in China, the 47 miles underwater Marmaray Tunnel in Turkey, or the cable stayed Russky Bridge in Russia with a length of over 10,000 feet and there are many to the list. With the increasing span and size of the civil engineering structures, their need for maintenance against earthquakes, strong winds, environmental effects and other unforeseen events is growing. Any sudden damage, failure or collapse in these structures will result in catastrophic consequences.

Structural Health Monitoring (SHM) provides real time monitoring of structural behaviour and assures safety by detecting damages and change in load patterns. This performance assessment is carried out using sensors installed in the structures. SHM has many processes including data acquisition from structures, data processing for damage sensitive features and decision making for accurate damage detection. Development of SHM for large civil structures needs multi-disciplinary involvement from various technical areas for effective monitoring.

Different types of sensors; wired and wireless can be used to gather various information about the structure such as acceleration, strain, temperature, tilt and so on. Wired sensors

have low initial cost but their labor intensive installation, data infidelity and inflexibility in the monitoring system are resulting in their replacement by wireless sensors. Wireless sensors have high initial cost but their ease of placement, flexibility in the network, on chip processing and high reliability outweigh the initial cost and prove economical in the long run. Wireless sensors also have some limitations; time synchronization, command dissemination, data packet loss and energy source. Energy harvesters prove to be a boon for supplying power to wireless sensor nodes and have a promising role in autonomous monitoring system.

The data collected by sensors from structures is complex and needs analysis to be meaningful. Structural response data is non-linear non-stationary. Various damage detection algorithms exist for SHM utilizing the dynamic properties of the structure or the statistical features of the structural response. Mode shape curvature, damage detection based on flexibility matrix, model updating methods, stochastic subspace identification, wavelet transform, Hilbert-Huang transform, neural network, machine learning, data mining and several other methods and algorithms are used in SHM. In this plethora of damage identification methods and data acquired from structures, it is essential to find their best suitability and develop a robust and accommodating method to assess damages effectively.

1.2. Research objectives

This thesis aims to study and improve the SHM and damage detection process using the vibration response of structures and the use of Wireless sensors for that purpose. The main objectives of the present research are:

- (1) To develop a damage detection method utilizing vibration energy harvester for increasing robustness in the monitoring system and capturing sensor malfunctioning along with powering the wireless sensors.
- (2) To investigate the applicability and robustness of the recently introduced energy-based method of damage detection using Hilbert-Huang Transform (HHT).

In order to achieve these objectives both numerical and experimental studies would be conducted to determine the vibration response of sample structures to be used for testing and validation.

Power supply is an important issue for wireless sensors, and with technological advances, this scenario is improving. The sensors monitor the structures are critical and any fault in them will misguide the SHM results which could have adverse effects. To verify sensor readings, application of energy harvesters is proposed in this thesis. This damage detection and verification method with suggested damage metrics are aimed to be examined and validated in this research. The applicability of this proposed concept and performance of its detection capabilities are the expected outcomes.

The above method to be developed here is a step to ensure accurate sensor readings but efficient data processing of these structural responses is also critical for SHM. With the non-linear and non-stationary complex structural data, most of the signal processing methods fail to preserve the original nature of the recorder response for solving conveniences. A relatively new method, Marginal Hilbert Spectrum by Hilbert-Huang Transform is under research nowadays. It is still not fully developed in the light of civil engineering SHM and is a prime current research area. New proposals of damage detection procedures using this method have been suggested by current researchers. This thesis aims

to test and examine those new methods on structures by conducting experiments using wireless sensors. The scope and effectiveness of this damage detection method is aimed to be evaluated.

1.3. Thesis organization

This thesis has been organized into six chapters. The first chapter is an introduction to the research explaining the motivation of this thesis. Chapter 2 provides the literature review about SHM using wireless sensors, the advent of energy harvesters for supplying power to wireless sensors for SHM and different types of damage detection techniques for civil engineering structures. Chapter 3 explains the methodology of the two damage detection techniques in this thesis: damage detection by energy harvesters and by Marginal Hilbert Spectrum (MHS) using HHT method. Chapter 4 shows the simulations and results by the application of the damage detection by energy harvesters on bridges. Chapter 5 shows the results for the simulation and experimental tests for detecting damages by HHT method. Chapter 6 summarizes this research with conclusions and provides scope for future work.

CHAPTER 2: LITERATURE REVIEW

2.1. Introduction

Infrastructure is very critical for sustenance of the society and its operations. Any damage or failure in infrastructure not only hinders all operations; it also takes a toll on lives and property. Three lanes of the De la Concorde overpass in Laval, Quebec suddenly collapsed in September, 2006, killing five people and seriously injuring six others (The Associated Press, 2006). Poor construction supervision and misplaced reinforcements caused this collapse even though, the bridge passed an inspection the previous year to collapse. The Interstate 35W bridge across the Mississippi River in Minneapolis suddenly collapsed in August, 2007, killing 13 people and injuring 144 more (AASHTO, 2008). Increased traffic and other environmental loads caused its deterioration and failure. I 35W bridge was 40 years old and this problem of aging infrastructure subjected to varying loads is not rare. The aging issue of infrastructure, the unpredictable advent of natural disasters and utilization of innovative construction materials demand the need of efficient inspection and maintenance of structures to ensure its safe performance. Structural Health Monitoring (SHM) aims to evaluate structural behaviour and provide early damage warnings based on the anomalies in its structural conditions for safety and sustainability of infrastructure.

With the progress in technology, sensors are utilized for SHM to obtain reliable information of structural behaviour. Sensors are categorized as wired and wireless. Wired sensors have drawbacks related to installation of wires, high cost and inflexibility in the

monitoring network design. Wireless sensors provide an advantage with these factors and are replacing the conventional wired sensors for structural health monitoring applications. Despite these advantages, the wireless sensors have some concerns as well. Time synchronization, power supply, command dissemination and accuracy of data after multi-hop are some current focus areas of improvement. To combat the problem of power supply which is truly essential in order to make the wireless sensor network autonomous, energy harvesting technology is used. This chapter reviews state-of-art of structural health monitoring applications using wireless sensors and the advancements of power supply by energy harvesters in recent projects. The application of energy harvesters for increasing sensor data reliability along with power supply function and improving SHM quality is proposed and discussed in Chapter-3.

The sensors record data from structures which is processed and analyzed for detection of damages in the structure. Damage detection techniques range from acoustic, electromagnetic, vibrational and visual techniques. A large majority of SHM methods are focussed on Vibration Based Damage Identification (VBDI) techniques. Vibration characteristics of a structure namely frequency, damping, mode shapes, etc. alter with damage in the structure. Mode shape curvature method, stiffness and flexibility matrix method, strain energy based methods are some of the VBDI techniques and their detailed reviews could be found in Fan and Qiao (2011) and Humar et al. (2006). VBDI methods can be broadly classified into time domain, frequency domain or modal analysis and time-frequency domain analysis. For joint time-frequency domain analysis, Hilbert-Huang Transform (HHT) is a relatively new approach capturing non-linear and non-stationary

features of vibration (Huang et al. 1998). The review of these methods is presented in this chapter.

2.2. Structural Health Monitoring (SHM)

SHM is defined as monitoring the structure with arrays of sensors and accumulating damage sensitive features which represent damage upon analysis due to any change in the structural properties. An extensive review of SHM methods are presented by Doebling et al. (1998) and Sohn et al. (2003). SHM is a combination of diagnostics and prognostics. Diagnostics includes damage detection based on presence, location, type and severity. Prognostics refers to the estimation of remaining useful life of the structure. SHM process has been described by Farrar and Worden (2007) to satisfy its objectives:

1. Operational evaluation – The operating environment, expected damage modes, and any data acquisition limitations must be taken into account. The economic and life-safety case must be outlined by these parameters.
2. Data acquisition – The sensing modality along with all the data acquisition process particulars must be chosen. Data processing is considered to obtain more representative and damage sensitive features.
3. Feature selection – Features have to be chosen for appropriate distinction between damaged and undamaged conditions of the structure.
4. Statistical model development – The analysis of the chosen features for accurately detecting damage into quantifiable metrics is attained in this step.

SHM can be done by model based or data based approach. In model based approach, data recorded by sensor is compared with some numerical or analytical model of the structure. On the other hand, the non-model based approach is carried out by considering only the data collected from the sensors without the need of actual modeling the entire structure. Modeling the actual structure is cumbersome and often might lead to errors if not updated accurately. Data based approach needs a correct baseline for comparison or an efficient algorithm to compare with the actual undamaged structural condition. A combination of both the methods serve as verification and leads to higher accuracy (Sohn et al. 2003).

Some common research focus areas in SHM are application of composite and innovative materials, appropriate feature and classifier selection, integrated sensor design with optimal sensor placement and power supply, operational and environmental fidelity for data acquisition (Boller 2013). The long-term installation of SHM system on super-tall buildings, long span bridges and large scale structures is the current research trend to monitor loading conditions and detect damages for safe and sustainable infrastructure.

2.3. Wireless monitoring of structures

Wireless and wired are the types of sensors used for SHM of civil engineering infrastructure. Wireless sensors have an edge over the long cables and their problems associated with wired sensors such as high installation cost and inflexibility of the network. In general, a wireless sensor is composed by four components: a sensing interface, a computing core, a wireless transceiver, and a power source (Lynch and Loh 2006). For some of them, the actuation interface is also integrated. Wireless sensors record data from structures and process it in the computing core subsystem before sending it to either another

node or the base station. Node to node and then base station interaction is termed as *multi-hop* network whereas only node to base station direct interaction is known as *single-hop* network. All these processes are carried out using electrical energy making power supply very critical.

The work presented in Straser and Kiremidjian (1998) represents one of the early applications of Wireless communication instead of wired communication within a structural monitoring system since when Wireless Sensor Networks (WSNs) in SHM has gained considerable attention. Signal reliability and power supply are the prime concerns for wireless sensors but with the latest advancements in technology, wireless sensors are applied to many full scale monitoring applications (Farinholt et al. 2010). While Wireless operated SHM projects are becoming more popular in recent years, there is a need for further advancement in this area in terms of research and development. Some of the recent SHM project using WSNs are summarized as follows.

Golden Gate Bridge, San Francisco:

The Golden Gate Bridge (GGB) is a cable-supported bridge, with the main span of 1280 metres length. A Wireless Sensor Network (WSN) for Structural Health Monitoring (SHM) is developed, implemented and tested on the main span and the south tower of the GGB. 64 wireless nodes are distributed over the main span and the tower constituting a 46-hop network as shown in Figure 2.1, recording ambient vibrations synchronously at 1kHz rate, with an accuracy of $30\mu\text{G}$ and less than $10\mu\text{s}$ jitter. This deployment is the largest WSN for SHM (Kim et al. 2007).

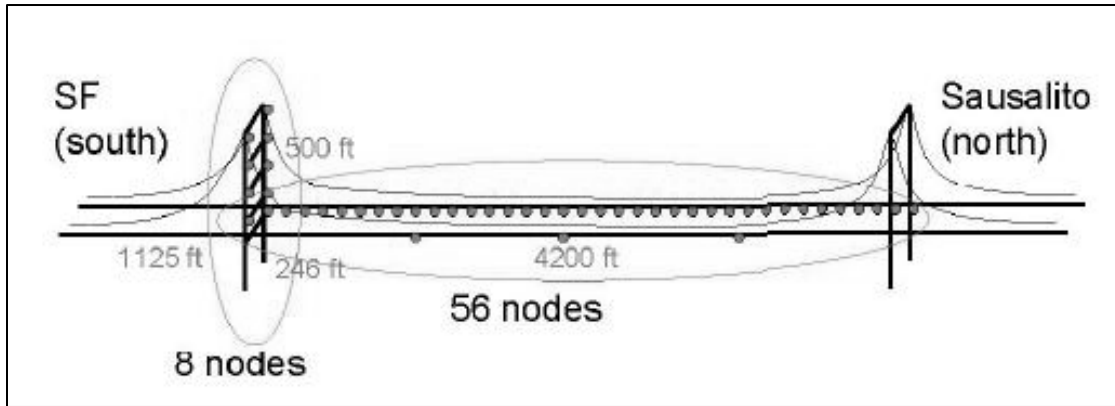


Figure 2. 1: Layout of nodes on the Golden Gate Bridge (Kim et al. 2007)

The 64 wireless sensor nodes were integrated by Crossbow MicaZ motes and acceleration boards. The high resolution vibration data identified the vibrating modes accurately. One complete cycle of sampling and data recording generates 20 MB of data and takes around 9 hours to download to the base station. The data acquisition system needs improvement for faster data collection.

New Carquinez Bridge, Vallejo:

The New Carquinez Bridge is a long suspension bridge with main span of 728 metres and total length of 1056 metres. Its main structural components are the two concrete towers, steel box girder and two suspension cables. The WSN installed is termed as Narada WSN and is presented in Figure 2.2 (Kurata et al. 2013).

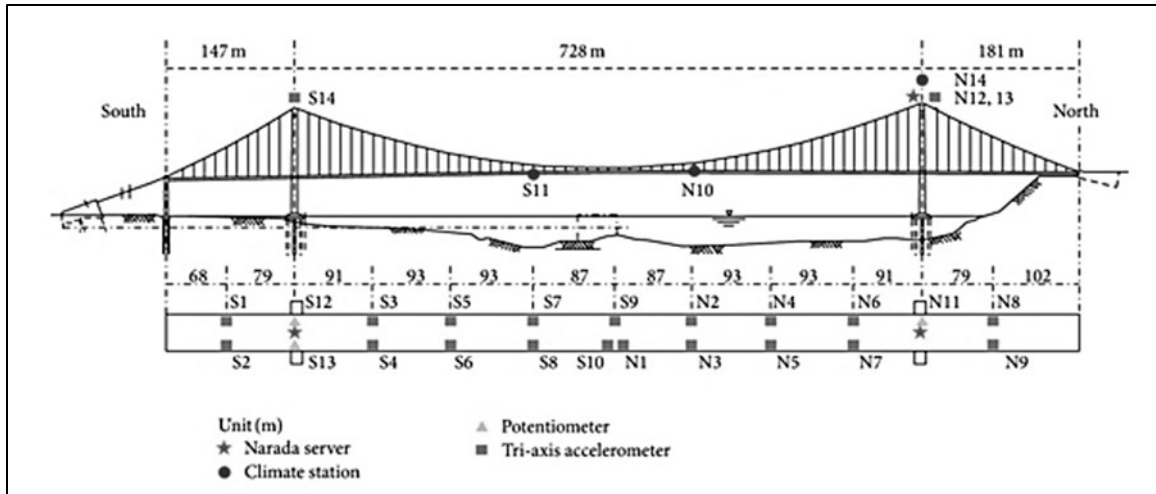


Figure 2. 2: Layout of WSN on the New Carquinez Bridge (Kurata et al. 2013)

The WSN system has two layers in this bridge. The lower layer comprises of low power wireless sensor nodes to capture ambient bridge vibration. The upper layer is the cyberinfrastructure framework for response data interrogation and storage. Communication between WSN servers and upper internet enabled layer is by a cellular modem. This WSN comprises of 28 Narada nodes collecting data from 80 channels. Also, this bridge incorporates solar energy harvesting to supply power to the sensors. The sensors are responsible for acquiring modal properties of the structure for continuous model updating and monitoring (Kurata et al. 2011). System identification, data mining, internet storage and permanent power solution makes this bridge an important SHM using WSN case study.

National Stadium, China (generally known as “Bird’s Nest”):

The National stadium of China is a huge structural building constructed for 2008 Beijing Olympic Games with a capacity of more than 90,000 occupants. The schematic plan is shown in Figure 2.3. It weighs over 40,000 tons and is monitored by multi-type WSN. Due

to its on-site environment and large scale structural properties, multiple parameters such as stress, displacement, acceleration, wind, and temperature are monitored by sensors (Shen et al. 2013). The WSN sensor deployment is presented in Figure 2.4.

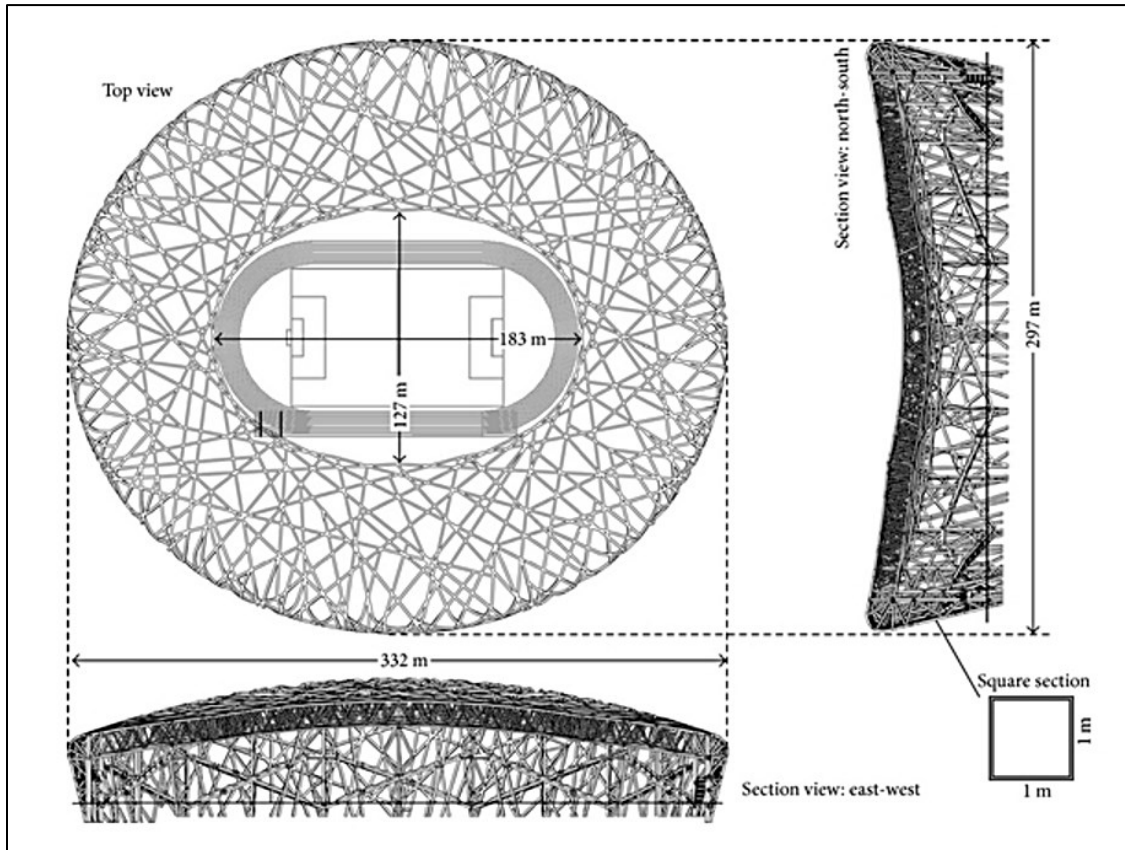


Figure 2. 3: Structural plan of National Stadium, China (Shen et al. 2013)

The sensor installation is rapid and low cost with accurate results after data analysis. Some specific features of this WSN are adjustable chain type topology, artificial control work mechanism and multi type sensor monitoring for super large scale structure.

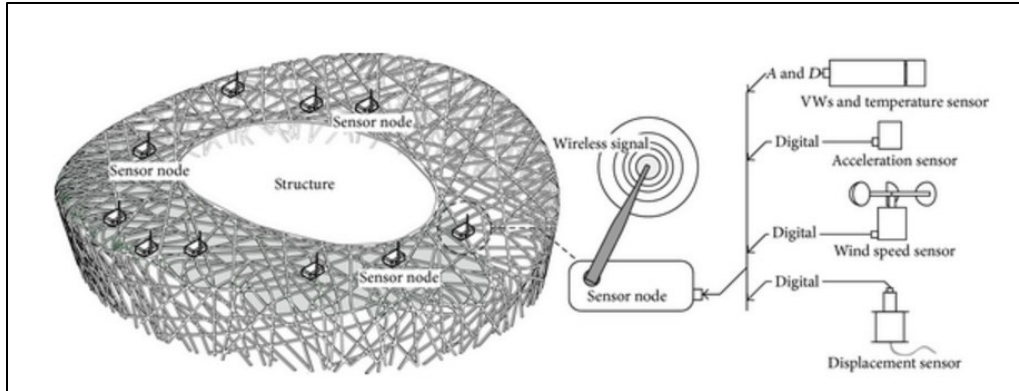


Figure 2. 4: Multi type WSN for National Stadium, China (Shen et al. 2013)

2.4. Power supply of wireless sensors

Life of the WSN is dependent on the lifetime of the batteries conventionally used in sensor nodes. This can affect the monitoring system especially if sensor nodes are in inaccessible locations of the structure. Hindrance in functioning of any node might result in collapse of the entire network. Several options are available to maximize the battery lifetime. As summarized by Sudevalayam and Kulkarni (2011), routing and data dissemination protocols, power aware storage, strategies for duty-cycling, tiered system architectures, adaptive sensing rates, and redundant node placement in the network are effective in increasing battery life time. Periodic monitoring is more efficient for power management than continuous monitoring because in the former, the nodes can go to sleep mode while not acquiring and transmitting any data. The ratio of energy consumed by the sensors between the active and sleep modes may be as high as 100 (Cardei and Du, 2005). Communication protocols like IEEE 802.15.4 is more efficient in terms of power management and is usually used for low data rate transfer (Callaway et al., 2002). Nevertheless, the battery lifetime is still finite. This raised the demand of a permanent solution to power supply.

Energy from the surrounding environment can be captured and transformed to electrical energy. This process is defined as *energy harvesting* (Park et al. 2008). The generated electrical energy can be used for powering wireless sensors for structural health monitoring proving to be a long-term solution. Especially in rural areas, where electric power lines may not be available near the bridges, energy harvesters are a suitable and significant means for power supply.

Different sources of energy have their own considerations for being utilized in supplying power to low power microelectronic sensors for SHM. Some of the recent SHM applications of energy harvesters for powering WSN are listed in this section. The most common viable sources are solar and mechanical currently.

2.4.1. Solar energy:

Photovoltaic cells harvest electrical energy from light energy, which is already an established technology. For solar energy harvesting, outdoor applications are preferred due to high solar energy availability in outdoor conditions, and could be very useful for SHM of outdoor infrastructure like roads and bridges. Its widespread applications in SHM are as follows.

- Miller and Spencer (2009) have deployed solar powered IMote2 wireless smart sensor system for monitoring Jindo Bridge in South Korea.
- Musiani et al. (2007) developed SHiMmer which is a solar energy harvesting system for sensing and actuating civil engineering structures. It uses super-capacitors for energy storage and low power consuming micro controller and radio.

- Chae (2012) developed and tested 45 solar powered sensors on Yongjong Grand Bridge.
- Hassan et al. (2012) have proposed and tested a wireless sensor system powered by harvested solar energy for monitoring cracks in concrete structures.
- Ho et al. (2012) developed a solar powered autonomous smart wireless sensor system and validated it on cable-stayed Hwamyung Bridge in Korea.
- Inamdar (2012) designed a photovoltaic system to monitor strains in bridges.
- Kurata et al. (2011) created and installed solar powered autonomous wireless monitoring network using Narada sensing unit (Zimmerman and Lynch 2009) on New Carquinez Suspension Bridge in California.

2.4.2. Piezoelectric Transducers:

Piezoelectric transducers can couple electrical and mechanical energy. Civil engineering structures have low frequency excitation. Piezoelectric harvesters require vibrations in at least close to 100s of Hz. Hence, they are not in a mature state of technology for powering SHM sensors currently. Still, some SHM advancement has been achieved.

- Wischke et al. (2011) designed piezoelectric harvester from vibrations of railways ties to sufficiently power the wireless sensor nodes.
- Peigney and Siegert (2013) developed a device to generate power from traffic on highway with a piezoelectric cantilever bimorph consisting of a tip mass and two piezoelectric patches attached to the clamped end of a steel plate.

- Cahill et al. (2014) experimentally validated use of Piezo-polymer Poly Vinyl Dene Fluoride (PVDF) based piezoelectric energy harvesters and an energy harvesting circuit for damage detection in reinforced concrete beam.
- Xie et al. (2015) introduced a novel Piezo-ceramic lead Zirconate Titanate (PZT) piezoelectric harvester design containing two groups of series piezoelectric generators connected by a shared shaft which is driven by a linking rod attached with a hinge to a proof mass on the tip of a cantilever fixed on the roof to harness energy from a high rise building, and can act like a tuned mass damper to dissipate energy.

2.4.3. Electromagnetic Induction:

Electromagnetic induction is the process of generating voltage due to varying magnetic flux around the conductor by movement of the magnet. Electromagnetic harvesters show great potential for scaling to lower frequencies of bridges. However, they are bulky in size for MEMs integration and further research also focuses on achieving resonance. Some full scale SHM applications are as mentioned below.

- Sazonov et al. (2009) developed a linear electromagnetic energy harvesting system and deployed it for powering wireless sensors on a rural highway bridge, RT Bridge in Potsdam, NY with low traffic volume.
- University of South Hampton's company Perpetuum developed electromagnetic energy harvesters for rail monitoring (Perpetuum 2013).

Electromagnetic induction proves successful in harnessing low frequency bridge vibrations even for rural traffic (Sazonov et al. 2009). There is a lot of data related to harvested energy

by the generator which can be tapped and analyzed for SHM. This is a novel concept presented in this thesis and is described with complete details in Chapter-3.

2.4.4. Thermal energy:

Seebeck effect is generation of electricity at the junction of two dissimilar metals with temperature difference (Park et al. 2008). Thermoelectric generators (TEG) work on this principle. TEG is constructed by arranging p-type and n-type junctions thermally in parallel and electrically in series. TEGs have an advantage over vibration energy harvesters as they do not operate on moving parts. But TEGs have the disadvantage of low efficiency with small thermal gradient and not easy to integrate with Micro Electro Mechanical Systems (MEMs). Not many applications in SHM are present due to lack of high thermal gradient in civil engineering infrastructure.

- Abbaspour (2010) demonstrated how heat flow and temperature difference between inside and outside of buildings which is waste energy can be harvested to power wireless sensor nodes.
- Inman and Grisso (2006) developed a system to carry out structural health monitoring of a panel using ambient vibrational and thermal energy.

A brief summary and review of the application in powering microelectronics for SHM by all these methods are presented in Table 2.1.

2.5. Analysis of vibration data

After sensor deployment and data collection, the next step is to analyze the data recorded for damage identification known as Vibration Based Damage Identification (VBDI). The

acquired data depicts the vibration characteristics of the structure and can be studied in different domains; time, frequency (modal), time-frequency. Some background of these methods with details about a relatively new method Hilbert Huang Transform (HHT) is presented.

Table 2. 1: Overview of energy harvesting systems for SHM applications

Energy harvesting system	Advantages	Limitations	SHM application state-of-art	Suitable deployment for maximum output
SOLAR	Mature technology, easy to install.	Not periodic and not available 24 hours.	Mostly outdoor SHM.	Outdoor structures like bridges, buildings.
PIEZO-ELECTRIC	Direct generation of desired voltage and easy integration with MEMs.	Variation in properties with age, stress, temperature and charge leakage.	Most work for SHM applications is in lab stage.	Bridges with preferably heavy passing traffic, impulse loads from railways.
ELECTRO-MAGNETIC	High reliability.	Difficult to integrate with MEMs, low output voltage	Promising for bridges and railways.	Traffic induced bridges and railways.
THERMAL	Low maintenance and high reliability	High cost with low conversion efficiency	Not much progress yet.	It can be used in buildings due to their environment inside and outside.

Frequency domain analysis:

The most common analysis in frequency domain is Fourier analysis. It was formulated by Joseph Fourier in the early 1800s (Brigham 1998) with the concept that an arbitrary

function could be expressed by a single analytical expression constructed as a sum of harmonic (sine and cosine) functions. For a continuous function of time period T, its Fourier series is expressed as

$$f(t) = \frac{a_0}{2} + \sum \left(a_n \cos\left(\frac{n\pi}{T}t\right) + b_n \sin\left(\frac{n\pi}{T}t\right) \right) \quad (2-1)$$

The Fourier coefficients are calculated as

$$a_n = \frac{1}{T} \int F(t) \cos\left(\frac{n\pi t}{T}\right) dt$$

$$b_n = \frac{1}{T} \int F(t) \sin\left(\frac{n\pi t}{T}\right) dt$$

These coefficients represent the contribution of the sine and cosine signal at all frequencies allowing the signal to be analyzed in terms of its frequency components. The frequency of each sinusoidal function must be time-independent due to which the Fourier analysis is able to construct stationary data only. Stationary data means that the frequency of the signal being analyzed is assumed to not change with time. The Fourier transform is unable to accurately represent functions that have non-periodic components which are localized in time or space. This is based on the fact that the Fourier transform is based on the assumption that the signal to be transformed is periodic in nature and of infinite length.

Mode shape curvature analysis:

This method uses mode shape as a damage detection metric as structural damage changes the vibrational mode shapes. The greatest variation is expected to occur at the location of damage. An issue is that the difference between the mode shape of a healthy and a damaged structure is not particularly sensitive to damage (Ratcliffe 2000). However, the second

derivative of a mode shape known as the mode shape curvature is inversely proportional the flexural rigidity of the structure and it provides a better damage diagnostic metric. Numerical differentiation is subjected to noise and this method is meaningful only for simple structures but fails for complex structures.

Time-domain analysis:

Time-synchronous averaging and auto-correlation of the signal are common techniques in time domain analysis. They are not common nowadays as they are not very sensitive to damage. Time synchronous averaging uses the average of the signal over a large number of cycles. This is expected to remove any contributions due to noise or non-synchronous vibrations. The auto-correlation function is the average of the product. This is performed to indirectly obtain information about the frequencies present in the signal. These functions only provide a limited amount of additional information about the response signal and are not robust for damage detection (Pines and Salvino 2006).

Time-frequency domain analysis:

To study non-linear and non-stationary signals, response data should be studied in time-frequency domain. Ville (1948) provided two basic approaches for time–frequency analysis. The first approach is related to dividing the signal into slices in time, and then to analyze each of these slices separately for their frequency content. This is used in the construction of Short-Time Fourier transform (STFT) and the Wigner–Ville Transform (WVT) (Ville, 1948). The concern related to WVT is the presence of negative power for some frequency ranges and its associated cross terms. Also, the WVT of discrete time signals suffers from aliasing errors. The STFT method (Cohen 1995) uses sliding windows

in time to denote the frequency characteristics of the signal as functions of time. It has issues related to modulating between time and frequency resolutions. A finer frequency resolution reduces the time resolution and vice-versa.

The second approach is to first filter different frequency bands, and then cut each frequency band further into slices in time and analyze their energy contents. This is used for the Wavelet transform. Wavelet transform can be considered as a decomposition of the signal into its set of basis functions or wavelets. These basis functions are derived from scaling and translations of the mother wavelet. This basic wavelet is used for the entire signal making it non-adaptive. As a result, only signal features that correlate effectively with the shape of this basic wavelet function are particularly sensitive (Staszewski 2000).

Developed by Huang et. al (1998), the Empirical Mode Decomposition (EMD) method is based on the assumption that any signal consists of different simple Intrinsic Mode Functions/ Oscillations (IMFs). The signal IMFs possess their characteristic time scale in the signal and decompose the signal accordingly. This approach is adaptive and can be applied to any time-series. On application of the Hilbert Transform, IMFs yield instantaneous parameters as functions of time that give sharp identification of fundamental features of vibration signals.

The IMFs represent the oscillation mode of the data instead of simple harmonic function and thus have to satisfy two necessary conditions: (1) the number of extrema and the number of zero crossings must either equal or differ at most by one in the entire data set under consideration; and (2) at any point, the mean value of the envelope defined by the local maxima and the envelope by the local minima is zero.

The IMFs are created to incorporate Hilbert transform which provides the instantaneous features of the signal and it needs to remove mode-mixing from the original signal. The procedure of the IMF construction is:

1. Identify all the local extrema, and connect all the local maxima by a cubic spline line as the upper envelope. Repeat the same procedure for the local minima to produce the lower envelope. The upper and lower envelopes should cover all the data between them.
2. The mean of upper and low envelope value is marked as m_1 ; and the difference between the signal $x(t)$ and m_1 is the first component, h_1 :

$$x(t) - m_1 = h_1 \quad (2-2)$$

3. h_1 is treated as the original signal and steps (1) and (2) have to be repeated, then

$$h_1 - m_{11} = h_{11} \quad (2-3)$$

After repeated sifting, i.e. up to k times, h_{1k} becomes an IMF, that is

$$h_{1(k-1)} - m_{1k} = h_{1k} \quad (2-4)$$

Then it is designated as

$$c_1 = h_{1k} \quad (2-5)$$

The first IMF component, c_1 is obtained from the original data.

4. Separate c_1 from $x(t)$ by

$$r_1 = x(t) - c_1 \quad (2-6)$$

where r_1 is treated as the original data and the above processes have to be repeated until the second IMF component c_2 of $x(t)$ has been derived. This process is repeated n times until n -IMFs of the signal $x(t)$ are constructed.

The decomposition process can be stopped when r_n becomes a monotonic function from which no more IMFs can be extracted. The original signal can be shown to be reconstructed as:

$$x(t) = \sum_{j=1}^n c_j + r_n \quad (2-7)$$

Hence, the signal is decomposed into n-IMFS (c_j) and a monotonic residue (r_n). The frequency content in each IMF changes with time and at the same time instant, no two IMFs contain the same frequency. Although, the frequency band in one IMF might overlap other IMF.

Once the IMFs are obtained, the next step is to perform Hilbert transform on them to obtain the instantaneous parameters. Hilbert transformation process is defined as

$$Y(t) = \frac{1}{\pi} P \int_{-\infty}^{\infty} \frac{X(t')}{t-t'} dt' \quad (2-8)$$

where P stands for Cauchy Principal value. The MATLAB library function ‘hilbert’ is used for the above transformation as used in the present work. Hilbert transform provides complex conjugate of X(t). So, an analytical signal, Z(t) is obtained which is

$$Z(t) = X(t) + iY(t) \quad (2-9)$$

This determines the instantaneous amplitude, phase and frequency of the signal as follows:

$$\text{Amplitude, } A(t) = \sqrt{X^2 + Y^2} \quad (2-10)$$

$$\text{Phase, } \theta(t) = \arctan \frac{Y(t)}{X(t)} \quad (2-11)$$

$$\text{Frequency, } \omega(t) = \frac{d\theta(t)}{dt} \quad (2-12)$$

Therefore, the signal can be represented in the HHT plot by considering the real part of the analytical signal as

$$x(t) = \text{Real Part} \sum_{j=1}^n A_j(t) e^{i\theta_j(t)} \quad (2-13)$$

The HHT plot is in time-frequency plane with amplitude contoured on it. This distribution is coined as the Hilbert Spectrum, $H(\omega, t)$. Marginal Hilbert Spectrum $h(\omega)$ is described as

$$h(\omega) = \int_0^T H(\omega, t) dt \quad (2-14)$$

where T is the total data length.

MHS shows the total amplitude contribution from each frequency.

HHT based techniques are promising for SHM in comparison with traditional methods such as Fourier Transform, Wavelet Transform. The development of HHT is still in progress now since it is a relatively new method. The EMD may generate undesirable IMFs at the low-frequency region with the problem of mode mixing to induce inaccurate SHM results. The first IMF may cover a very wide frequency range which might result in the inability of achieving the properties of mono-component signal, this can hamper damage detection with noise contamination. Although this method has some limitations, but the advantages outweigh them and currently, it is one of the most reliable SHM methods providing the true nonlinear and non-stationary nature of the vibration data.

Some HHT applications in SHM are listed below:

- Kunwar et. al (2013) applied HHT a 4×1 m single span-bridge model instrumented with 10 wireless sensor nodes. Bridge vertical accelerations are measured as a

- wheel and axle is rolled on the model to simulate passing vehicles. HHT method could detect and locate damage under transient vibration loads.
- Hsu et al. (2013) proposed a damage detection index known as the ratio of bandwidth to perform damage detection of a steel structure through experiment by stiffness reduction of the structure. The study supported that HHT is a powerful method for analyzing the acceleration data obtained from the steel structures with initial damage from earthquakes.
 - Rezaei and Taheri (2010) proposed and analyzed a new damage index for damage detection in beams, EMD energy damage index. A cantilevered steel beam with a transverse notch was examined for various notch sizes located at different locations along the beam.
 - Xu and Chen (2004) studied EMD method on a three-story shear building model on a shaking table with two springs horizontally connected to the first floor of the building to provide additional structural stiffness. Structural damage was simulated by varying the stiffness or removing the pre-tensioned springs and various damage severities were assessed.
 - Ghazi and Büyüköztürk (2015) developed a new energy based algorithm to capture nonlinear effects of damage on structural response with the proposal of new damage metrics. They incorporated Mahalanobis distance to employ multiple damage sensitive features for higher precision on a steel laboratory prototype. This thesis verifies some of the algorithms proposed by Ghazi and Büyüköztürk (2015) on experimental data.

2.6. Summary

In this chapter, structural health monitoring and damage detection methods were discussed. SHM can be conducted using wired and wireless sensors. Wireless sensors are more popular than wired sensors due to their ease of installation, performance, maintenance and cost benefits. An overview of SHM procedure with some wireless SHM applications on real structures was provided. Despite the numerous advantages of wireless sensors, they carry some limitations of their own. One such concern is the issue of power supply. Power is supplied to wireless sensors conventionally by batteries which need to be replaced or recharged eventually. Energy harvesters can resolve this issue by harnessing energy from surrounding and removing the need for replacement or manual recharging. This reduces the demand for human interference and help in making the monitoring system autonomous. SHM applications of various energy harvesting sources like solar, thermal, electromagnetic and piezoelectric were reviewed in this chapter.

Finally, damage detection methods based on structural vibration responses were discussed. The methods included analysis with time, frequency (modal), time-frequency domain with focus on Hilbert-Huang Transform (HHT) method. The procedure of HHT method and its recent SHM applications were reviewed.

Based on the literature review, it is clear that there is no method available for vibration-based damage detection using the amount and pattern of the energy generated by the vibration energy harvesters for powering wireless sensors. Objective 1 of this thesis will address this gap. Time-frequency method of analysis of vibration data for damage detection using HHT is relatively new for Civil Engineering structures. Although the review of the literature indicates that there are some viable methods available in this regard, they are not

tested extensively and there is a scope for further development. Objective 2 of the thesis will attempt to address it to some extent.

CHAPTER 3: METHODOLOGY

3.1. Introduction

This thesis is broadly segmented into two methods of damage detection in structures. This segmentation is briefly depicted in Figure 3.1. The first method proposes the use of energy harvesters as damage detectors along with powering wireless sensor nodes for monitoring bridges. The linear generator utilized in this study harvests vibrational energy from the passing ambient traffic on bridges by electromagnetic induction. The other damage detection method utilizes Marginal Hilbert Spectrum (MHS) of structural responses constructed by Hilbert-Huang Transform (HHT) method to detect damages on a simply supported beam simulation and by experiments on a book-shelf structure. Further details of both the procedures are discussed in this chapter.

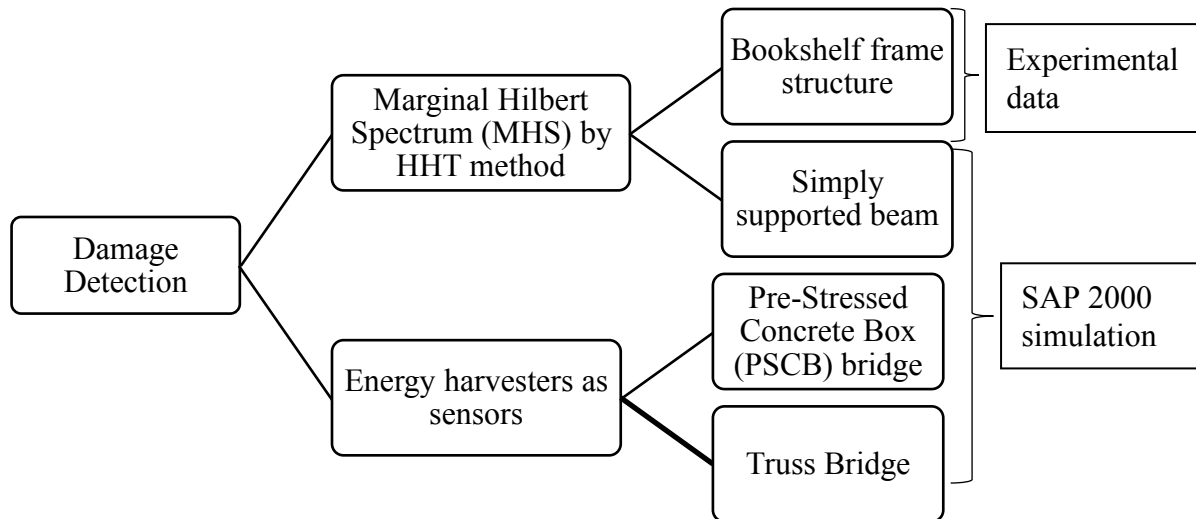


Figure 3. 1: Overview of damage detection methods in thesis

The vibration energy harvesters can harness energy effectively when deployed on large structures which have more vibration like bridges and tall buildings. Hence, the first method related to harvesters are examined on the case studies of bridges. The second method, damage detection based on HHT is directed to attain high accuracy with preservice of non linear and non stationary parameters of the vibration response signal. This phenomenon is best captured in real structures. Therefore, this method is intended to be tested by conducting experiments on a three storey steel structure and a steel simply supported beam. The structures have been tested numerically and the frame has been investigated experimentally. The simply supported beam is due for experiments at CBRI, India.

3.2. Damage detection by energy harvesters

Wireless sensors have several advantages of flexibility, accuracy and cost. Civil engineering structures are huge and their long-term monitoring need several sensors located at inaccessible locations. Wireless sensors are conventionally powered by batteries which either have to be recharged or replaced over passing time. Lately, energy harvesters prove to be a viable solution for this problem by removing the need of battery replacement or recharging. Energy harvesters scavenge surrounding energy and convert them to electrical energy supplying power to the wireless sensor nodes providing enduring operation of the monitoring system.

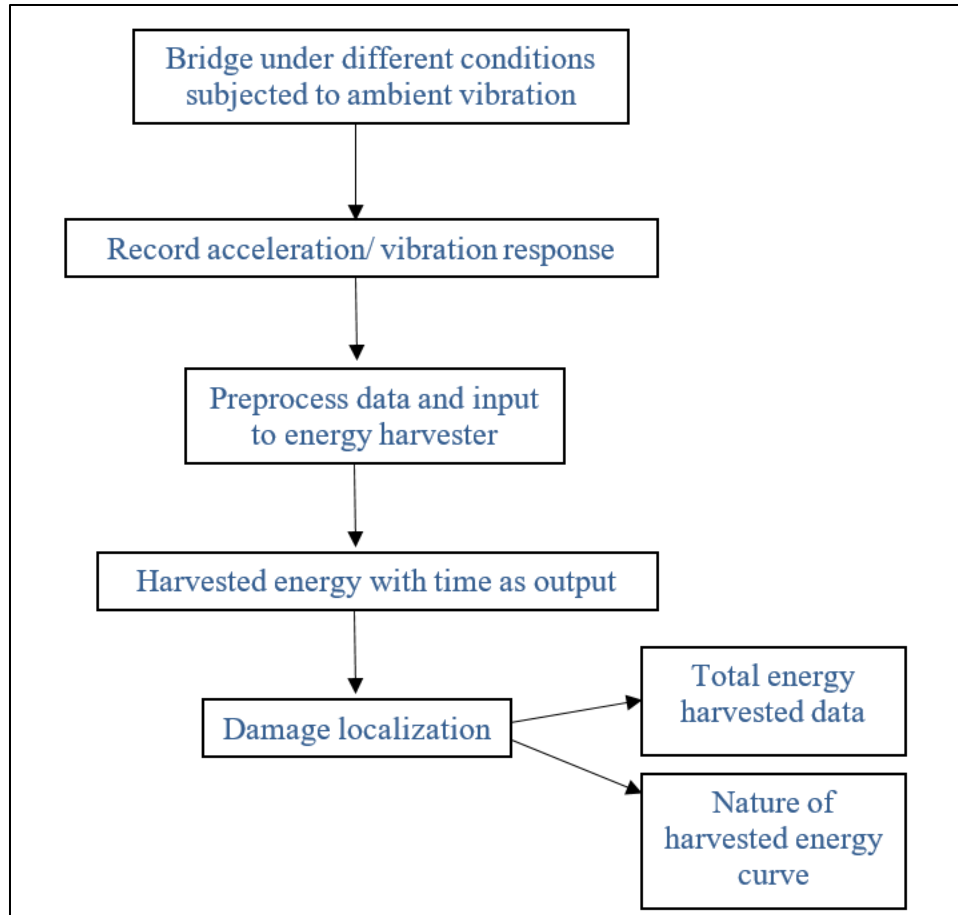


Figure 3.2: Flowchart of damage detection method by energy harvesters

This thesis proposes the use of these energy harvesters as sensors as well; along with their existing function of supplying power to sensors. The energy harvested vs time data can be obtained from the harvesters. In damage scenarios, the amount of the harvested energy and its pattern changes with time. This characteristic can be used in determining damage in a structure. This novel damage detection method is tested on a Pre-Stressed Concrete Box (PSCB) Bridge for which ambient vibration test data is available for the undamaged case along with a Warren truss bridge similar to Nieporęta rail bridge and various damage scenarios have been simulated using a correlated SAP 2000 (SAP 2000 user manual, 2015)

model developed here. The proposed damage detection method is described in the following sub-sections.

3.2.1. Pre-Stressed Concrete Box (PSCB) Bridge

Bridges vibrate by ambient traffic and are a feasible option for harvesting vibrational energy. This study proposes use of electromagnetic harvesters for bridges to function as damage detectors as well. Electromagnetic generators can harness even low frequency vibrations and power wireless sensors. The bridge considered for this study is a PSCB bridge in Gangwon province of South Korea built in 1994. The total span length is 780 metres with deck width 12 metres. It comprises of 16 spans where the first and last span lengths are 40 metres and rest of the spans are 50 metres. The wireless data acquisition was used for ambient vibration tests conducted on this bridge. The tests have been carried out by Korea Expressway Corporation in 2012.

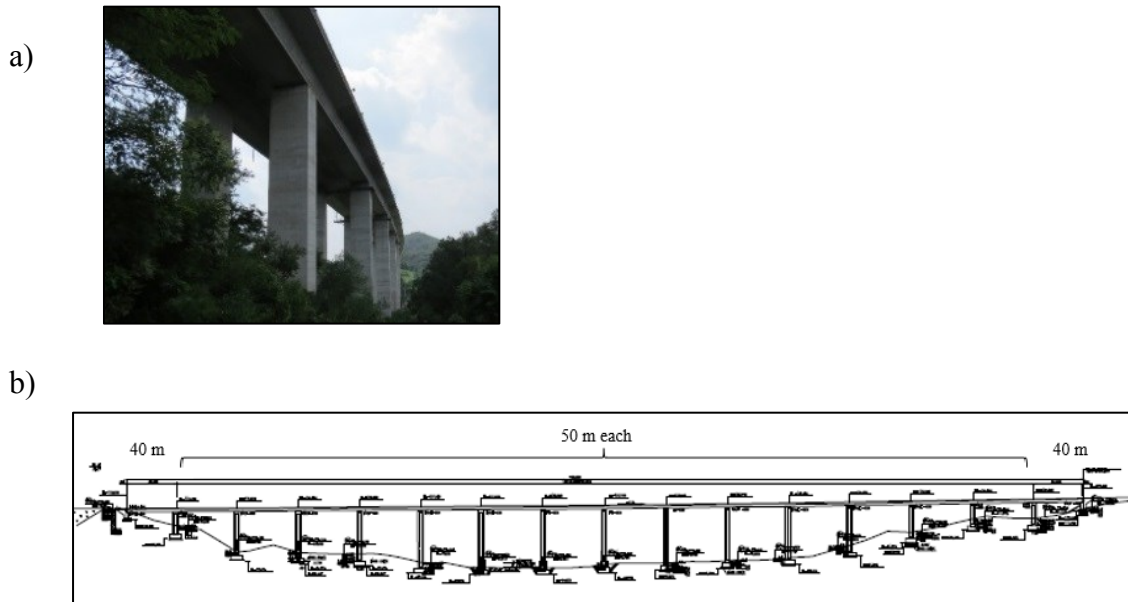


Figure 3.3: PSCB bridge details: (a) photograph of the bridge; (b) longitudinal elevation

3.2.2. Wireless monitoring of PSCB Bridge

30 wireless accelerometers PCB 393B12 with 10000 mV/g sensitivity and ± 0.5 g range have been placed along the full-length of the bridge with sampling rates of 256 Hz recording vibration data from ambient passing traffic. The first and the last span have one sensor located at the middle of the span. Rest of the 14 spans have two sensors; each located one-third span distance apart.

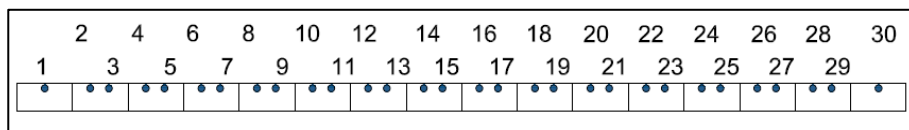


Figure 3.4: Sensor locations on PSCB bridge

3.2.3. Energy harvester design

Sazonov et al. (2009) designed a linear generator harvesting vibrational energy from low frequency vibrations using electromagnetic induction. The harvester's base is mounted on the bridge and is driven by bridge vibrations. The applied vibration moves the magnet around the conductor in the harvester relative to a coil and this varying magnetic flux generates electricity. Resonant spring-mass concept is used which means that matching the main frequency of bridge vibration with the natural frequency of the harvester can result in greater displacements of the moving mass generating more electrical energy.

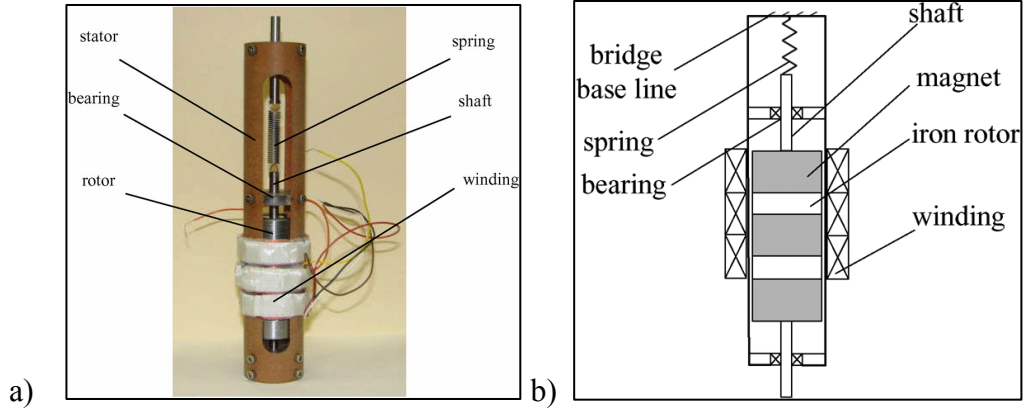


Figure 3.5: a) Schematic diagram; b) picture of linear generator

The transient vibration process is depicted by the vibration differential equation 3-1.

$$\ddot{z} + \frac{c}{m}\dot{z} + \frac{k}{m}z = a_i \quad (3-1)$$

where ‘ c ’ is the vibration damping, ‘ m ’ is the mass of the moving body, and ‘ a_i ’ is the input acceleration to the spring-mass system from the bridge excitation. The total vibrational damping ‘ c ’ comprises of mechanical damping ‘ c_m ’ and electrical damping ‘ c_e ’. The vibration of the bridge oscillates the mass in the harvester. The electrical energy generated ‘ Q_{he} ’ depends on the electrical damping and is calculated as shown.

$$Q_{he} = \int c_e \dot{z}^2 dt \quad (3-2)$$

The natural frequency of the generator is designed according to the main frequency of the bridge excitation. The vibration amplitude is different at different locations of the bridge. So, the first bending mode is considered optimal. The idea is that if the energy can be harvested at a lower displacement like at one-fourth of the span, then it works at the maximum displacement state in the middle of the span.

3.2.4. PSCB Bridge model

For the study, the bridge vibrations for undamaged and damaged scenarios are required. The undamaged response data for ambient vibration is provided by Korea Expressway Corporation but the data for different damage cases study is not available. The damage scenarios are simulated in SAP 2000 model of the bridge. The model constitutes a total of 782 frame elements.

The first bending mode is at 2.47 Hz and the SAP 2000 model is updated to its first bending frequency of 2.43 Hz which is in close proximity of that of test data. Also, Fast Fourier Transform (FFT) of all the 30 sensor nodes is carried out and the lowest main frequency is similar as the first bending mode of the SAP 2000 model.

The first natural frequency of the PSCB bridge is 2.47 Hz and this should be equal to the harvester's natural frequency. It must be noted that the real bridge is not installed with any energy harvesting system. However, in the present study, it is assumed that the energy harvesters are installed at specified sensor locations and the amount of harvested energy is computed based on the equations discussed in Sec 3.2.3 above using MATLAB (MATLAB user manual, 2008) and Simulink (Simulink user's guide, 2016).

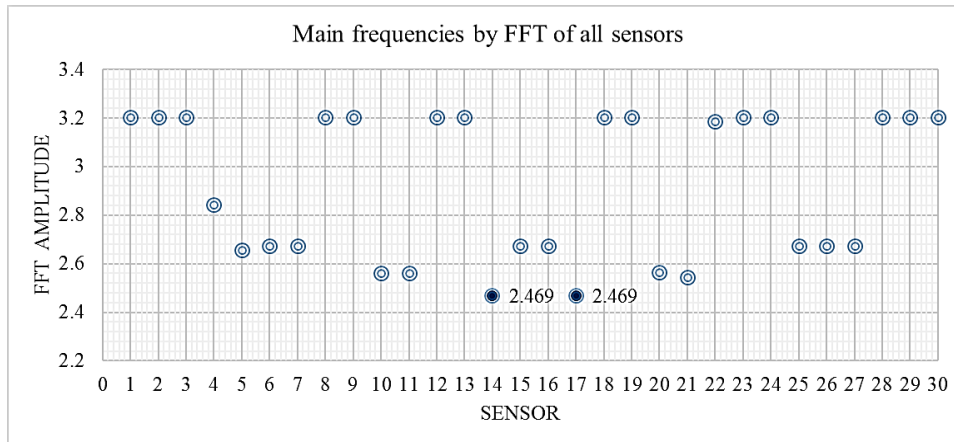


Figure 3.6: FFT results of all 30 wireless accelerometers on PSCB bridge

3.2.5. Truss Bridge model

Railway bridges are critical to infrastructure system. Railways carry large number of people and goods. Any disruption in their operation can take a heavy toll. So, this novel damage detection method is extended to another bridge model to investigate its applicability for railway bridges. Truss type bridges are common for railway bridges infrastructure. Warren truss type bridge is selected for this study. The bridge model considered here is adapted from Nieporęta rail bridge near Warsaw in Poland (Kolakowski et al. 2011). This steel bridge was constructed in the 1970s and its model is similar to over one thousand rail bridges in Poland. The bridge is 40 metres in span and 8 metres in height consisting of five bays as shown in Figure 3.7.



Figure 3.7: Nieporęt truss bridge, Poland (Kolakowski et al. 2011)

The structural configuration of this steel truss bridge is shown in Figure 3.8 (Favai et al. 2014) and the truss bridge considered in this thesis is similar to the bridge shown in Figure 3.7 and 3.8. However, since some of the specific details of the bridge shown in Figures 3.7 and 3.8 is missing, those details have been assumed in the adapted bridge model used in this thesis, and in SAP 2000 for generating its dynamic response in damaged and undamaged cases. The truss structure is hinged at one end and has roller bearing on the other end. All the floor beams and cross beams are of I-section with two main stringer double-tee beams. For the analysis model, two portal frames were also added to increase the stiffness of the truss bridge (Kolakowski et al. 2011).

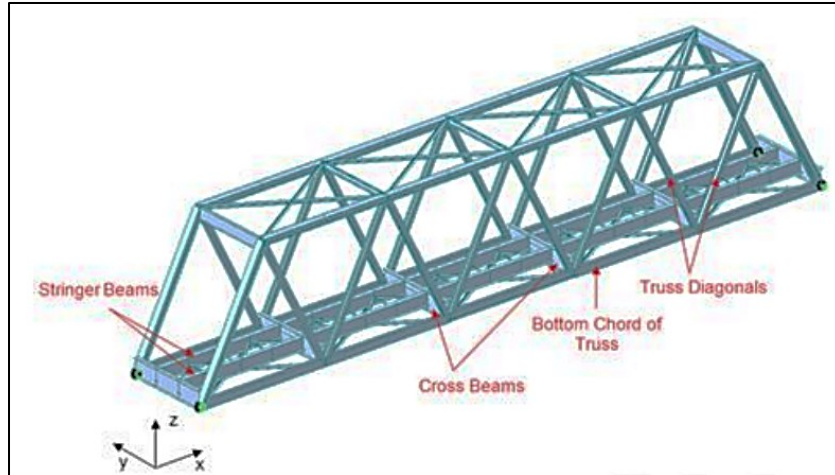


Figure 3.8: Structural configuration of Nieporęt truss bridge, Poland (Favai et al. 2014)

A representative model of this bridge is constructed in SAP 2000 for the analysis of damage detection using energy harvesters. Due to lack of complete structural details, a deck is assumed on the truss bridge instead of rails and sleepers. Although, by this study, the behaviour of truss bridges can be assessed for this method. The first bending mode of the model is at 4.65 Hz. Energy harvesters with wireless sensors are assumed at certain locations along the span on the deck and cables. Damage is simulated for various cases and the harvested energy curve parameters are analyzed for damage detection. The details of the SAP 2000 model constructed for the bridge here are discussed in Chapter 4.

3.2.6. Harvester simulations

The generator's natural frequency can be attained by varying its spring constant. The rest of the parameters of the linear generator for the energy harvester are as shown in Table 3.1.

Table 3. 1: Parameters of linear generator

Symbol	Parameter	Value
m	Rotor mass	0.604 kg
c _m	Mechanical damping	0.006 kg/s
c _e	Electrical damping	0.1513 kg/s
c	Vibration damping	0.1573 kg/s

The natural frequency of the spring can be calculated from Equation 3-3.

$$f = \frac{1}{2\pi} \sqrt{\frac{k}{m}} \quad (3-3)$$

The transient vibration process based on Equations 3-1 and 3-2 is simulated for this case as shown in Figure 3.9. The source block ‘accelin’ represents the time history data for the structural response under applied ambient vibration. ‘1’, ‘2’ and ‘3’ in the diagram denote external acceleration force, damping and stiffness components respectively which are fed into the block u(1)-u(2)-u(3) which is the transient vibration process shown in Equation 3-1. The resultant acceleration is integrated (1/S) by the next block to attain velocity. So, this represents how the transient vibration process is modelled and the energy is calculated using the velocity and electrical damping as shown in Equation 3-2. The output of the simulink model is taken into ‘scope’ block which provides the cumulative energy harvested over time. As shown in Table 3.1 and equation 3-3, the linear generator’s natural frequency can be tuned to attain resonance by varying its spring constant.

For the PSCB, the stiffness ‘k’ of the spring in the generator is calculated to be 145.33 N/m from this, which results in the natural frequency to be 2.47 Hz. For the truss bridge, ‘k’ is 515.59 N/m for simulation of natural frequency of 4.65 Hz.

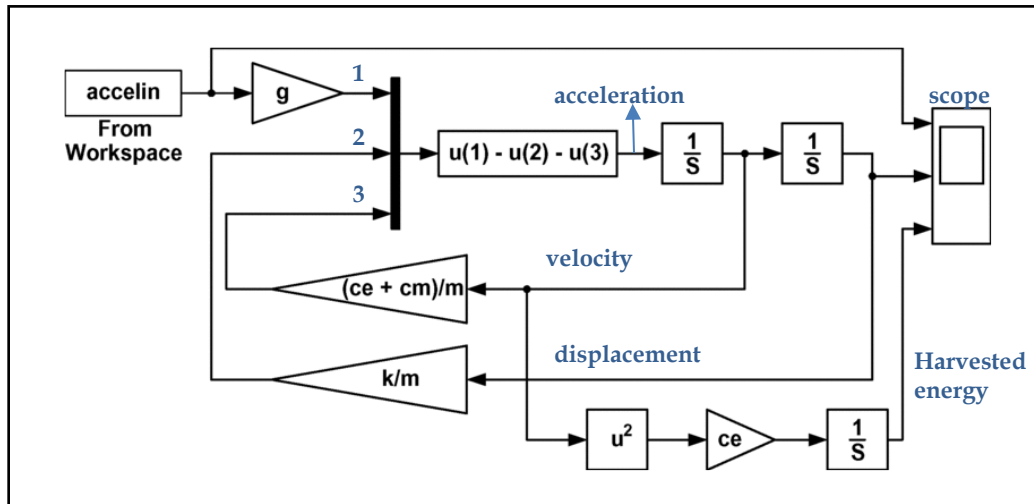


Figure 3.9: Transient vibration process

The harvester is modeled using Simulink in MATLAB to calculate the energy harvested from the bridge vibration. The sensor node acceleration data is inputted and the energy harvested for 50 seconds is considered for damage analysis.

3.2.7. Damage detection method

The energy harvested by linear generator depends on the bridge vibration. Any damage in the bridge leads to alteration of expected energy to be harvested. Hence, energy harvesters are proposed to be utilized as sensors as well for a more accurate structural monitoring. For validation of this concept, this case study is utilized. The undamaged and damaged responses of the bridge are simulated from the SAP 2000 PSCB model and truss bridge

model under White Gaussian Noise (WGN) for ambient vibration shown in Figure 3.10. The damage scenarios are created as follows. The acceleration responses are normalized before further analysis for clearer results as they are subjected to WGN (Balsamo et al. 2014).

$$data_{normalized} = \frac{data - data_{mean}}{data_{standard\ deviation}} \quad (3-4)$$

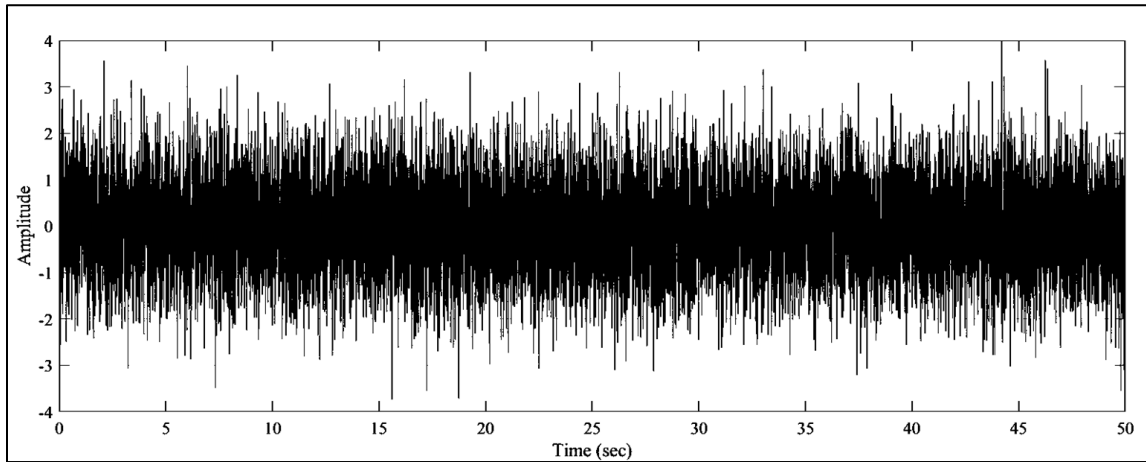


Figure 3.10: White Gaussian Noise applied as ambient vibration

Damage detection is carried out by comparing the total harvested energy in 50 seconds and the nature of the energy harvested vs time plot.

First, the PSCB bridge case study is considered. Four damage scenarios are considered for testing the proposed damage detection method. Damage is simulated by reducing the stiffness of 10 frame elements in particular spans corresponding to the damage scenarios by 20%. 10 frame elements signify 10 metres of length. 10 harvesters are placed at 10 sensor locations selected out of 30 total sensor locations. Comparison of all these 10 generator readings for harvested energy helps localize the damage in the bridge.

Table 3. 2: PSCB bridge damage cases

Damage scenarios	Damaged span	Location of damage	Sensors on damaged span
Damage 1	3 rd span	Close to sensor 5	4,5
Damage 2	8 th span	Close to sensor 14	14,15
Damage 3	6 th span	6 th span	10,11
Damage 4	16 th span	Close to the support connecting 15 th span	30

Four damage scenarios are considered for the truss bridge as well. Damage is simulated on the decks or cables by reducing its area by 20%, hence decreasing the moment of inertia of the deck and axial strength of the diagonal rods or cables. In total there are 8 harvesters for this analysis, 5 placed on each span and 3 placed on the three cables. The damage scenarios are summarized in Table 3.3. The first two cases are based on damage simulation on the deck. The third case is related to damage in one of the cables with energy harvester. The fourth case is for damage in cable without any harvester installed on it. Comparison of these different energy harvester locations for the four simulated damage cases is attained using two damage metrics which is discussed below.

Table 3. 3: Steel truss bridge damage cases

Damage scenarios	Damaged span	Sensors closest to the damage
Damage 1	1 st span	4,1
Damage 2	3 rd span	6,3
Damage 3	2 nd span cable	2,5
Damage 4	5 th span cable	8

The responses of all these damage scenarios and undamaged scenario are fed into the harvester model to obtain harvested energy. Damage is detected in two ways in this thesis.

Total energy harvested:

The first metric is to compare the total energy harvested in 50 seconds for all the cases. Damage in the structure will alter the input vibrations to the harvester and hence, damage location can be identified.

$$Damage\ metric\ 1 = \frac{Total\ energy\ harvested\ by\ undamaged\ bridge}{Total\ energy\ harvested\ by\ damaged\ bridge} \quad (3-5)$$

Energy harvested curve:

The next metric is related to the curve representing the variation of the harvested energy with time. The pattern of the curve is associated with the excitation input to the generator; which changes with the bridge damage. This pattern is determined by kurtosis of the generated energy curve. Kurtosis relates with the sharpness or peakedness of the curve. The energy peaks at near resonant frequencies are altered under damage.

$$\text{Damage metric 2} = \frac{\text{Kurtosis of harvested energy curve of undamaged bridge}}{\text{Kurtosis of harvested energy curve of damaged bridge}} \quad (3-6)$$

The passing traffic patterns are important in the context of damage metrics calculation. The amplitude of bridge vibrations is dependent on the type and volume of vehicular traffic, and higher traffic load will generate higher amplitudes of bridge vibration. The traffic patterns of particular bridge to be instrumented should be identified and the energy harvesting curve trend should be correlated with the traffic pattern. Any change in the harvested energy curve behaviour under consistent traffic pattern can be related to the structural damages which changes the vibration pattern of the bridge. Damage can be related to harvested energy curve in this manner and any deviation from the expected curves can be correlated to the sensors data which can provide information about the type and location of damage or possible malfunction of a sensor, if the correlation is not followed.

3.3. Damage detection by MHS

Data generated from real structures are usually non-linear and non-stationary. MHS by HHT method can detect damage for these responses preserving their non-linear and non-stationary features. The process of MHS construction from structural response is explained below followed by an example demonstrating its working.

The signals decomposed to several Intrinsic Mode Functions (IMFs) in their intrinsic time-scales. The IMFs are adaptive to signals and they allow well behaved Hilbert transform on them to obtain instantaneous frequency and amplitude. This preserves the non-stationarity of the signal providing instantaneous details rather than analysing the signal in a global

form like Fourier spectrum. This approach is adaptive and can be applied to any time-series. The detailed step by step procedure is described in Chapter-2.

The entire process is performed by codes developed using MATLAB. To examine the codes written and detection ability of MHS by HHT method, the following input signal is considered as an example:

$$x(t) = 2 \sin(2\pi 15t) + \sin(2\pi 5t) \sin(2\pi 0.1t) + 4 \sin(2\pi t) \quad (3-7)$$

HHT method should be able to determine the frequency (15, 5, 1) and amplitude (2, 1 4) components of $x(t)$ accurately. The original signal is shown in Figure 3.9, the IMFs in Figure 3.10 and HHT plot in Figure 3.11. For comparison, FFT is performed in Figure 3.12 as well and results by HHT method were very precise showing the instantaneous components of the signal.

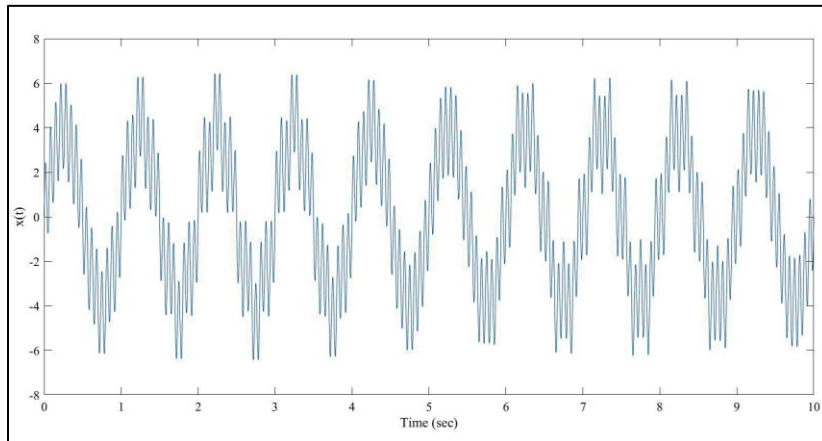


Figure 3.11: Plot of signal $x(t)$

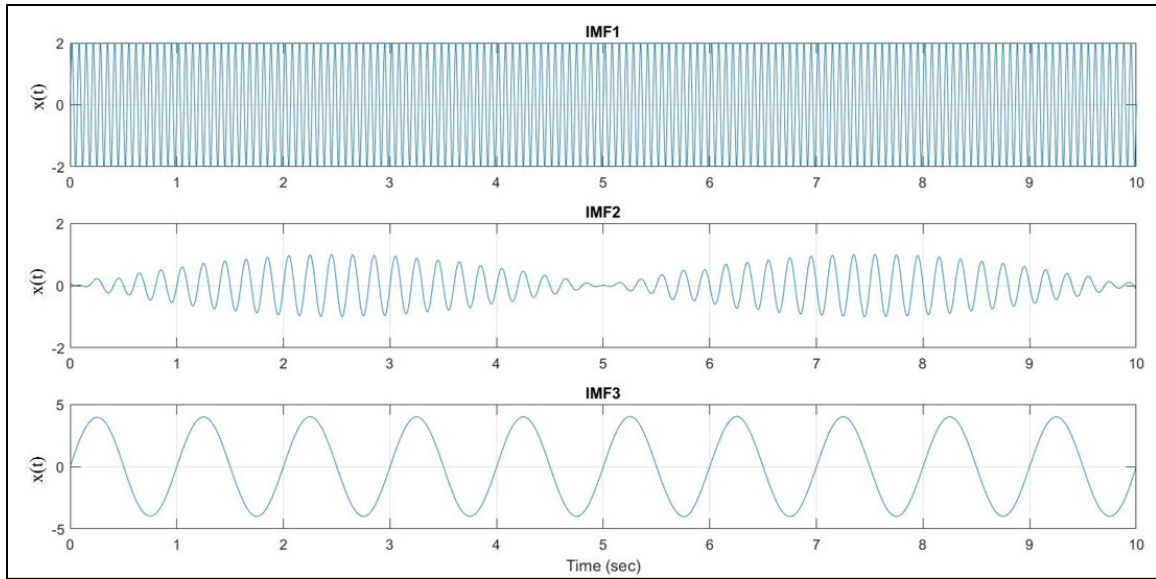


Figure 3.12: IMFs of signal $x(t)$

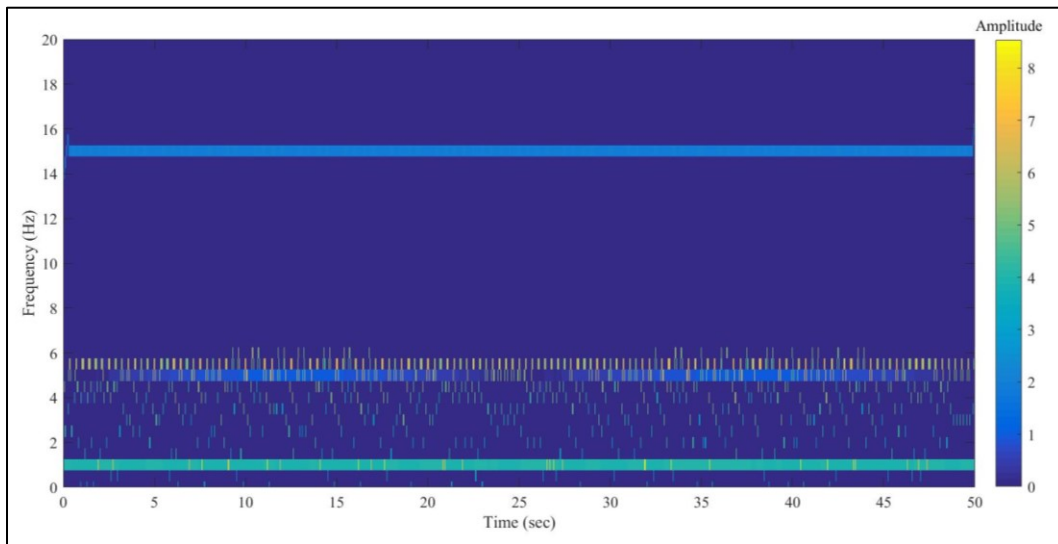


Figure 3.13: Hilbert-Huang Transform (HHT) plot of signal $x(t)$

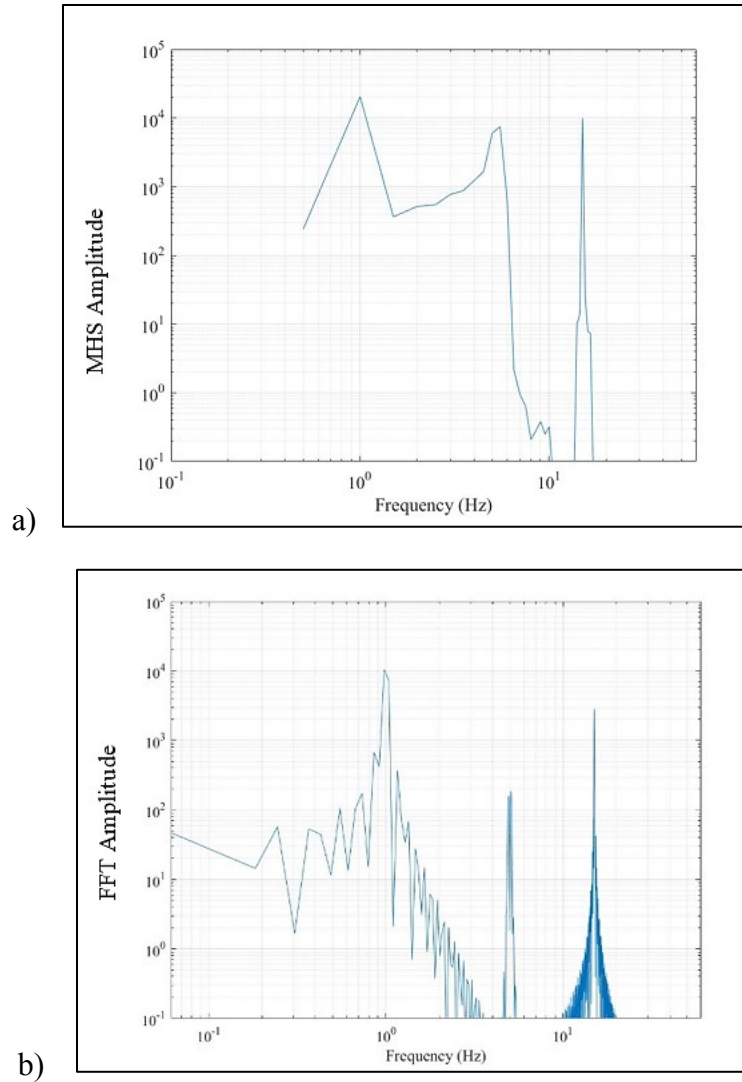


Figure 3.14: a) MHS; b) FFT of signal $x(t)$

The procedure for obtaining the plots in Figure 3.10-3.12 is discussed elaborately in Section 2.5. Figure 3.10 shows the Intrinsic Mode Functions (IMFs) obtained by Empirical Mode Decomposition (EMD) which results in the decomposition of the signal into its main frequencies. The first 3 IMFs represent 15, 5 and 1 Hz inherent to the signal. No two IMFs have the same frequency at the same time instant. Once the IMFs are obtained, they can accommodate well-behaved Hilbert Transform on them to provide instantaneous parameters. Referring to Section 2.5, the instantaneous amplitude corresponding to the

frequencies and time can be obtained in the HHT plot as shown in Figure 3.11. The color bar represents different amplitude values. Three color bands are clearly visible in Figure 3.11 which correspond to the amplitudes of 2, 1 and 4 to 15, 5 and 1 Hz respectively. Marginal Hilbert Spectrum (MHS) is plotted from the HHT curve using Equation 2-14 in Figure 3.12.a. It represents the total amplitude contribution from each frequency in a probabilistic sense. The peaks of this curve correspond to the main frequencies. Figure 3.12.a shows the 3 frequencies of 1, 5 and 15 Hz accurately identified with comparison to the FFT plot which is very noisy for this mathematical simulation. This accurate HHT method is not widely used for damage detection of civil engineering structures currently. The goal is to validate this method using different response signal data collected by experiments. Firstly, this concept is tested on a structural simulation of a simply supported beam in SAP 2000. As mentioned by (Ghazi and Büyüköztürk 2014), experimental data is better than numerical simulations for this study. Thus, experimental data is also used from a steel bookshelf structure. HHT method testing procedure for them is described in the following sections. The work for experimental data acquisition for the beam structure is under progress at Central Building Research Institute (CBRI), Roorkee, India and is a part of future research.

Sampling rate selection

The sampling rate of the sensors considered for recording structural response is very important and must consider the range of frequencies of the structure to be determined. Taking into consideration, the Nyquist or the folding frequency occurs at half of the sampling rate. So, the selected sampling rate should be more than twice the structural frequencies to be captured. The size of the data window, or the number of data points also

play an important role. The data points should not be too few such that useful information is lost and may produces unacceptable results due to the effect of aliasing error. Sufficient number of data points or zero padding can be used to minimize that effect. Also, higher number of required data points can induce noise. Hence, the sampling rate has to be optimally selected for the frequency analysis of the structures.

3.3.1. Beam structure

The HHT method is tested on a simply supported steel beam of length 1.2 metres before moving on to conducting experiments on it. Its geometry and dimensions are shown in Figure 3.13 and its properties are presented in Table. 3.4. The beam experiment is to be carried out at CBRI, India by deploying wireless sensors and this simulation is performed in SAP 2000 corresponding to that experiment. The beam is to be wirelessly instrumented to record its vibration data at three different equidistant points under undamaged and damaged scenarios. Here the vibration response of the beam has been generated using its numerical model constructed using SAP 2000.

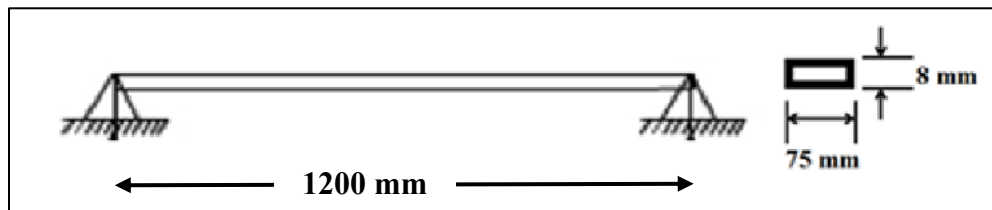


Figure 3.15: Simply supported beam section details

Table 3. 4: Properties of the simply supported beam section

Property	Value
Length (mm)	1200
Width (mm)	75
Thickness (mm)	8
Elastic Modulus (MPa)	2.10×10^5
Density (kg/m ³)	7.800×10^3
Poisson's Ratio (ν)	0.3

The sampling rate of the Wireless acceleration sensors is assumed to be 256 Hz. The entire beam is subjected to White Gaussian Noise (WGN) for the software analysis to represent ambient vibration, and the vibration response was computed at the sampling rate of 256. The SAP 2000 model of the simply supported beam is shown in Figure 3.14.

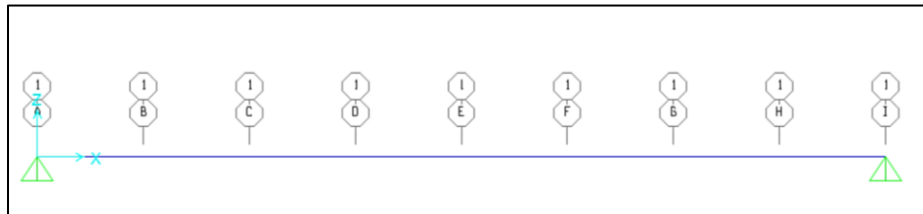


Figure 3.16: SAP 2000 model of simply supported beam

Damage scenarios of the beam

The instrumentation scheme for the beam is shown in Figure 3.17. The beam is instrumented with wireless sensors at three locations 300 millimetres apart from each other. Two damage locations are considered for this beam. One at the support with the label 'Damage 1' and another at the middle marked as 'Damage 2' to check the damage detection efficacy of HHT method. The sensor nodes locations and damage regions are demonstrated

in Figure 3.17. Damage is created by reducing the moment of inertia by 20% in the marked region. Each marked damage case covers 150 mm. The sensor located closest to the damage is expected to capture the maximum effect.

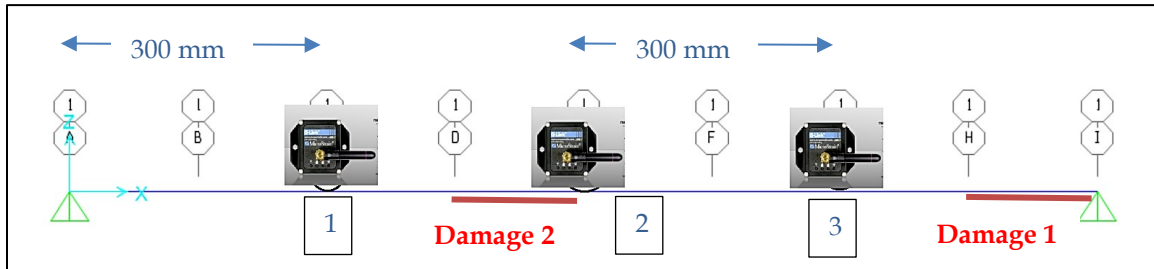


Figure 3.17: Sensor and damage locations on simply supported beam

3.3.2. Bookshelf structure experiment

The bookshelf structure experiment was conducted at Structures Laboratory, Concordia University, Canada. The material of the cantilever beam is galvanized steel. The steel frame is fixed to the base using concrete to depict it as a three storey structure model. Its geometry and dimensions are shown in Figure.3.16 and its properties are presented in Table. 3.5. The bookshelf frame is wirelessly instrumented to record its vibration data at three different points or levels under baseline and damaged scenarios. The frame is struck along its long span around 4 times in 20 seconds in order to study its vibration characteristics.

Table 3. 5: Bookshelf frame structure dimensions

Bookshelf – frame structure dimensions	
Height	140 cm
Length	60 cm
Width	27 cm



Figure 3.18: Bookshelf frame structure picture

Wireless monitoring of the frame

The frame consists of three levels representing a building with three floors. Each wireless sensor is positioned at the centre of each floor to record the vibration data. Microstrain

Wireless G-Link Accelerometers were used. The wireless data acquisition system used is Node Commander v1.5.26. Microstrain USB base station is used for collecting data from wireless nodes and transferring it to the computer for further processing. Communication with multiple nodes can be carried out through USB base station and data from the nodes can be downloaded and erased by commands using the Node Commander. The communication protocol is IEEE 802.15.4. The sensor units were produced in 2007 and they cost around 550 USD per sensor unit. The different data collection modes are high speed streaming, low duty cycle and data logging. This research used data logging mode for data recording in the sensors for the sake of accurate time stamps in multiple nodes. All the three wireless sensor nodes on each level were triggered for data collection at the same instant.



Figure 3.19: USB base station

For verification of sensor data, a model of the structure in undamaged scenario is created using SAP 2000. The frequencies of the structure after modal analysis from the SAP 2000

model and frequencies obtained from FFT of the data collected from experiment using wireless sensors are found to be similar. Verification results are explained in Chapter-5.

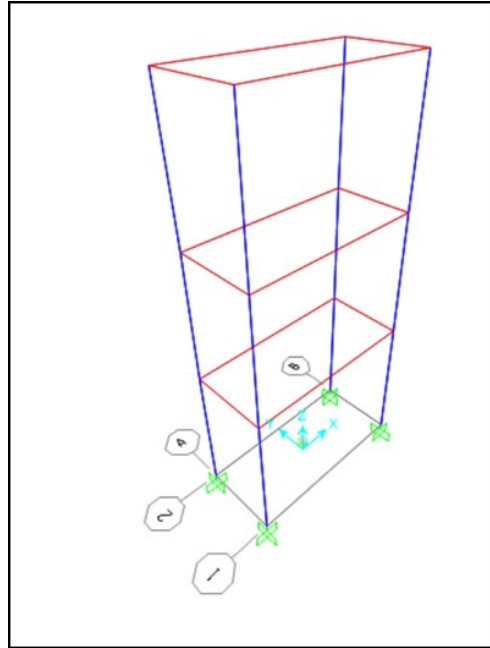


Figure 3.20: SAP 2000 model of three story steel frame

Damage scenarios of the bookshelf frame structure

Each rack of the bookshelf depicts a storey level of a building. Each level is rectangular in shape and bolted with the columns in its all four directions. Two bolts at each corner are used with a total of eight bolts for one level. To induce damage at a level, all the eight bolts

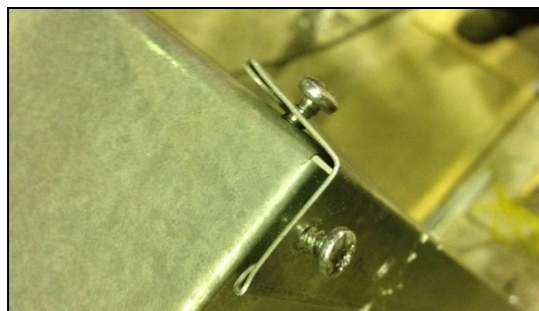


Figure 3.21: Top level damage scenario by loosening bolts

are loosened as shown in Figure 3.19. Two damage scenarios are considered, first on the top floor and second in the middle floor.

3.3.3. Damage indices

The steps of instrumentation of the structure, data collection and data processing aim to detect damages and localizing them accurately. To attain this goal of measurement, some Damage Indices (DI) are required. Several energy distribution curves are plotted for the calculation of MHS and their distribution changes with induction of damage in the structure. The method to obtain damage indices for detection of this change are described below.

Normalized energy vs IMF no. plot:

Due to structural damage, its response characteristics change. This leads to change in energy distribution of the modes or IMFs. The square of amplitude provides energy with respect to IMFs. The damage index (DI) deals with analyzing the change in the pattern of energy distribution among the existing IMFs or any newly created IMF after damage with respect to the undamaged structure. A necessary condition is to keep the same input energy for both the undamaged and damaged structural vibration data. It is important since this method works with energy variation in the vibrating modes of the structure. This can be sufficed by normalizing the energy in the energy distribution curves for both the cases. As proposed by Ghazi and Büyüköztürk (2014), the fourth central moment, kurtosis of such distribution can be considered as DI since, kurtosis is measure of shape or peakedness of the distribution. Also, skewness, which is the third central moment indicates the amount of asymmetry around the mean value of the distribution.

These two metrics can be calculated for DI and their formulae are as shown. Kurtosis aims to find changes in existing modes or creation of new modes in the structure. Whereas, skewness detects nature of transfer of energy between the modes.

$$DI_1 = \frac{kurtosis(Energy_{undamaged})}{kurtosis(Energy_{damaged})} \quad (3-8)$$

$$DI_2 = \frac{skewness(Energy_{undamaged})}{skewness(Energy_{damaged})} \quad (3-9)$$

Marginal Hilbert Spectrum (MHS) curves:

The Marginal Hilbert Spectrum (MHS) shows the amplitude accumulation of a signal with its frequencies. It includes the non linearities of the signal captured from the structure without least possible energy leakage. Under the scenario of damage, the peak frequencies of a structure will also vary and MHS can capture it precisely. This change in the distribution of MHS curves is accounted in DI. Normalizing the MHS curves for both the scenarios is important for relevant interpretation.

$$DI_3 = \frac{kurtosis(NMHS_{undamaged})}{kurtosis(NMHS_{damaged})} \quad (3-10)$$

Normalized Cumulative Marginal Hilbert Spectrum (NCMHS) curves:

NCMHS curves were proposed by Ghazi and Büyüköztürk (2014). MHS curves are non-smooth and hence, difficult to interpret. NCMHS curves are smooth and strictly increasing. They are obtained by calculating the cumulative sum of MHS curves for a particular sensor and then normalizing it to keep the input energy same for each case. The cumulative sum smoothens the curve while preserving its physics. The normalization of the curve assures the consistency of the input energy in the structural system. While DI based on NCMHS

was proposed by Ghazi and Büyüköztürk's (2015), it is used in the present work to test its accuracy and applicability which was not done earlier, independently. The area between the NCMHS curves of the two cases depict the energy transfer between the modes and how it varies with damage. The ratio of the NMCHS curves in the damaged and undamaged condition with respect to the average baseline provides DI_4 .

$$DI_4 = \frac{\sum |Area\ between\ damaged\ and\ undamaged\ NCMHS|}{Area\ of\ undamaged\ NCMHS} \quad (3-11)$$

To obtain the energy distribution baseline or undamaged structure curves for each DI , multiple readings have to be taken into consideration and their mean values are the final plots for calculations. This removes outlier effects in some readings, if present.

DI is found by a ratio of various curves for damaged to undamaged condition and the more it is deviated from unity, higher is the damage. The DI of all the sensor nodes are evaluated and the one with the highest DI is taken as the location of damage. In the two cases experiments presented here, the damage location is known and the vibration data is used to obtain the DI for all sensor locations. The node with the highest DI is the damage location by MHS method and it can be verified with the known scenarios.

3.4. Summary

In this chapter, the two damage detection methods utilized for this thesis are explained and their investigation procedure is discussed. The first method is damage detection by energy harvesters. Two bridges: PSCB and Warren truss bridge are modelled and analyzed in SAP 2000. Their vibration responses are fed to the linear generator model in MATLAB Simulink and the resultant output provides harvested energy. Damage is detected by the assessment of the amount of harvested energy and its energy generation curve pattern with

time. The second method is damage detection by Marginal Hilbert Spectrum (MHS) curves obtained from Hilbert-Huang Transform (HHT) method. This is further tested on two structures: simply supported beam model in SAP 2000 and steel bookshelf structure by laboratory experiment. The variation in the obtained curves of their Hilbert Spectral Analysis (HSA) helps in damage detection.

The next chapters show the validation of these methods and the results obtained.

CHAPTER 4: DAMAGE DETECTION BY ENERGY HARVESTERS

4.1. Introduction

Civil engineering structures are instrumented with sensors for their accurate monitoring and early damage detection. Wireless sensors are preferred over wired ones due to their several benefits like ease and cost of installation, flexibility in adding or removing sensor nodes in the existing monitoring network in recorded data as absence of wires make them less susceptible to human or environmental disturbances.

Another advantage of wireless sensor network is its very less requirement of human interference for its operations. Wireless sensors operate on batteries conventionally; which either have to be replaced or recharged from time to time. This fails the system to be autonomous in true sense. Also, sensors are mostly located at inaccessible locations of the structure and huge structure have many sensors installed which makes it even more difficult to administer. Energy harvesters prove to be a suitable long term solution for this problem of power supply. This study deals with electromagnetic type of vibrational energy harvesters which convert vibrational energy to electrical energy.

The electromagnetic generators harness bridge excitation and supply power to the wireless sensors monitoring the bridge. The harvested energy from the generator is dependent on the vibration of the bridge it is attached to. The ambient vibration of a bridge can be created by passing traffic and wind. Any damage in the structure is reflected in its response. The

idea of the damage detection method proposed in this chapter is rooted in this concept. The structural damage alters its response to ambient vibration and further, changes the dynamic characteristics of the structure and alters the energy harvested by the harvesters installed for the sensors. By tapping the data on the harvested energy and analyzing it, damage can be detected and localized as explained in Figure 3.2 of Chapter-3.

The purpose of putting forward this method is to verify the functioning of the sensors and making the most of energy harvesters to power the sensors. Any redundancy in the wireless sensor system adds to damage detection of the structure, detection and isolation of sensor faults. This added redundancy provided by harvesters have economic benefits as it performs dual applications by powering the sensors and detecting faults in the system. This leads to contributing more towards the autonomous nature of wireless sensor networks for structural health monitoring and early damage detection with higher accuracy.

4.2. Electromagnetic energy harvesters

A linear generator works on the principle of electromagnetic induction and can convert kinetic energy to electric energy for supplying power to wireless sensors. The bridge vibrates under ambient excitation and along with it, the linear generator moves up and down. The spring in the generator supports the moving mass in it. This motion of linear generator varies the magnetic flux through the winding producing voltage and generating electrical energy. The working principles and parameters of the generator are explained in detail in Chapter-3. The natural frequency of the generator is based on the moving mass and spring which is designed according to the fundamental frequency of the bridge vibration, so that the linear generator can undergo resonance and the more the moving mass

displaces, more electrical energy it generates. This process is modelled using Simulink in MATLAB as shown in Figure 4.1. It is based on Figure.3.9 which shows the transient vibration process. The mass, spring and damping forces of the spring in the linear generator are acted upon by the input acceleration 'accel' provided by the bridge excitation. After undergoing the transient vibration process, the block labeled as 'Integrator' outputs velocity which is converted to energy using Equation 3-2 which is demonstrated by $F_{cn1} \gg Gain3 \gg Integrator2$ in the Simulink model. The final output is 'energy_harvested' which is a time series providing cumulative energy harvested since the input acceleration is also a time series.

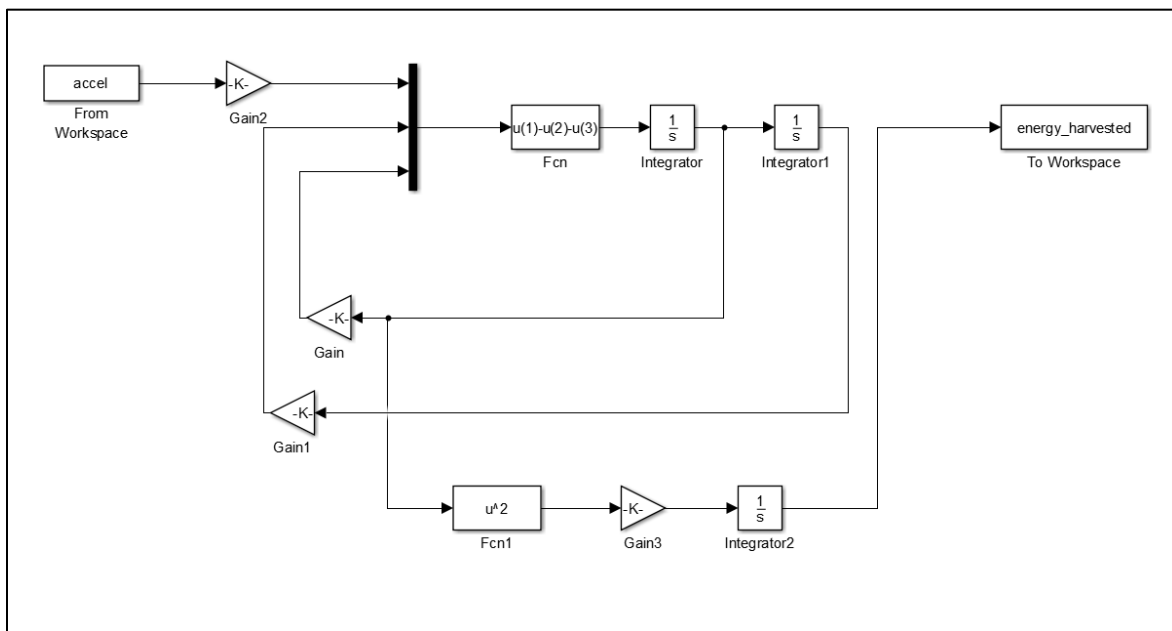


Figure 4. 1: Simulink model in MATLAB of acceleration to energy harvested data

The PSCB bridge and truss bridge models in SAP 2000 are subjected to WGN representing ambient vibration. The Simulink generator model takes the bridge vibration response as input to the harvester and produces energy harvested by it as output. This analysis was run

for 50 seconds for undamaged and damaged scenarios whose comparison demonstrates damage detection by this method. All the parameters as ‘gain’ are elaborated with values in Table.4.1. ‘Integrator’ provides displacement and ‘Integrator1’ gives velocity which is further integrated by ‘Integrator2’ to output the harvested energy. Separate inputs to the Simulink model were used for the two bridges owing to the variation in their bending frequencies and structural details.

Table 4. 1: Simulink generator model parameters

Label in Simulink	Meaning	Values inputted	
		PSCB	Truss bridge
Gain	$(c_e + c_m)/m$	0.26043	0.26043
Gain1	k/m	240.6126	853.6221
Gain2	g	9.8	9.8
Gain3	c_e	0.1513	0.1513

The simulation and analysis softwares used in this thesis are mainly SAP 2000 (SAP 2000 user manual, 2015) and MATLAB (MATLAB user manual, 2008). SAP 2000 is an integrated software operating on Finite Element Analysis and used for structural analysis and design with its built in user interface and design codes. This research uses SAP 2000 for modeling and analysis of the bridges and beam. MATLAB is a platform for performing computational mathematics. Its built-in features help to execute signal processing tasks and other mathematical operations. Simulink (Simulink user’s guide, 2016), which is a part of

MATLAB is also utilized in this thesis. It helps perform simulations for dynamic systems using block diagram environment.

4.3. PSCB Bridge model and harvester deployment

The frequency of the first bending mode of the bridge under ambient vibration is experimentally found to be 2.47 Hz and the SAP 2000 model is updated to its first bending frequency of 2.43 Hz which is in close proximity of that of test data. The SAP 2000 model is shown in Figure.4.2. The PSCB bridge model has a length of 780 metres in total consisting of 782 frame elements. Each frame element represents about a metre in length. The deck width is 12 metres and its curved radius is 3000 metres. The Young's Modulus of Elasticity of the concrete used is 279 GPa, density is 2500 kg/m³ and Poisson's ratio is 0.167. The vibration response of the structure at the undamaged (baseline) and damaged states are obtained from the correlated structural model as described in Section 3.2.

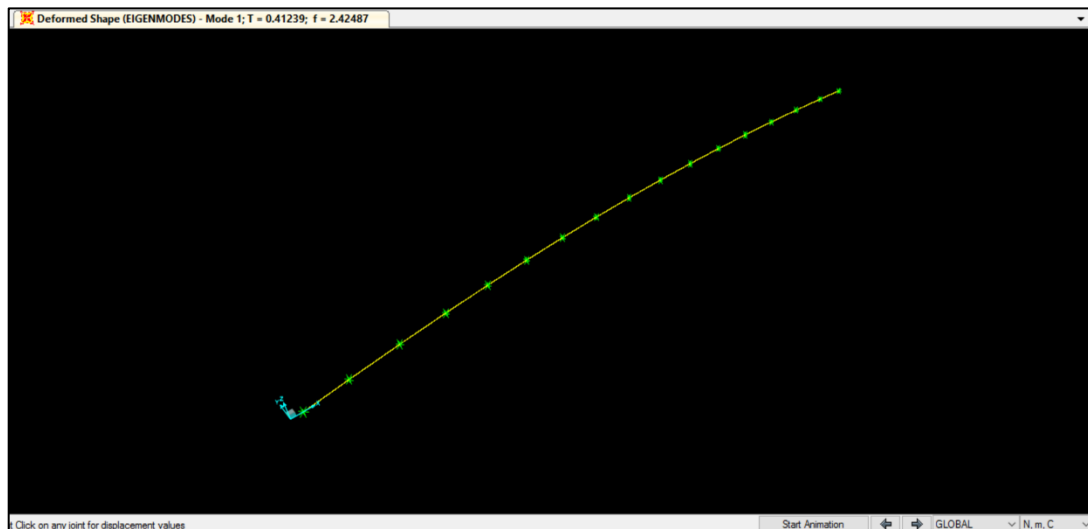


Figure 4. 2: SAP 2000 model of PSCB bridge

The energy harvesters are placed at 10 selected locations on the bridge where 30 sensors are deployed. 10 harvester locations were selected in order to study different types of

locations on the bridge for testing if the harvesters can detect damage at all bridge locations on spans; even including cases where the damage location is not instrumented with harvesters. The harvester locations are marked in blue along with sensors in Figure.4.3.a. The 10 harvesters with damages highlighted in red are shown in Figure.4.3.b. More details on damages are provided in Chapter-3. The next sections discuss the results obtained from this method and its efficacy.

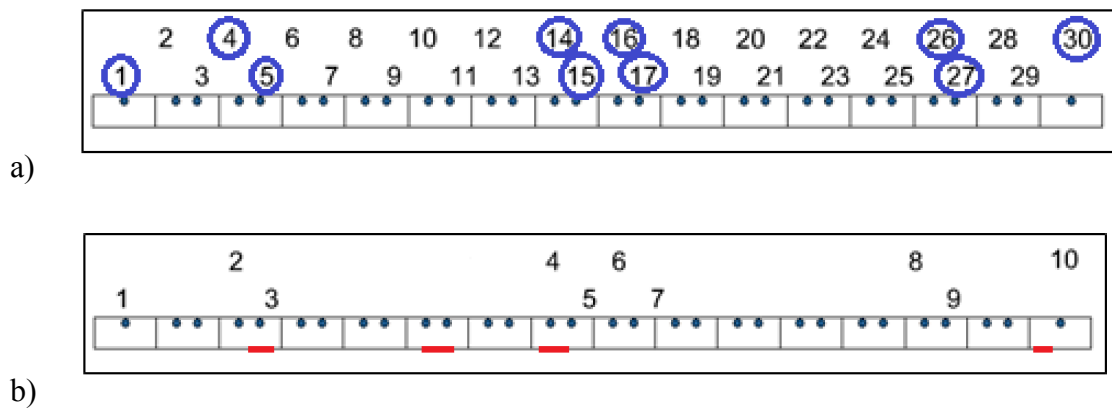


Figure 4. 3: a) Harvester and sensor locations; b) Harvester and damage locations

4.4. Truss Bridge model and harvester deployment

The first bending mode of the truss bridge model representing Nieporęt rail bridge, Poland is at 4.65 Hz. Its SAP 2000 model is shown in Figure 4.4. The bridge is constructed of steel with Young's modulus of 205 GPa, yield strength of 345 MPa and density of 7850 kg/m³. The deck is built of concrete material in SAP 2000 with density of 2350kg/ m³ and compressive strength of 28 MPa. The bridge length is 40 metres with a height of 8 metres and width of 6 metres supported on two stringers at the base. One end is hinged while the other end has roller support.

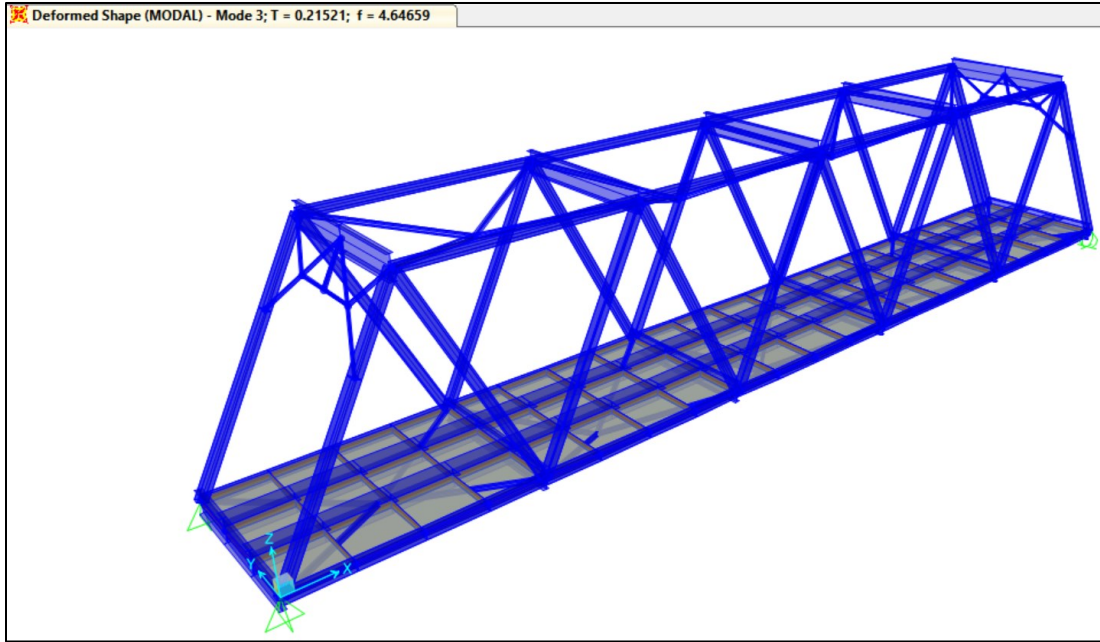


Figure 4. 4: SAP 2000 model of steel truss bridge

Eight energy harvesters are placed on the bridge to assess different damage scenarios. Their placement is depicted in Figure 4.5. Damage is simulated by reducing the member area which decreases the moment of inertia in the deck and axial strength in the cables.

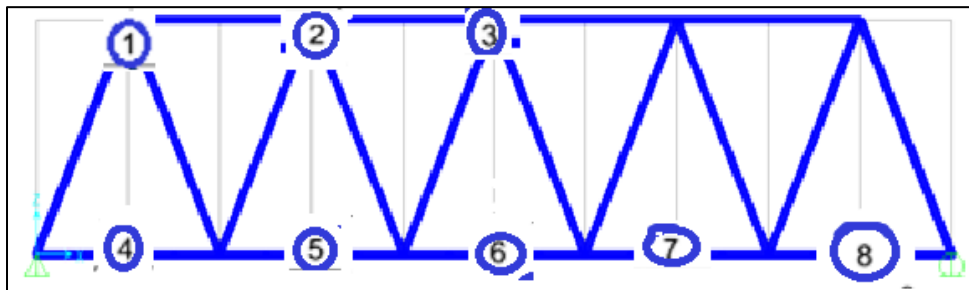


Figure 4. 5: Energy harvester locations on steel truss bridge

The damage locations are shown in Figure 4.6 corresponding to the four damage scenarios. The damages on the deck along the span are in the close proximity of the harvester. The middle cable damage is near a harvester as well. The support cable is not installed with any

harvester and is created on purpose to study the damage localization efficiency of this method.

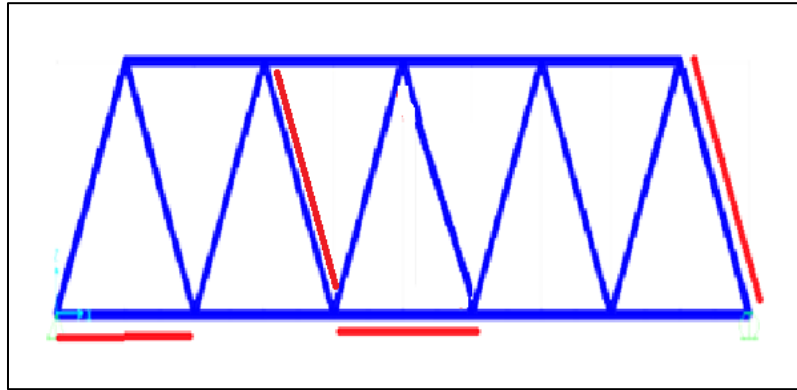


Figure 4. 6: Damage locations on steel truss bridge

4.5. Vibration responses and harvested energy

The bridge vibration data was collected at all the 10 harvester locations under baseline and damaged cases for the PSCB bridge. 10 data sets are created for 5 scenarios i.e. 1 undamaged and 4 damaged cases resulting in a total of 50 different data sets. For the steel truss bridge, vibrations from 8 harvester locations under baseline and damaged cases are analyzed. 8 data sets are synthesized for 5 scenarios i.e. 1 undamaged and 4 damaged cases resulting in a total of 40 different data sets. The entire data sets with respect to harvester and damage scenarios were fed into the generator model and the harvested energy with respect to time plot is obtained for both the bridges. The harvested energy plots are cumulative in nature. The total energy generated and the nature of the curve are analyzed for damage detection metrics. Damage metric 1 is based on total energy harvested by harvesters at different locations under damaged and undamaged states of the bridge. Damage metric 2 calculates the ratio of the kurtosis of the harvested energy distribution patterns for damaged and undamaged cases.

One set of vibration data of PSCB bridge for energy harvester 3 under 5 scenarios is shown in Figure.4.7 for input WGN as a specimen. The harvested energy curve for it under all the scenarios are shown as well in Figure.4.8. Acceleration response to WGN and harvested energy curve for all cases by harvester 5 is demonstrated in Figure 4.9 and Figure 4.10 respectively. It should be noted that the harvested energy curve varies for different scenarios whereas the first bending mode frequency is almost similar to the baseline case and constant under all the damage scenarios.

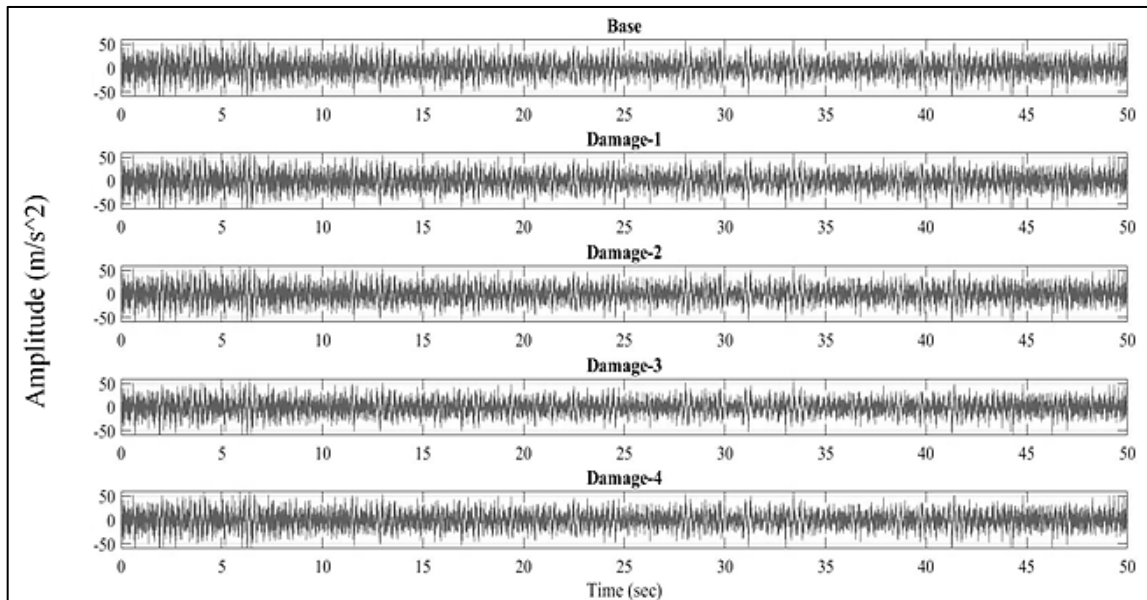


Figure 4. 7: Acceleration response to WGN for PSCB energy harvester 3

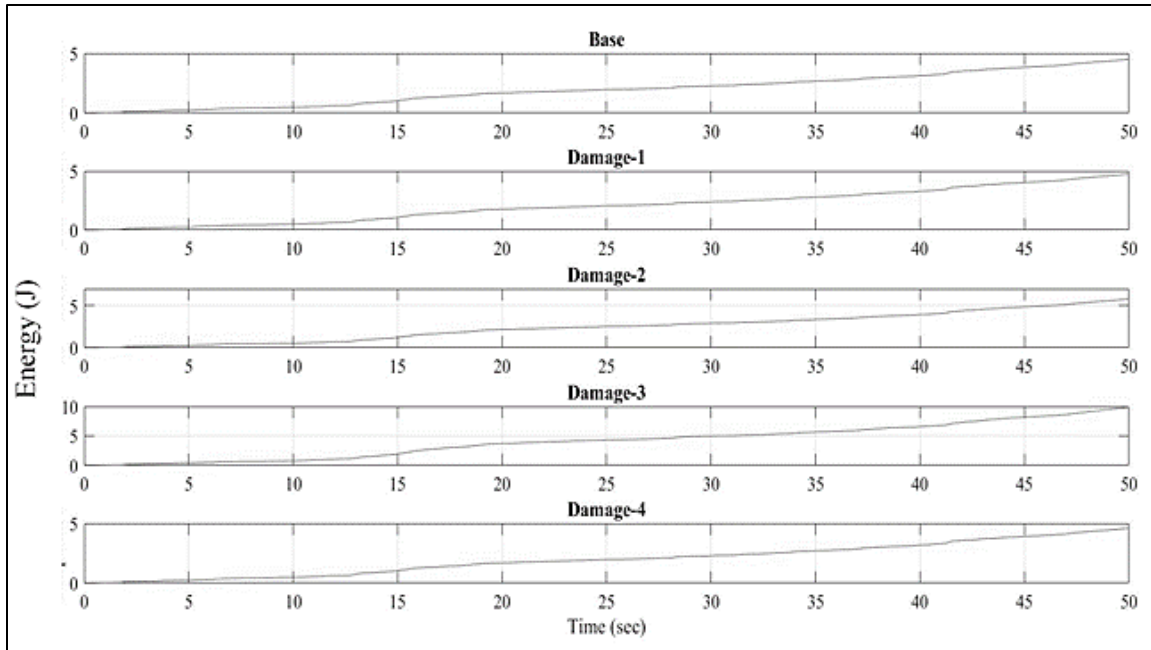


Figure 4. 8: Harvested energy for PSCB energy harvester 3

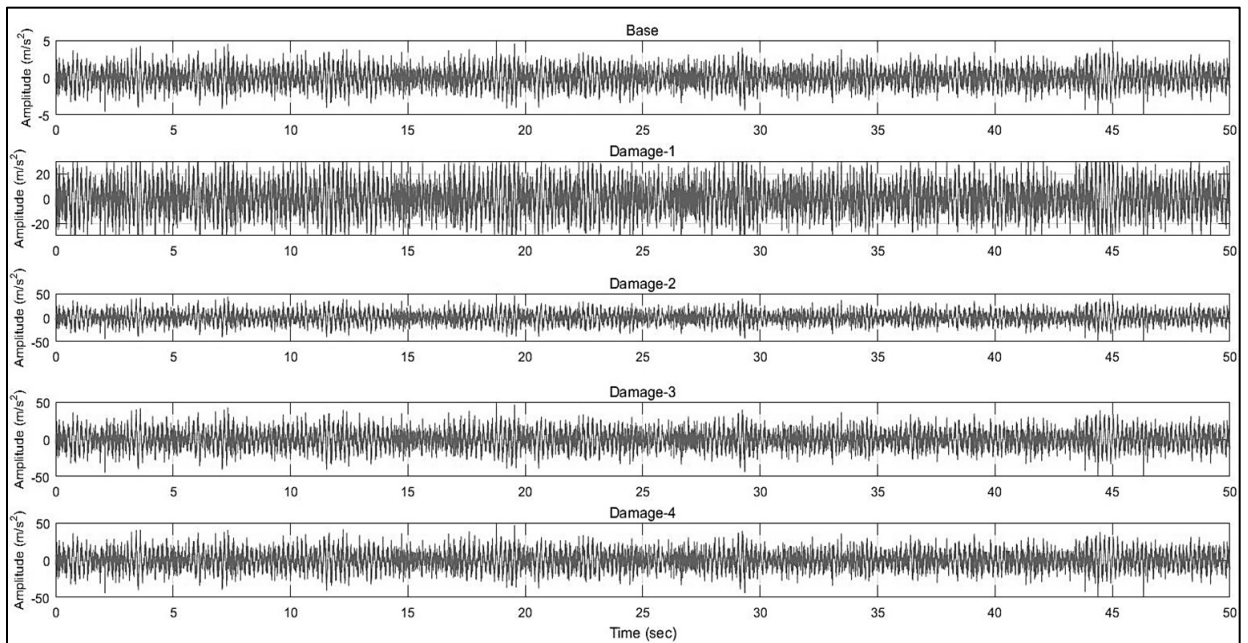


Figure 4. 9: Acceleration response to WGN for truss bridge energy harvester 5

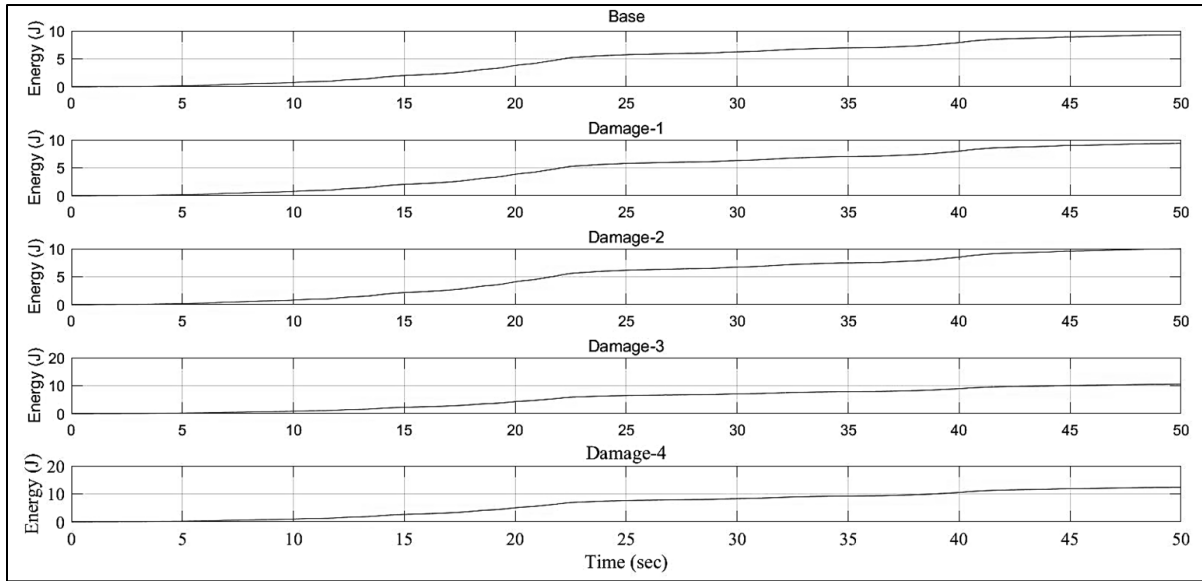


Figure 4. 10: Harvested energy for truss bridge energy harvester 5

4.6. Results

The entire procedure discussed for damage detection by energy harvesters is performed and the energy harvested from all the harvesters are analyzed. For a clear understanding, the damage scenarios with their locations next to harvesters are displayed for PSCB in Figure.4.11 and for truss bridge in Figure 4.12.

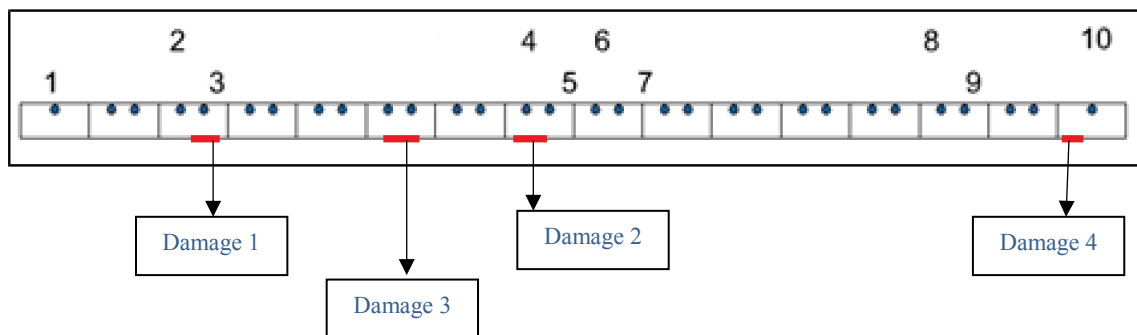


Figure 4. 11: Energy harvesters and damage scenario locations for PSCB

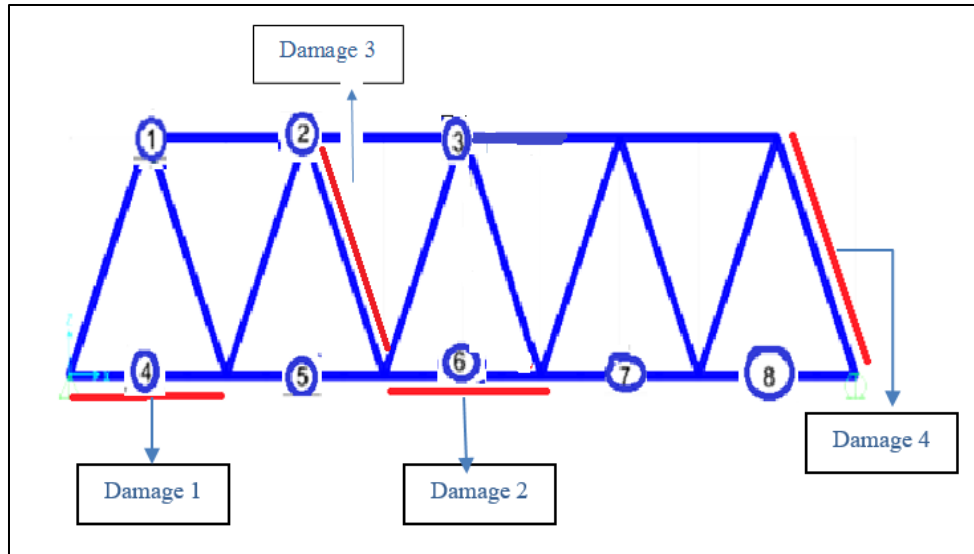


Figure 4. 12: Energy harvesters and damage scenario locations for truss bridge

First, the PSCB bridge results are calculated. The damage metric 1 for all damage scenarios are shown in Figure 4.13. The damage metric 2 results are in Figure 4.14. The x-axis shows the energy harvester and y-axis represents the value of damage metric.

Higher the value of the damage metric, higher is the damage at that location. Energy harvested may increase or decrease depending on the nature of the damage, so the ratios of damaged to undamaged state may be greater or less than 1. This creates inconsistency in results. Such cases should be dealt separately and should not be compared together as some damage may reduce the energy harvested bringing the ratio lower but has higher severity of damage.

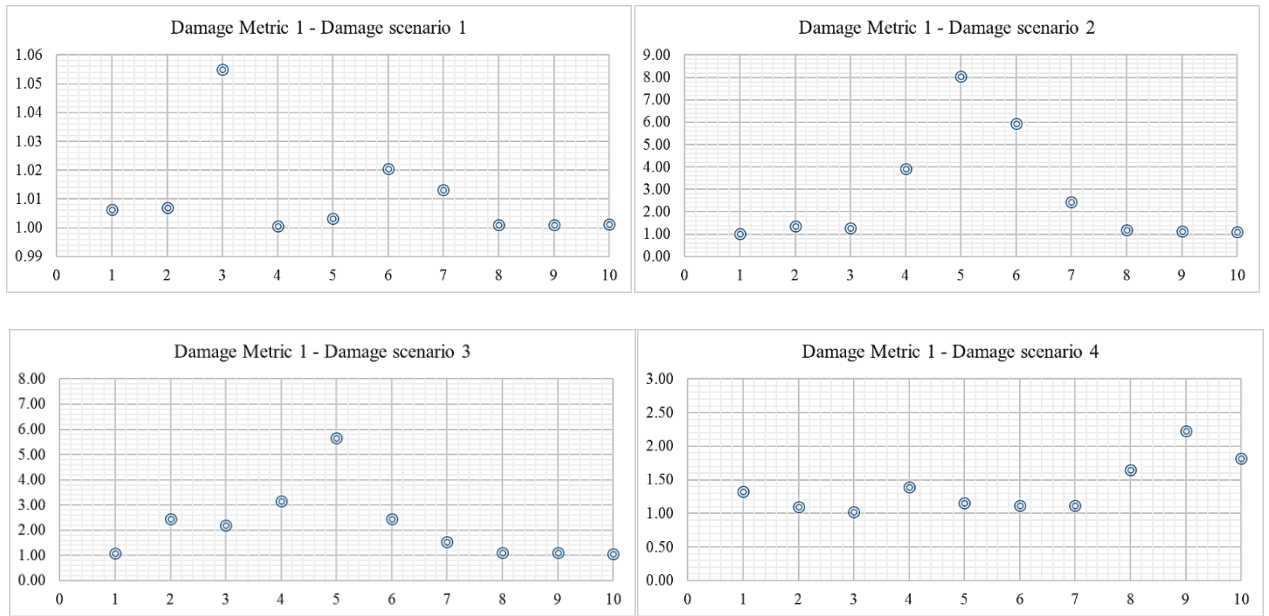


Figure 4. 13: Damage Metric 1 results for all damage scenarios of PSCB

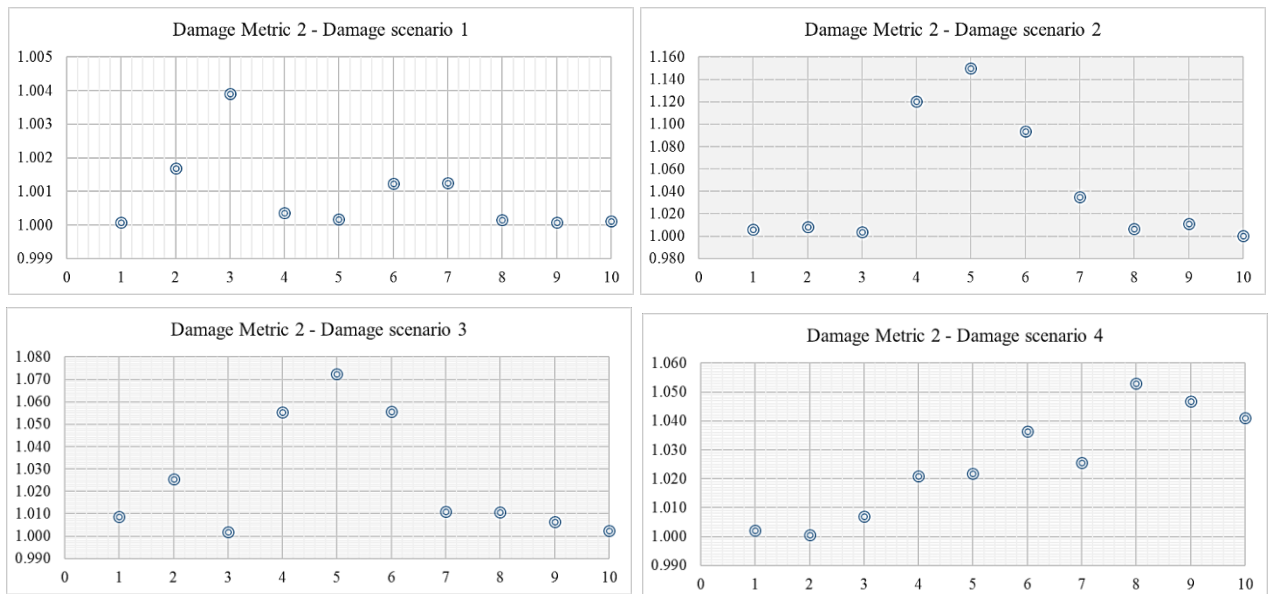


Figure 4. 14: Damage Metric 2 results for all damage scenarios of PSCB

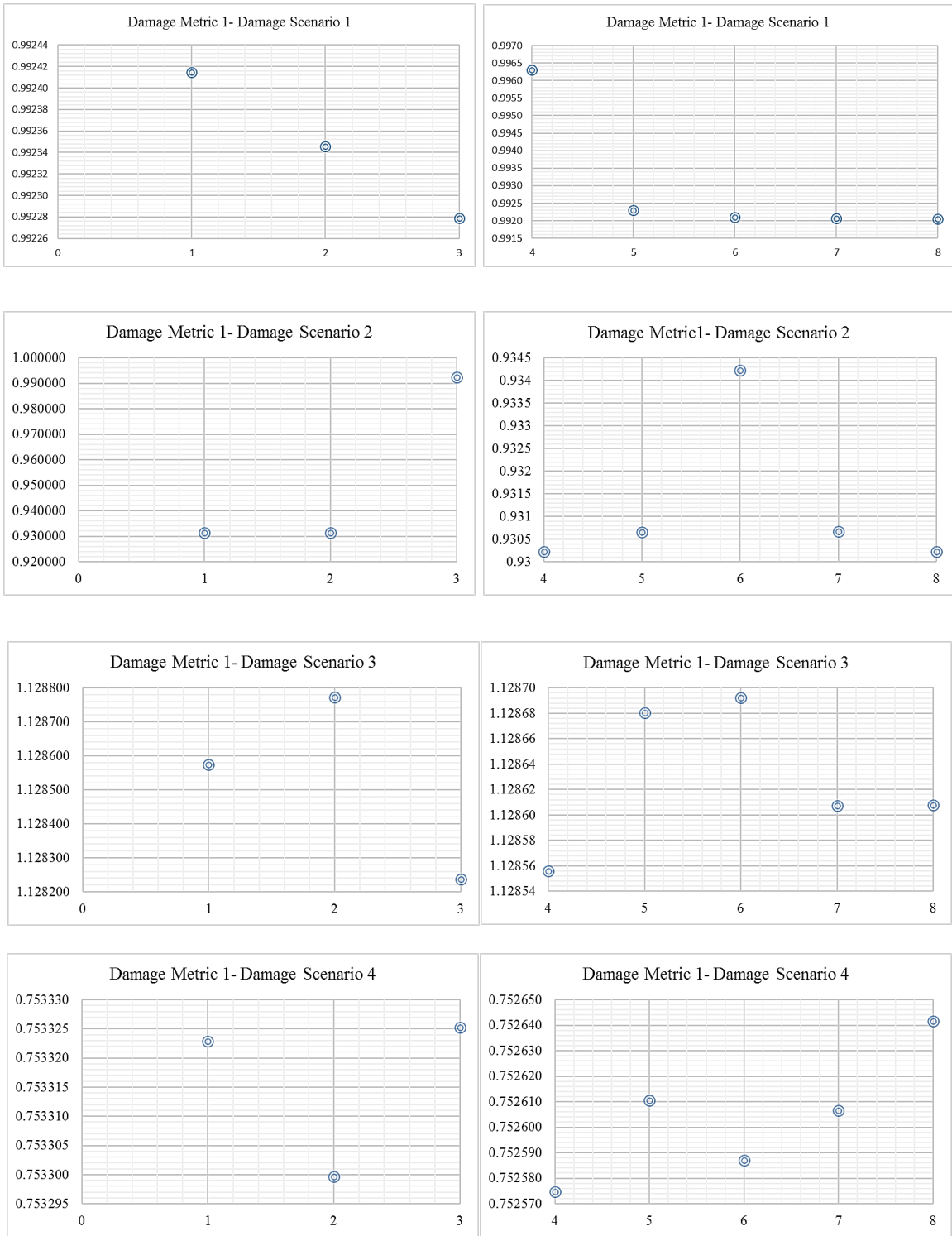


Figure 4. 15: Damage Metric 1 results for all damage scenarios of truss bridge

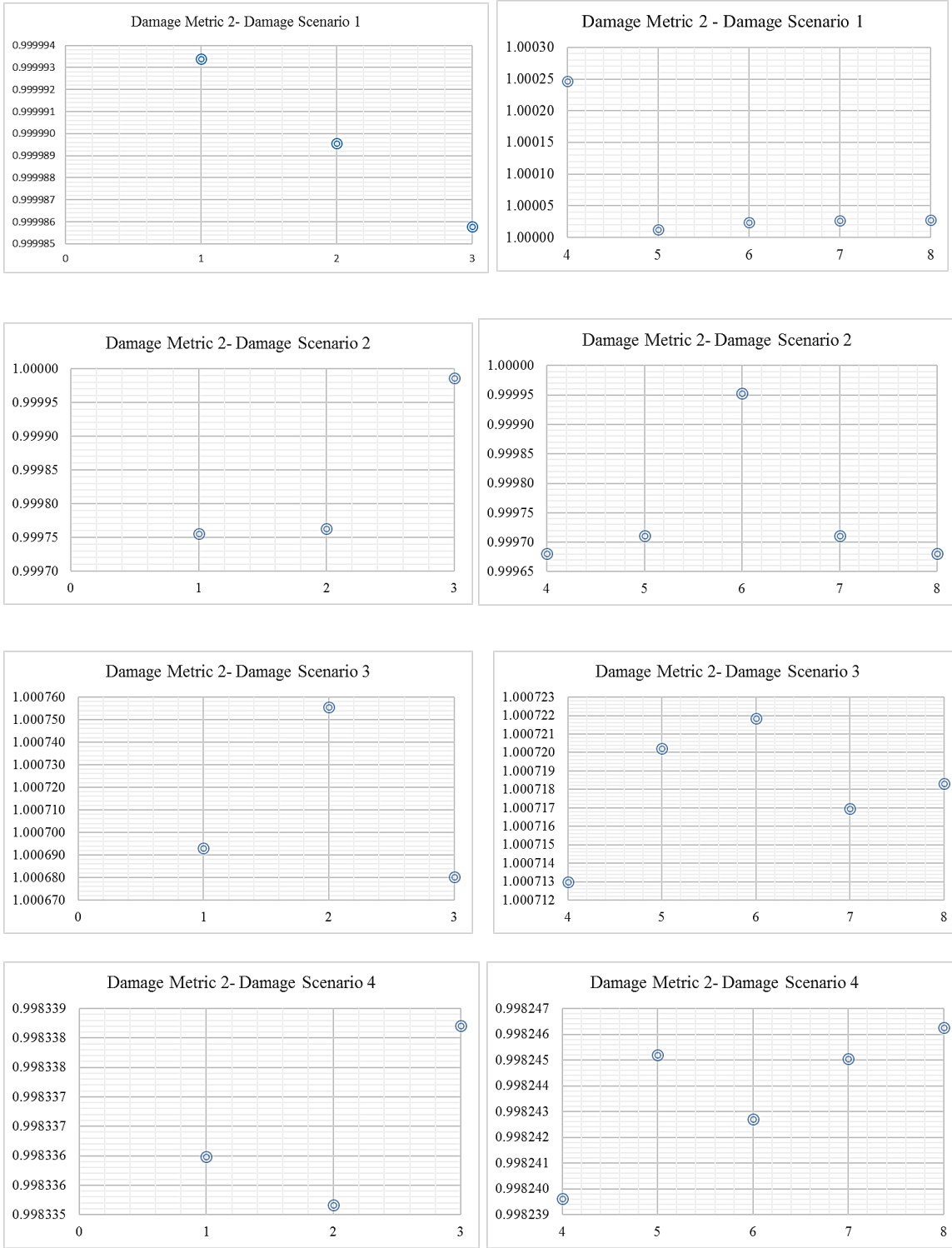


Figure 4. 16: Damage Metric 2 results for all damage scenarios of truss bridge

The truss bridge harvesters are considered in two segments: harvesters on cables and deck. Cables are axial members and deck is a slender member viable to bending. This difference in behaviour changes the energy harvested in different ways with respect to the undamaged condition of the bridge. Thus, they are assessed separately. Harvesters 1,2, and 3 are on the cables as shown in Figure 4.12; the rest of the harvesters 4,5,6,7,8 are on the deck. The damage metrics for all the harvesters are presented under all the damage conditions. Damage metric 1 is shown in Figure 4.15 and damage metric 2 is in Figure 4.16.

4.7. Discussion

The results of the case study presented in this chapter demonstrates the viability of the proposed damage detection technique using the amount of energy harvested for powering wireless sensors using vibration-based energy harvester utilizing induction motor or linear generator. The aim of this analysis is to validate the proposal of using energy harvesters as damage detecting sensors to increase robustness of the monitoring system along with its existing role of extending the life of the wireless monitoring network by replacing batteries with energy harvesters. The harvesters are assessed for authenticating the sensor data and detecting sensor faults. Vibrational energy harvesters based on electromagnetic induction are used for this study as they are capable of harnessing low frequency vibrations from civil engineering structures like bridges.

Two damage metrics are assessed for investigating the efficacy of this method. Damage Metric 1 is the ratio of the total energy harvested and Damage Metric 2 is the kurtosis of the harvested energy distribution curves between the undamaged and damaged states of the

structure. Different damage scenarios are introduced for verifying the robustness of the proposed method. Some damages are near to the harvesters whereas some are located away from them. Table 4.2 and Table 4.3 show the harvesters nearest to the damage and obtained damage detection results for PSCB and truss bridge respectively. The harvesters are mentioned in decreasing order of damage. Figure.4.17 displays the variation of damage metrics for the energy harvesters under all the damage scenarios. The occurrence of peaks is visible for some harvesters. These peaks indicate the damage location for that damage scheme.

Table 4. 2: Comparison of damage metric results for PSCB

Damage scenario	Harvesters nearest to damage	Harvesters detected by Damage Metric 1	Harvesters detected by Damage Metric 2
1	3, 2	3	3, 2
2	5, 4	5,6,4	5,4,6
3	4, 5	5,4	5,4,6
4	9, 10	9, 10, 8	8, 9, 10

Table 4. 3: Comparison of damage metric results for truss bridge

Damage scenario	Harvesters nearest to damage	Harvesters detected by Damage Metric 1	Harvesters detected by Damage Metric 2
1	4,1	4,1	4,1
2	6,3	3,6	3,6
3	2,5	2,6,5	2,6,5
4	8	3,1,2,8	3,1,2,8

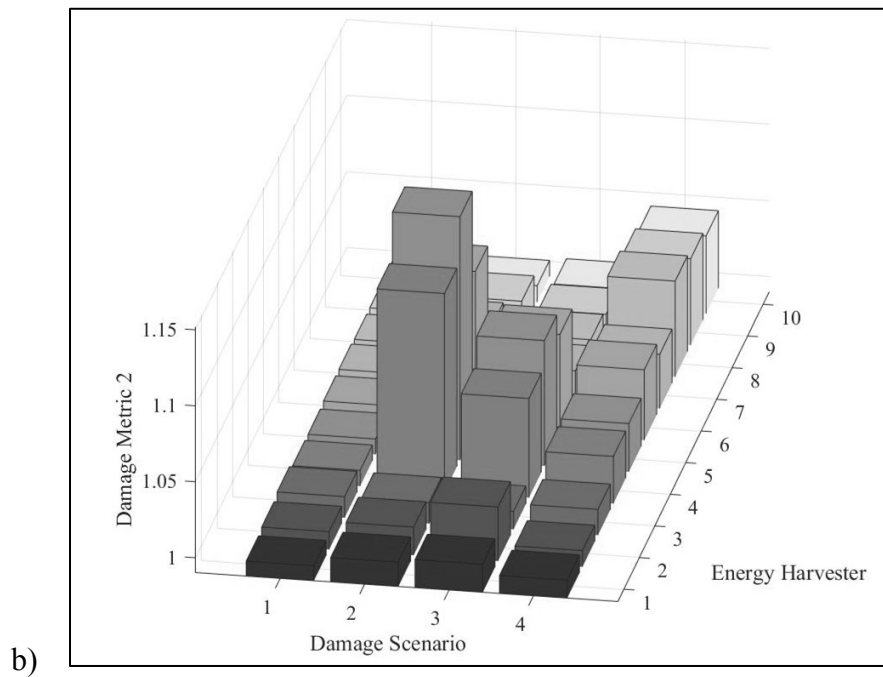
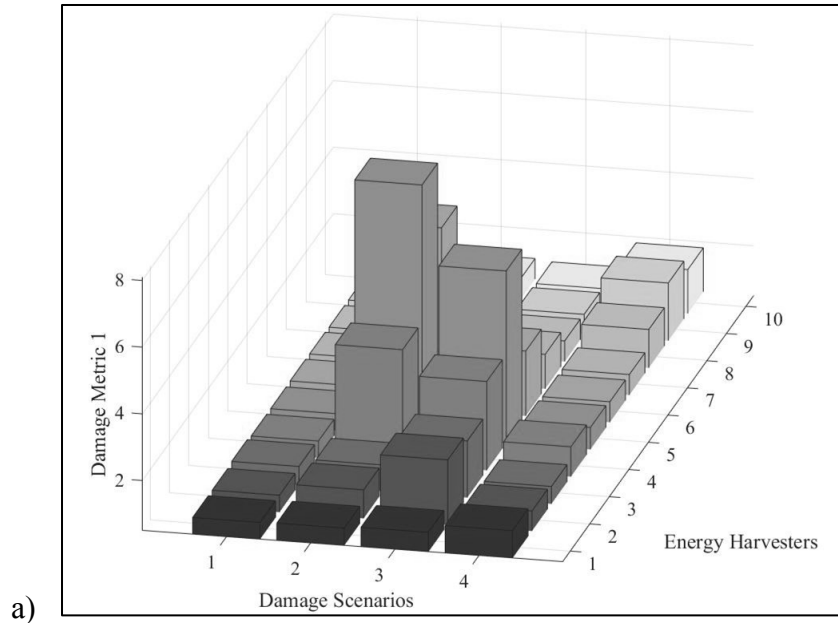


Figure 4. 17: Variation of a) Damage Metric 1; b) Damage Metric 2 under all the damage scenarios for PSCB

For damage scenario 1, the damage is located in the third span near harvester 3. Expected results should show maximum damage in harvester 3 and then harvester 2. Metric 1

identified harvester 3 accurately but could not detect effects of damage in 2 distinctly. Metric 2 is effective in precisely detecting harvester 3 and then harvester 2 in order of damage extent. In damage scenario 2 results, the damage is expected to affect harvesters 4 and 5 the most; as the damage is created in the 8th span where they are considered to be installed. Both the damage metrics denote harvesters 4 and 5 as damaged along with harvester 6 as well. It is quite possible because harvester 6 is located in the adjacent span and is expected to suffer the damage. However, metric 2 identifies damage more precisely than metric 1 showing the correct order of damage extent. Damage scenario 3 is in the sixth span where no harvesters are located. This damage is generated with an intention to study the effectiveness of this method for such cases. Metric 1 pointed out 5 and 4 harvesters but the damage extent order is not correctly assessed. Metric 2 highlighted harvesters 4, 5 and 6 also with not truly representing the extent of damage from location point of view. Although, it localized the damage accurately to some extent. Damage scenario 4 is set up in the sixteenth span but closer to the support connecting the adjacent span. So, it is expected to attain higher damage in sensor 9 and then sensor 10 based on the distance from the damage. Metric 1 correctly determined the damage locations for harvesters 9 and 10 adding susceptibility to harvester 8 also. Metric 2 also identified harvester 8,9,10 but the localization order is not as expected.

Based on this analysis, it can be deduced that damage metric 2 is effective for cases when the harvester is very close or adjacent to the damage. Its sensitivity decreases as the damage distance increases. However, the damage metrics could localize the damage accurately to some extent to detect the vicinity of damage. More damage sensitive features and further signal processing tools can enhance this damage detection process. The aim of this study

is to validate the concept of using energy harvesters as fault detectors and it proves to serve this purpose satisfactorily. For a more coherent explanation of obtained results, the first mode shape of the bridge is examined. Figure 4.18 shows the first bending mode of PSCB bridge in SAP 2000.

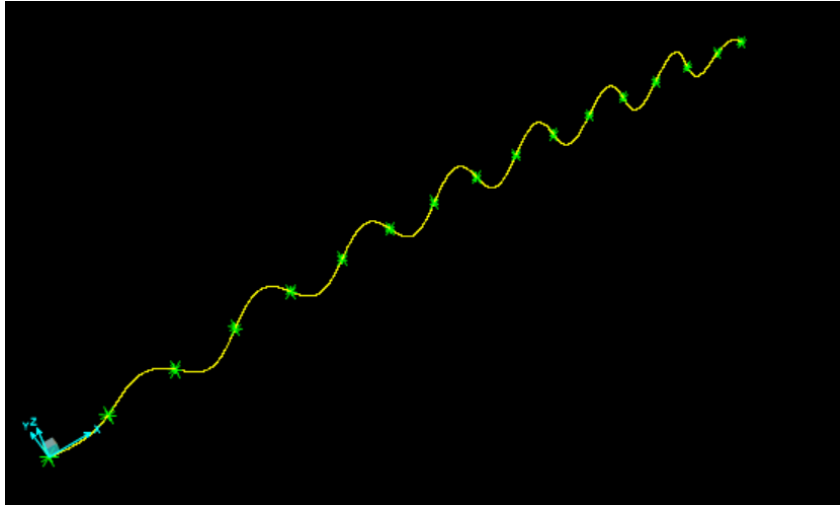


Figure 4. 18: Bending mode 1 of PSCB bridge in SAP 2000

From this mode shape figure, it is observable that for damage scenario 4, harvester 8 undergoes more displacement than harvester 10. Since, it is relatively closer to the damage compared to other harvesters, its effect is captured in the damage metrics. Similarly, for damage case 2 and 3, harvester 6 shows orderly displacement as harvesters 4 and 5. Therefore, the damage metrics are responsive to harvester 6.

Moving on to the case of the steel truss bridge, which is common for railway bridges is investigated for viability of damage detection by energy harvesters' method. 8 energy harvesters are deployed on the deck and cable for 4 damage scenarios. Damage is created by reducing the cross section area by 20% at the specified location. Figure 4.19 depicts the

variation of damage metrics for the energy harvesters under all the damage scenarios. The peaks have higher damage metric values and locate the damage for that particular case.

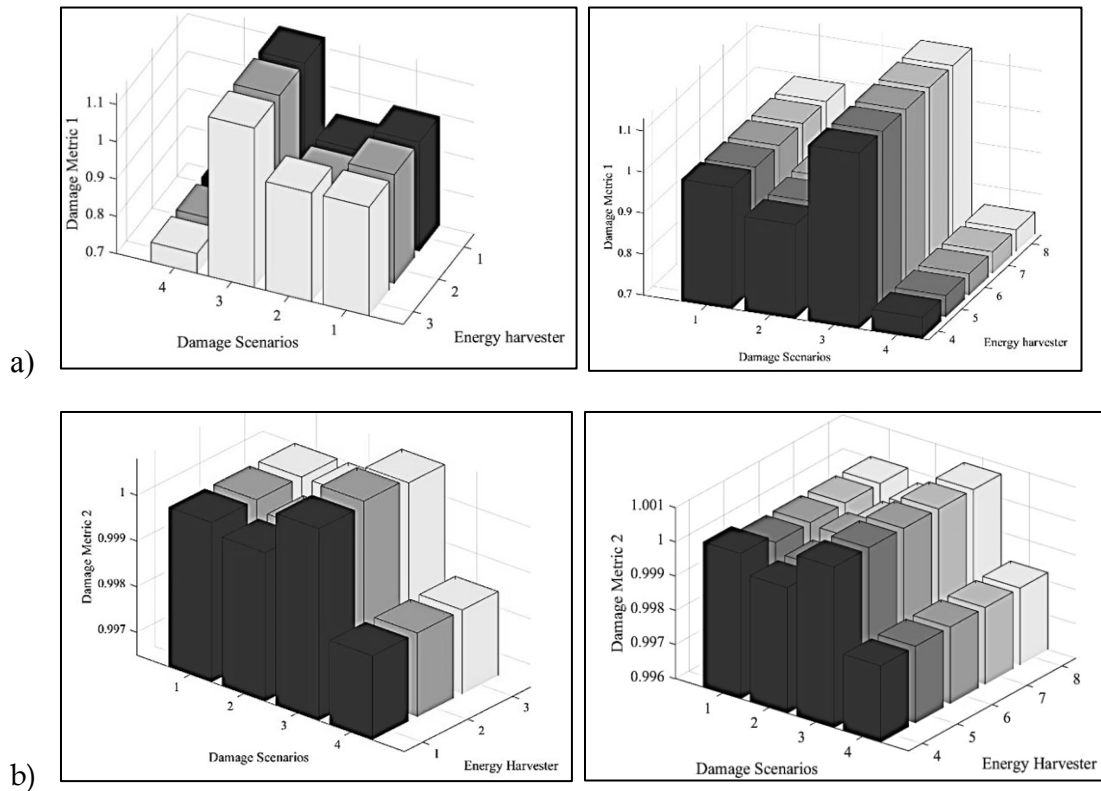


Figure 4. 19: Variation of a) Damage Metric 1; b) Damage Metric 2 under all the damage scenarios for truss bridge

In damage scenario 1, the damage is located on the first span and it should have the most effect that particular span and the connected cable. This is clearly captured by harvesters 4 and 1 by both the damage metrics in the correct order of expected severity. Damage scenario 2 is simulated at the mid span. The harvesters detect the damage by showing highest damage metric 1 and 2 at that span and the connected cable. But the cable possesses higher damage metrics than the span. Damage scenario 3 is generated at the cable with harvester 2 attached to it. Both the damage metrics showed the same results detecting

highest damage at harvester 2. They also showed damage at the adjacent span and the directly attached span. The last damage scenario is simulated to study the effect of distance on harvester's damage detection ability. Damage scenario 4 is at the end cable next to harvester 8. Both the damage metrics showed harvester 8 has the most damaged among the harvesters on the deck but all the harvesters located on the cables showed higher damage than harvester 8. This might be a result of different structural behaviours of different members and that is why it is a good practice to group different structural elements together and then perform this analysis.

To sum it up, the damage detection method proposed and evaluated in this chapter is effective in damage localization but other methods need to be incorporated to increase its efficacy and damage precision. More statistical features sensitive to such damages and pattern recognition techniques like neural networks, genetic algorithms accompanied with machine learning algorithms are potential candidates for further research to achieve better structural health diagnostic results.

4.8. Summary

A novel damage detection method using energy harvester is proposed and tested in this chapter. The energy harvesters powering wireless sensors for structural health monitoring is investigated to be used as a damage detector for structural and sensor faults. Linear generators working on the principle of electromagnetic induction are deployed on Pre Stressed Concrete Box bridge and Warren steel type bridge under different damage scenarios and ambient vibration. Damage metrics based on the amount of energy harvested and the pattern of the harvested energy curve are analyzed. The damage detection results

are found to be satisfactory validating the application of this method and adding to higher accuracy of the monitoring system. For more improvement in damage detection results, further research on data mining for sensitive feature selection and better data processing tools can be carried out.

CHAPTER 5: DAMAGE DETECTION BY MARGINAL HILBERT SPECTRUM METHOD

5.1. Introduction

Structural Health Monitoring (SHM) has gained popularity in civil engineering for monitoring the structural condition, detect damage and provide early warnings. With the new construction materials being used and varying loading conditions being created on structures by rising population, structural health monitoring is becoming more critical. Sophisticated sensors installed on structures can project the condition of the structures. Enormous data is collected by these sensors and their processing is very crucial for accurate structural condition assessment. This chapter presents the results of a method of a novel method developed based on Marginal Hilbert Spectrum for analyzing such data and detecting damage or anomaly in structures.

Structural response data from a real structure are usually non-linear and non-stationary in nature. Huang et al. (1998) introduced a new method based on the combination of Empirical Mode Decomposition (EMD) with Hilbert Spectral Analysis (HSA) known as Hilbert-Huang Transform (HHT). Integrating the HHT plot over time generates Marginal Hilbert Spectrum (MHS). The peaks of MHS correspond to the main frequencies of the system. This method preserves the non-linear and non-stationary features of the response data by considering instantaneous parameters while decomposing the response into

Intrinsic Mode Functions (IMFs) by EMD process. It is described in details in Chapter-2 with background and Chapter-3 with methodology. However currently, this method is not applied widely in monitoring civil engineering structures. It is relatively new and hence, this thesis aims to investigate its ability to detect and locate damages. In 2014, a research team under Prof. Buyukozturk at MIT, Cambridge (Ghazi and Büyüköztürk 2014) developed energy preserving curves by this method for locating damages in structures. The proposal involved construction of Normalized Cumulative Marginal Hilbert Spectrum (NCMHS) to obtain a smooth curve which is mathematically easy to deal with and its normalization removes the effect of varying input energies for vibrating the structure Ghazi and Büyüköztürk (2015). The entire process is shown in Fig. 5.1.

This chapter tests the non-linear energy curves proposed by Ghazi and Büyüköztürk (2014) along with some new curve metrics proposed in the present thesis. The method developed by Ghazi and Büyüköztürk (2014) has been studied using the vibration response of a simply supported beam and a three-storey frame. While the vibration response of both the structures has been generated numerically, the response of the frame is also generated experimentally at the Structures Laboratory at Concordia University. The Damage Indices suggested in Ghazi and Büyüköztürk (2014), including those which were not validated by them have been computed using the vibration data in the present study to determine their applicability and validity. DI labelled in the flow chart above indicates Damage Index and are explained in Chapter-3. IMFs are plots of the signal decomposed in such a way that at the same time instant, no two IMFs will contain the same frequency. The integration of the square of their amplitude over time provides energy of that IMF. The pattern of energy distribution for IMFs changes under damage scenarios and this leads to DI_1 and DI_2 . The

MHS represents amplitude variations corresponding to main frequencies of the structure which shift when subjected to damage and MHS captures them effectively as they preserve the energy and time locations of the response signal. This phenomenon is used for DI_3 . The next curve is NCMHS which changes its pattern and is distinct in case of damage and healthy states of the structure. This is incorporated in DI_4 .

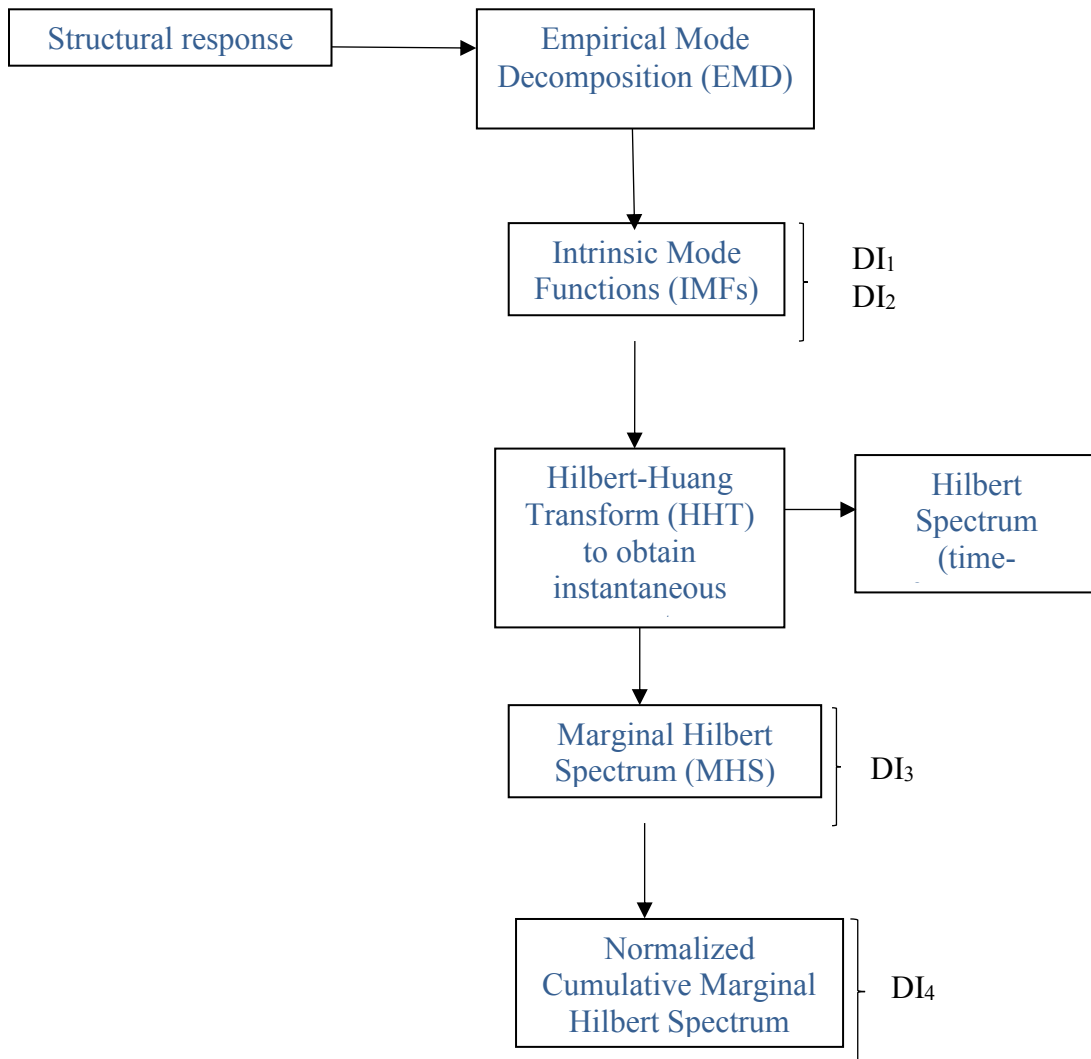


Figure 5. 1: Damage detection flow chart by Marginal Hilbert Spectrum (MHS)

Investigation of effectiveness of these DIs is carried out in the next sections. Experimental data is best suited for such study as it has non-linear and non-stationary features. Two case studies are developed to test this method. The first is a three-storey steel bookshelf frame structure and the other is a software simulation of simply supported beam whose experiments are to be performed at CBRI, India.

5.2. Description of the structures and data acquisition

Firstly, a simply supported beam model is utilized to test the relatively new HHT method for detection of simulated damages. A steel beam of 1200 mm length with cross section 75mm x 8mm is modelled in SAP 2000. The tests are to be carried out at CBRI, Roorkee, India and this is a preliminary study for the same. Three sensors are located at 300 mm apart from each other. White Gaussian Noise (WGN) is applied as ambient vibration. The SAP 2000 model is shown in Figure 3.14. The first three mode shapes of the beam are in Figure 5.2. Damage is simulated at different locations and is identified by HHT method in the following sections.

Since, experiments generate true non-linear and non-stationary data, they are more appropriate for this study. For this reason, an experiment is conducted at Concordia University, Montreal. A steel frame structure consisting of three racks or levels is fixed to the ground by setting the base with concrete. G-Link wireless accelerometer sensors are placed on each level i.e. total 3 sensors for data acquisition. Structure details and sensor information details are provided in Chapter-3. Figure 5.3 shows the picture of wireless sensor used. The green light remains constant during data collection and data sending process. It blinks while it is turned on but inactive and is off when the sensor is off.

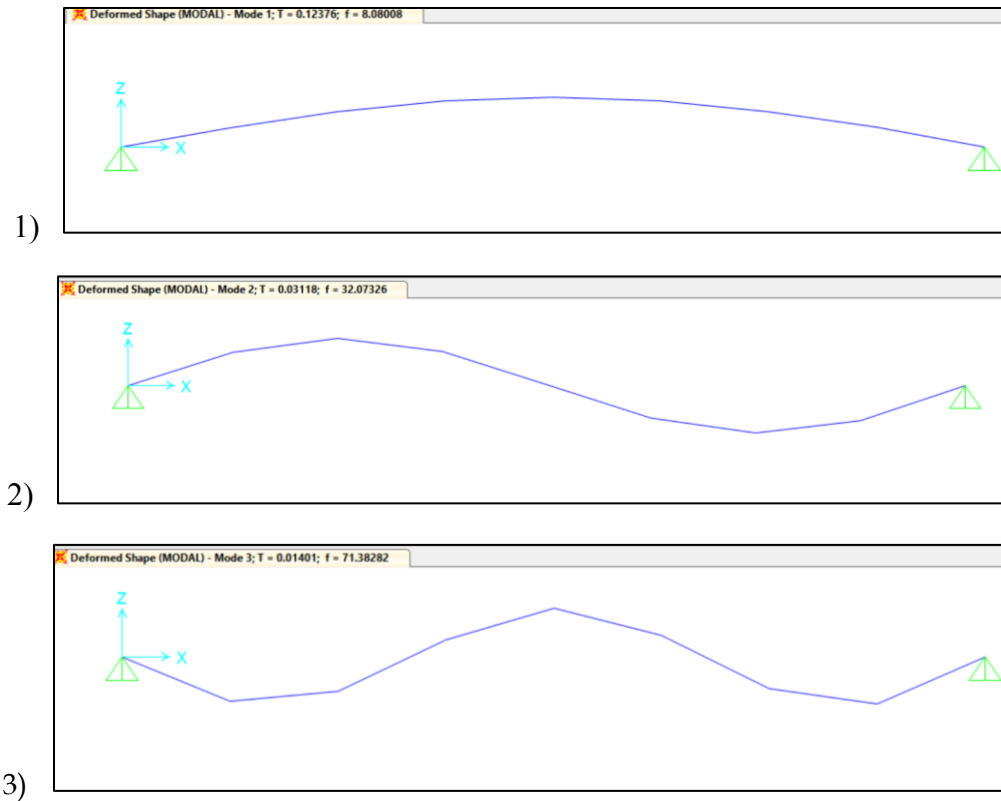


Figure 5. 2: First three mode shapes of the simply supported beam in SAP 2000

Data sampling rate is 512 Hz and data is recorded for approximately 20 seconds but 16 seconds data is analyzed for this study. Larger data sets need longer time for calculations and increase the computational effort and cost. The frame is struck on the top floor in the longitudinal direction to study the vibration characteristics for all the conducted tests.

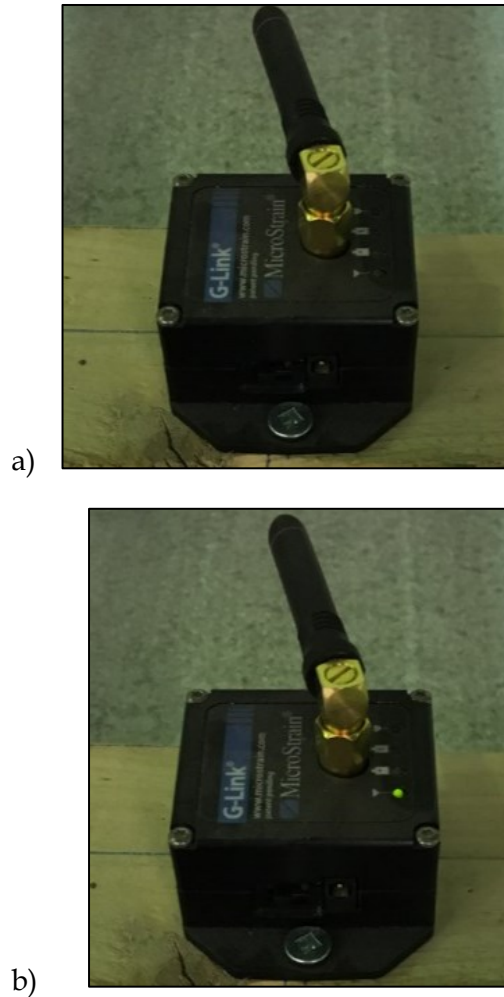


Figure 5. 3: Wireless accelerometer a) turned off; b) data transmission mode

For the purpose of data verification acquired by wireless sensors, the frequencies were compared with SAP 2000 model of the frame structure. The Frequency Domain Decomposition (FDD) of the signal provided the first three frequencies of the frame which are in the same range as that of the SAP 2000 physical modal analysis. The FDD program was developed by Farshchin (2015) and is able to perform modal analysis and calculate the mode vectors. The first 3 mode shapes of the frame in SAP 2000 are shown in Figure 5.4. and the FDD results are in Figure 5.5. Table 5.1 demonstrates comparison of experimental

results with simulation and the experimental data. Considering all these information, the authenticity of the experimental data is thus verified.

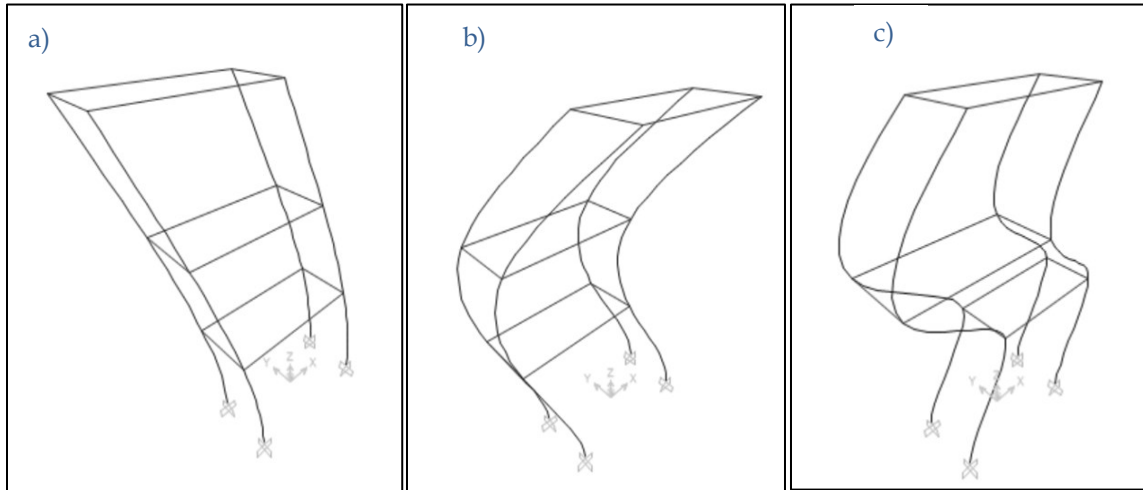


Figure 5. 4: First three mode shapes of the frame in SAP 2000

Table 5. 1: Experimental data verification for frame

Mode number	Frequency by real data	Frequency by SAP 2000 model
1	8 Hz	5.8 Hz
2	37.5 Hz	35.6 Hz
3	94 Hz	94.3 Hz

Only one USB base station is used for data recording and communication with all the three wireless sensors. The data recording mode is data logging. All the sensors are triggered together by Node Commander and the data downloaded after the experiment. The available interaction options include: triggering the nodes, downloading data, viewing/browsing the trigger and erasing the data. The power consumption for data logging mode is 25 mA and

for sleep mode is 0.5 mA. The batteries used are rechargeable Lithium Ions and are recharged using external power charger.

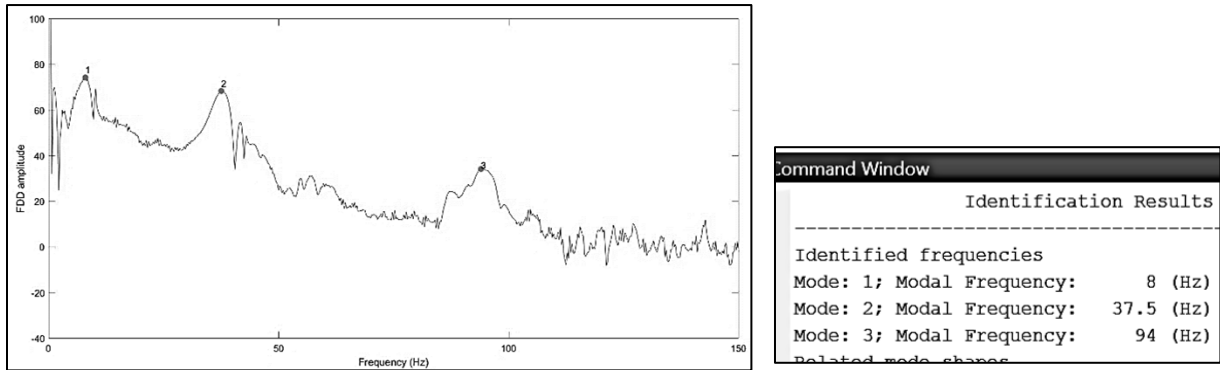


Figure 5. 5: Frequency Domain Decomposition (FDD) results in MATLAB

5.3. Structural response data

The steel simply supported beam is subjected to White Gaussian Noise as ambient excitation and vibration response data is analyzed for 15 seconds. Data is recorded at three nodes under three scenarios: undamaged and damage near sensor 2 and 3 as shown in Figure 3.15. The resultant vibration responses are preprocessed using Equation 3-4 for clearer results after analysis. Vibration responses of all the 3 cases for the node at 30 cm

(Node 1) are presented in Figure 5.6 under undamaged scenario for reference. Damage is simulated in SAP 2000 by reducing the moment of inertia at the marked locations in Figure 3.15 by 20%.

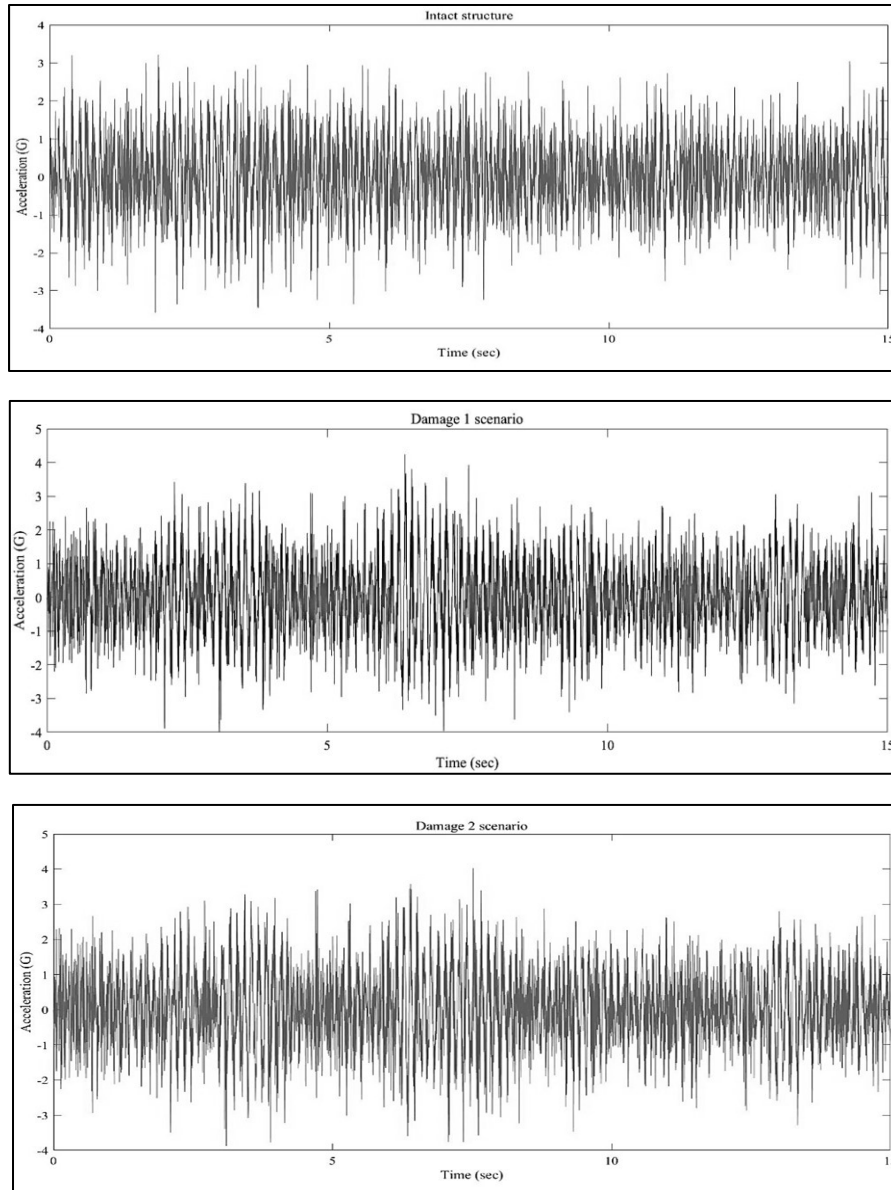


Figure 5. 6: Acceleration response of Node 1 on simply supported beam

For the first experimental case study of frame, response vibration data is recorded for healthy and damaged states. Damage is created by loosening all the four bolts of the rack

or story in which damage is considered. Two such scenarios are considered. One is on the top floor of the rack and second is in the middle or second level of the frame. The data is preprocessed for improving the results by offsetting it with the mean of the distribution. By removing the mean values from the signal data, identification results improve.

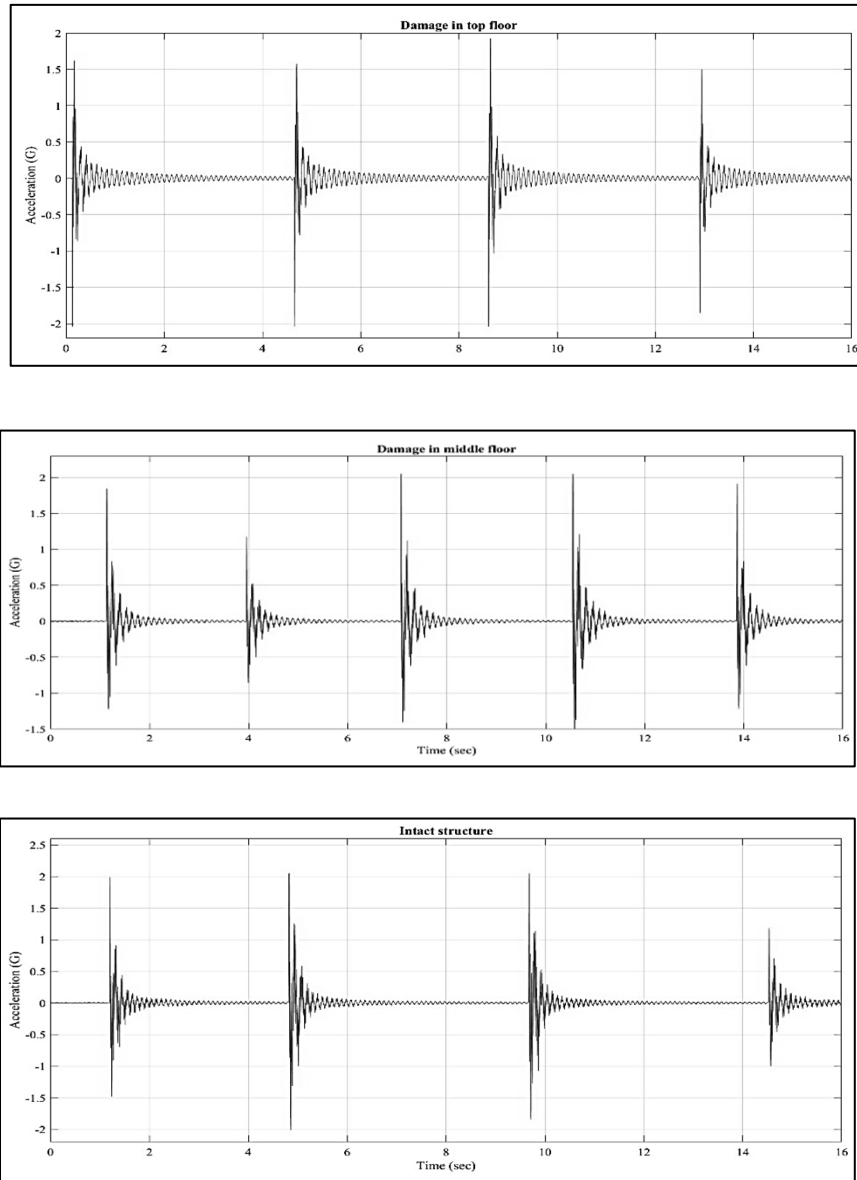


Figure 5. 7: Acceleration response of top floor sensor

There are effectively 3 sets of data: intact structure, damage 1 (in top floor), damage 2 (in second floor). The response data of all the three floors for the three damage scenarios generate nine datasets to be analyzed (3 x 3). Although, average of multiple tests is taken into account for the baseline data of undamaged structure for increased precision in results. Figure 5.7 shows the acceleration response data for the top floor sensor in the three cases: intact structure, damage in top floor and damage in middle floor.

It can be seen that the amplitude of vibration is different in all the cases for the same location. This is due to the varied input force applied for excitation while striking the frame. The high amplitudes are the time location of impacts applied to the structure. The energy curves are normalized during analysis to combat this effect of different energies in the input force to the structural system.

5.4. HHT and MHS plots

This section elucidates the IMFs and their energy plots obtained by EMD of the original signal, HHT plot of the IMFs and MHS. The next section is related to obtaining damage indices from these curves. The first case is the intact or undamaged structure. The plots from the intact state by the Node 1 (30 cm from left) for the beam and the first floor sensor in the frame are provided as follows. Figure 5.8 and Figure 5.9 shows the first five IMFs of the response signal for the node 1 of beam and the first floor sensor of the bookshelf structure respectively.

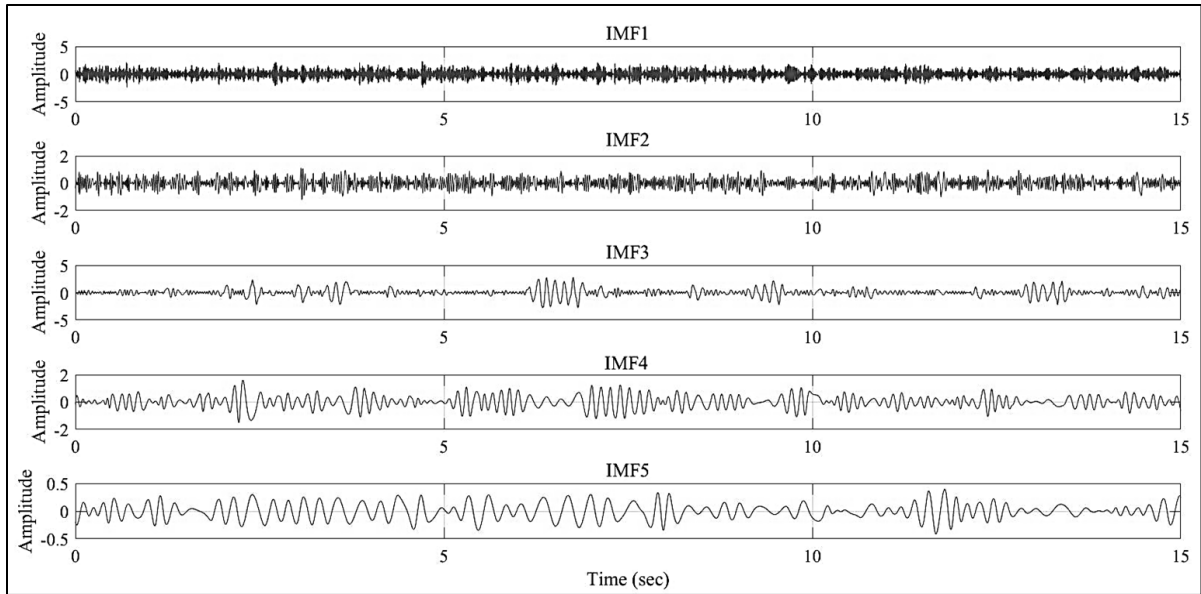


Figure 5. 8: Five IMFs of the Node 1 (30cm from left) sensor data for intact structure

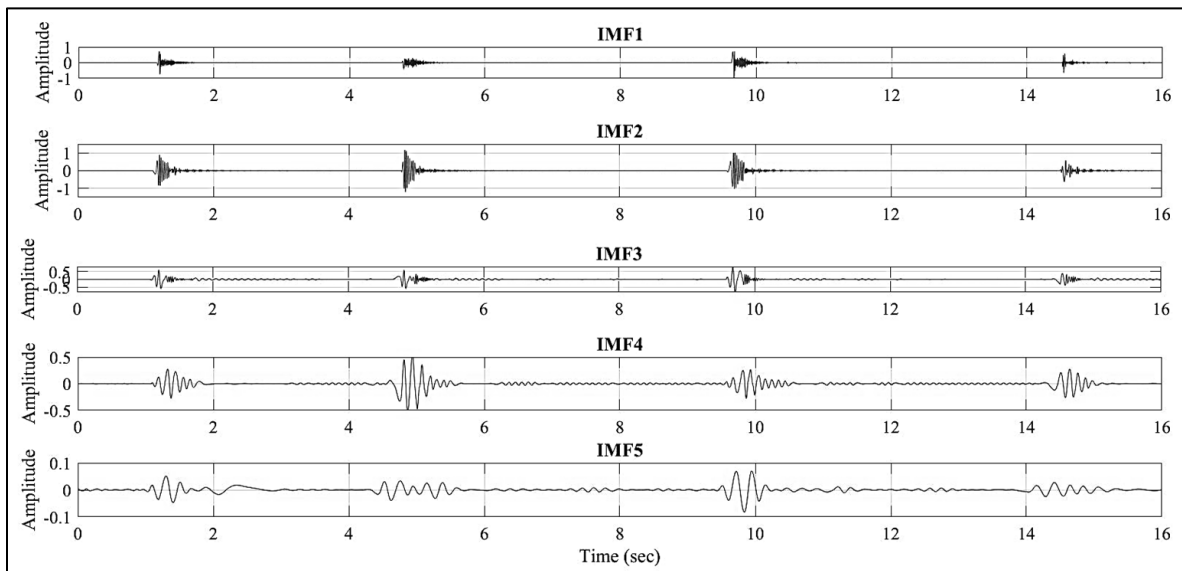


Figure 5. 9: Five IMFs of the top floor sensor data for intact structure

The IMF amplitudes are squared and integrated over time to get the energy contained in them. For removing input energy effects applied during excitation of the structure, they are

normalized by the summation of the data set. Figure 5.10 shows the node 1 and Figure 5.11 presents the first floor intact structure normalized energy vs IMFs plot.

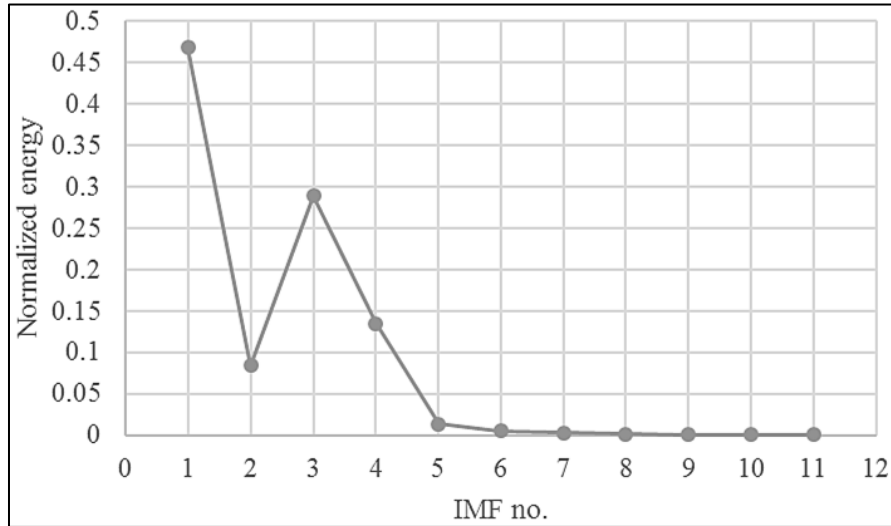


Figure 5. 10: Energy distribution with IMFs for Node 1 intact simply supported structure

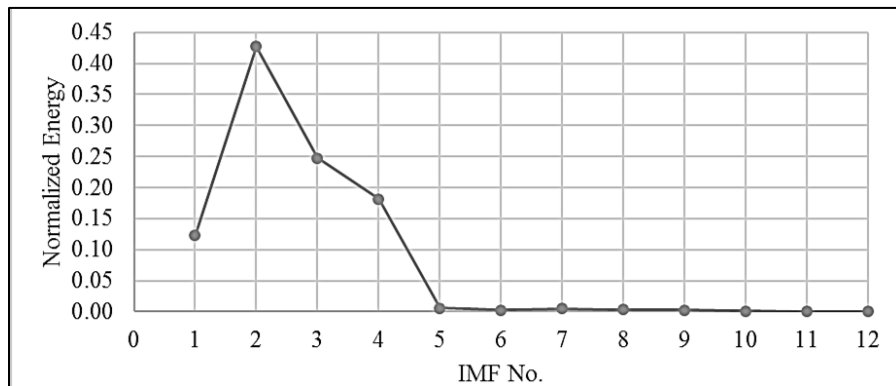


Figure 5. 11: Energy distribution with IMFs for first floor bookshelf intact structure

Application of Hilbert transform to the IMFs provide its instantaneous parameters. The frequency-amplitude plot of the response signal with respect to time instants known as Hilbert-Huang Transform (HHT) plot is demonstrated in Figure 5.12 for the bookshelf

frame structure. The time-frequency-amplitude content of the response signal can be clearly noted in this HHT plot.

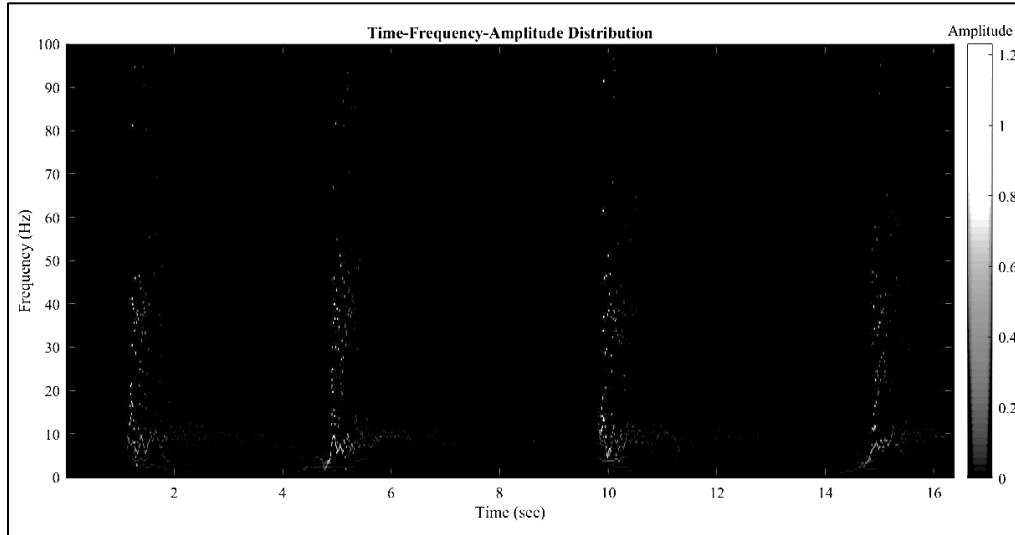


Figure 5. 12: HHT plot for first floor intact bookshelf structure

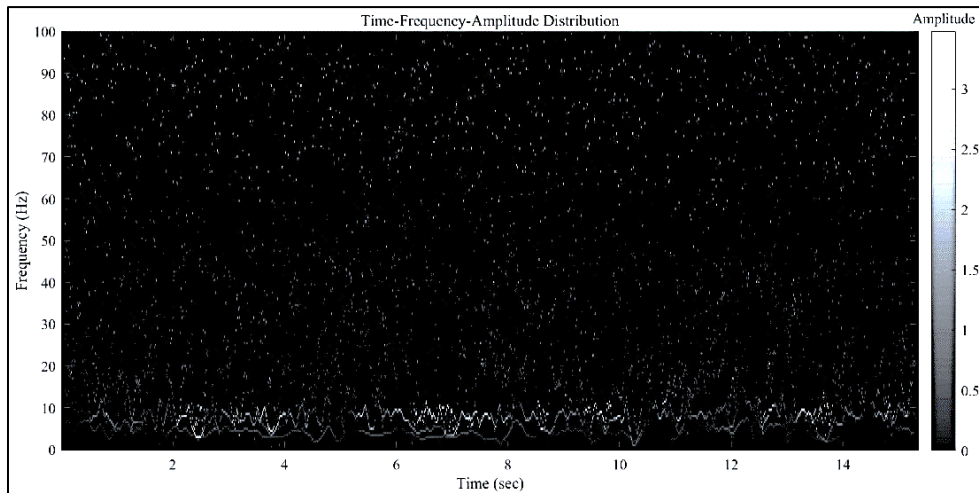


Figure 5. 13: HHT plot for Node 1 (30cm) on simply supported beam

The HHT plot for Node 1 on simply supported beam is presented in Figure 5.13. The WGN is synthetically generated comprising of various frequency contents and it can be observed in this HHT plot.

Marginal Hilbert Spectrum is measure of amplitude contribution from each frequency value. It is cumulative amplitude over the distribution in a probabilistic sense. The MHS plots for the Node 1 and the first floor intact structure are in Figure 5.14 and 5.15 respectively. In both the plots, the main frequencies are correctly identified and have been shown by ticks. The next plots are normalized MHS which remove the effect of the different input forces for clear identification of change in energy solely contributing from vibrating modes. The normalized MHS plots for Node 1 of simply supported beam is shown in Figure 5.16 and for first floor bookshelf in Figure 5.17. Both are in undamaged state of the structure.

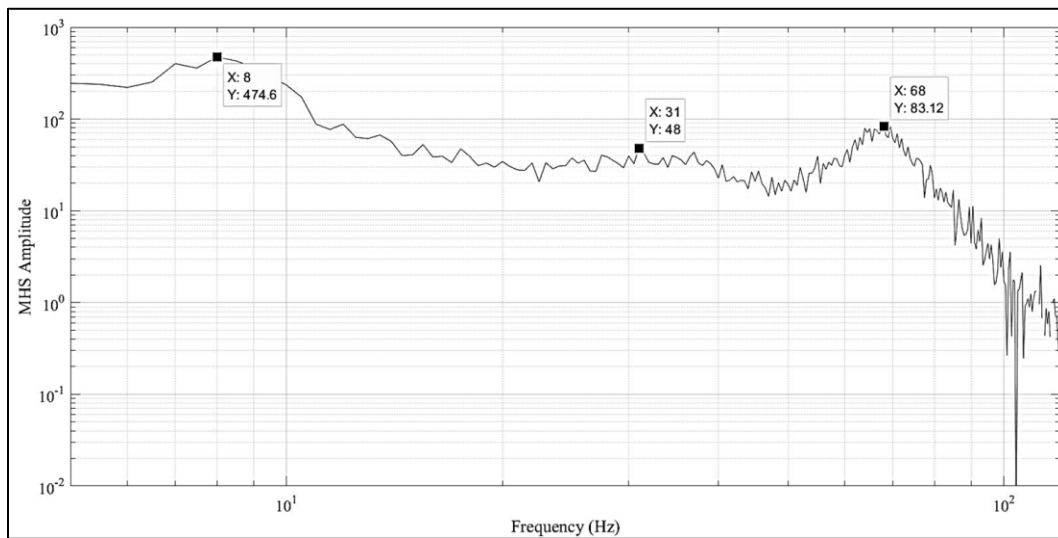


Figure 5. 14: MHS plot for Node 1 intact structure

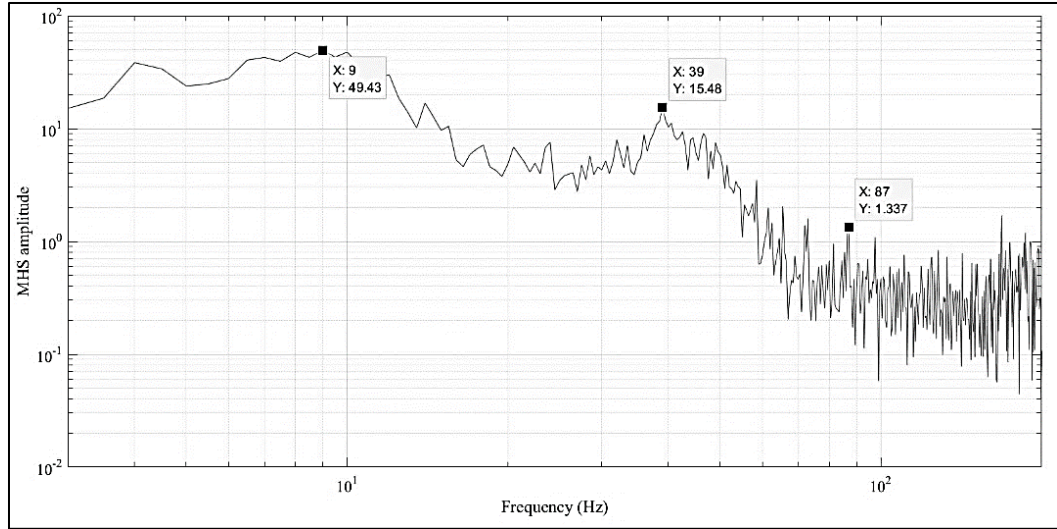


Figure 5. 15: MHS plot for first floor intact structure

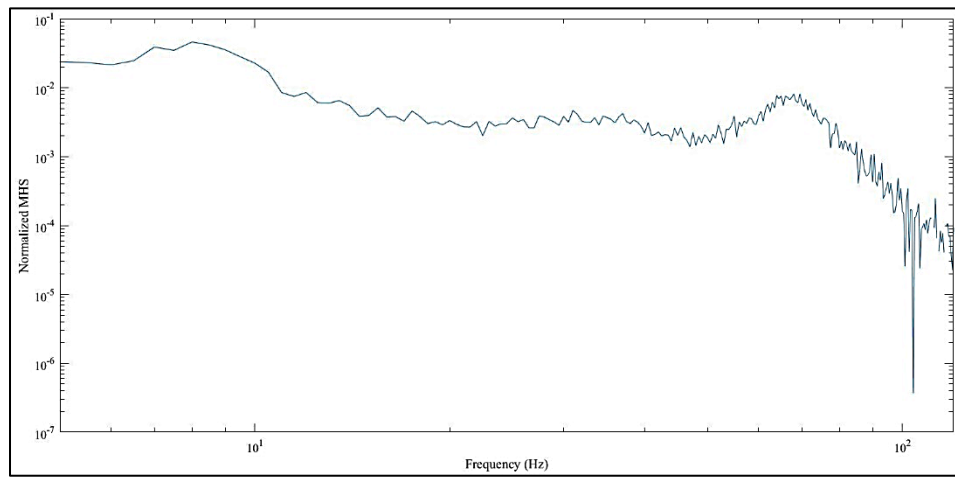


Figure 5. 16: Normalized MHS plot for Node 1 intact structure

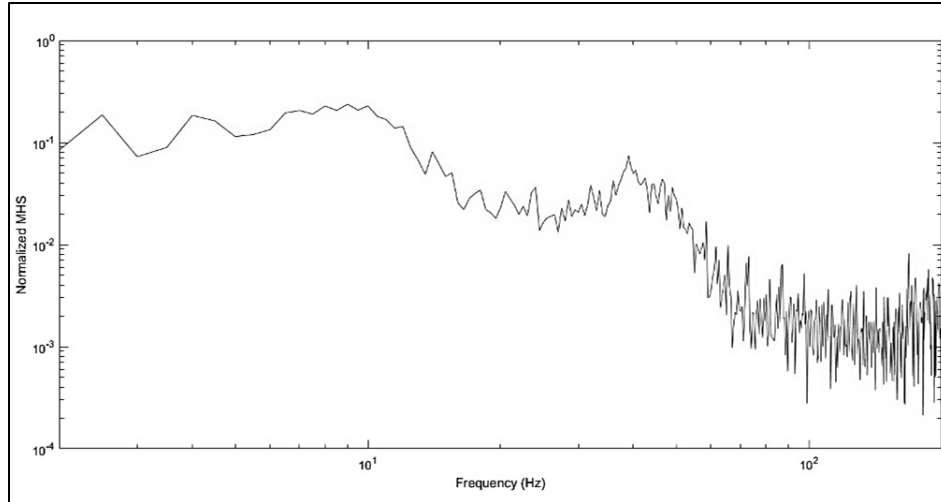


Figure 5. 17: Normalized MHS plot for first floor intact structure

The cumulative function smoothens the MHS curve and normalizing its cumulative sum maintains consistent input energy in the structural system. This is done for mathematical convenience as proposed by Ghazi and Büyüköztürk (2014) at the MIT. NCMHS plot of Node 1 intact simply supported beam structure is shown in in Figure 5.18 and for first floor intact structure is presented in Figure 5.19.

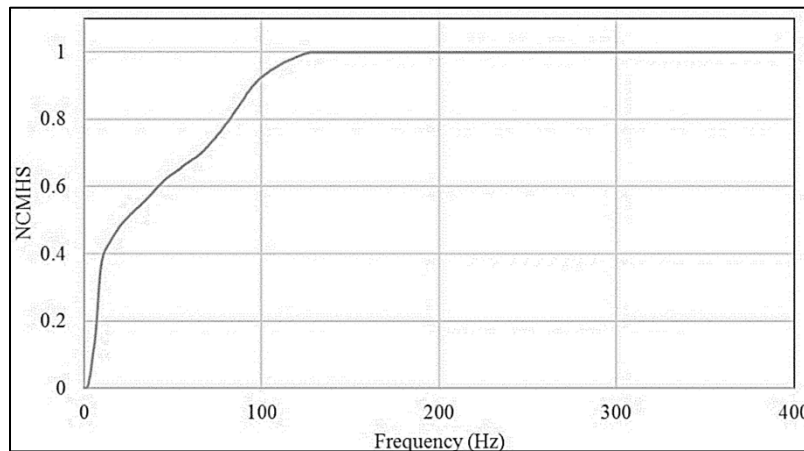


Figure 5. 18: Normalized Cumulative MHS (NCMHS) plot for Node 1 intact beam

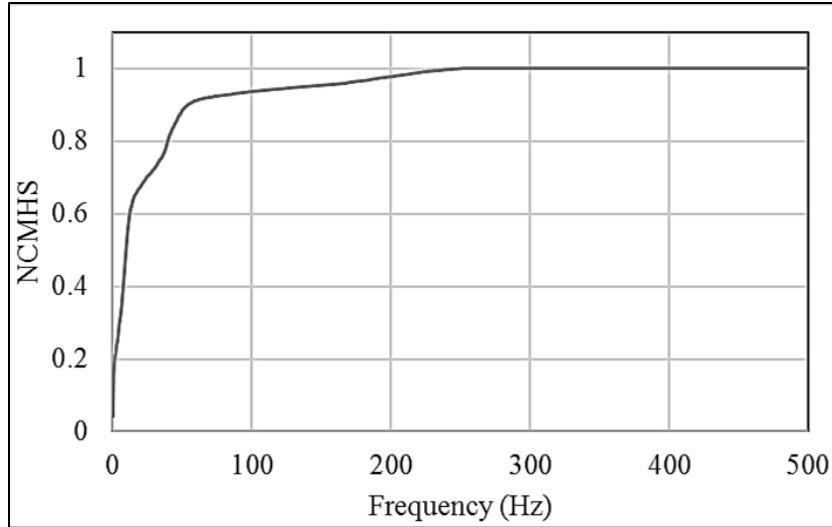


Figure 5. 19: Normalized Cumulative MHS (NCMHS) plot for first floor intact structure

All these curves are plotted step-wise to demonstrate the procedure for obtaining them using experimental data of frame structure. However, for damage detection indices, not all plots are to be used. Normalized energy vs IMFs distribution, normalized MHS and NCMHS plots are analyzed for damage localization which is explained elaborately in the following section.

5.5. Damage Detection

The first case study considered for damage detection is the simply supported beam. The two damage cases are damage 1- near the support (node 3) and damage 2- near the centre (node 2) of the beam. Figure 3-15 provides the exact picture of damage locations created by reducing the moment of inertia of the beam in SAP 2000. The second case study is experimental data set from the steel bookshelf structure. It involves two damage scenarios by loosening the bolts at first floor and second floor. This section analyzes the curves for both the cases to investigate the application of EMD and HHT for damage detection in civil

engineering structures. It is assumed that the first damage scenario is damage on first floor and the second on the second floor. The data will be compared with the healthy structure state calculating DI_1 and DI_2 .

$$DI_1 = \frac{kurtosis(Energy_{undamaged})}{kurtosis(Energy_{damaged})} \quad (5-1)$$

$$DI_2 = \frac{skewness(Energy_{undamaged})}{skewness(Energy_{damaged})} \quad (5-2)$$

Figure 5.20 and Figure 5.21 show the normalized energy vs IMF damage detection curves for both the structures considered. Their damage indices 1 and 2 are displayed in Figure 5.22 and Figure 5.23. For the bookshelf structure, the 1st floor is the top floor, 2nd is the middle and 3rd floor is near the base. For the simply supported beam, Node 1 is at 30 cm from left support, Node 2 is at 60 and Node 3 is at 90 cm from the left support.

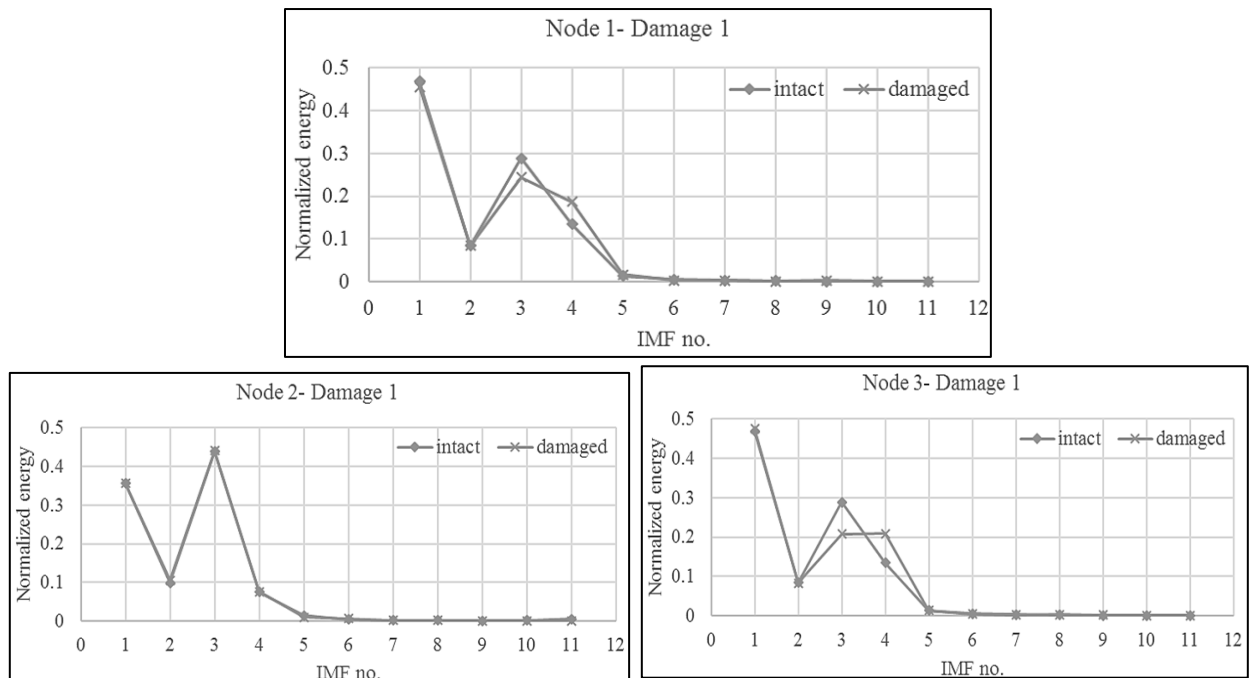


Figure 5. 20: Normalized energy vs IMF number curves for damage near Node 3

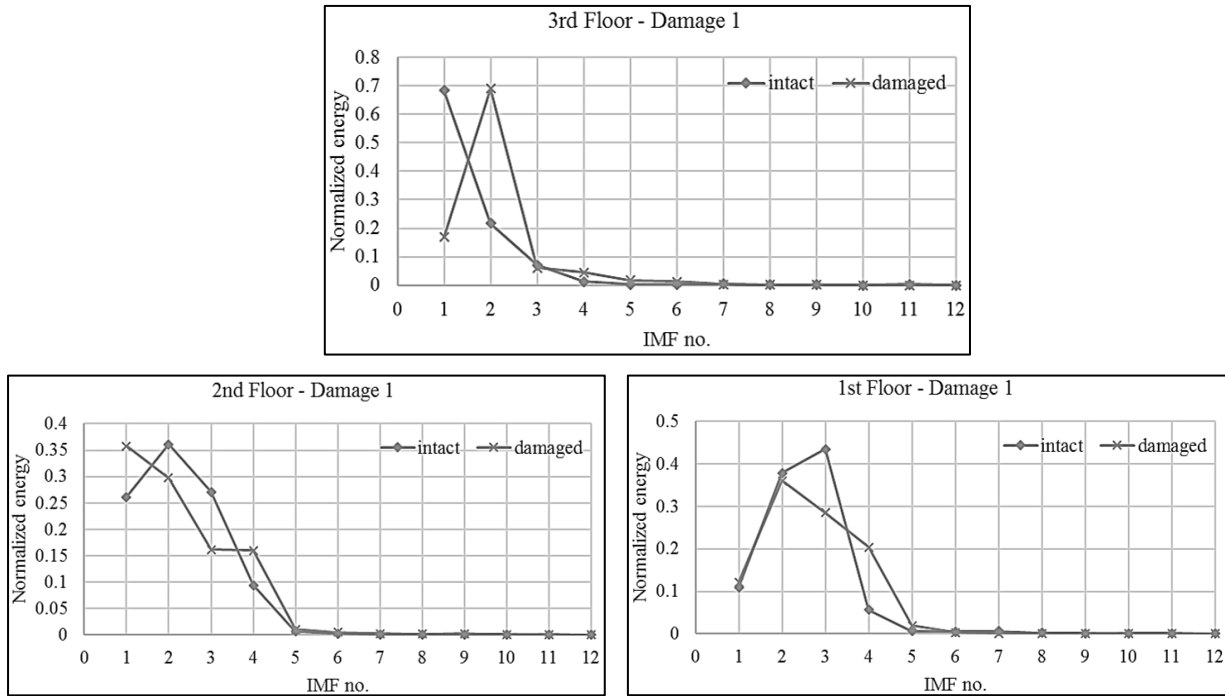


Figure 5. 21: Normalized energy vs IMF number curves for damage in top floor of bookshelf frame structure

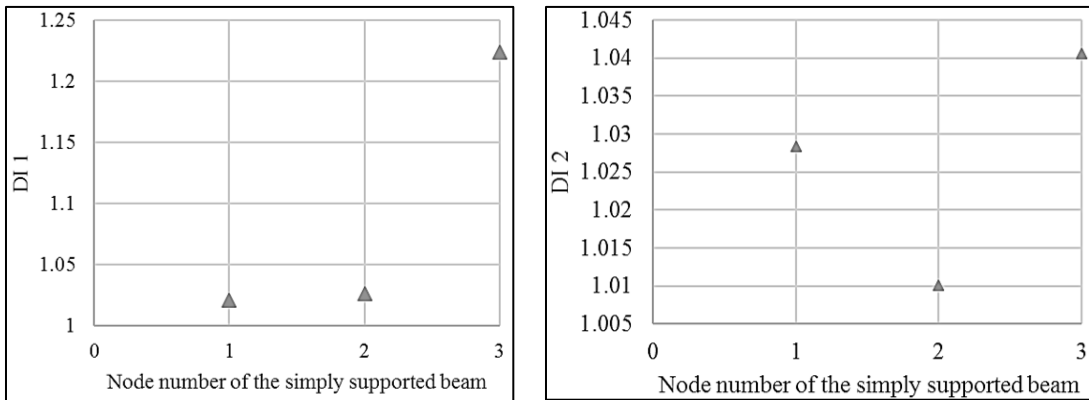


Figure 5. 22: Damage indices plots for damage near node 3 of the beam

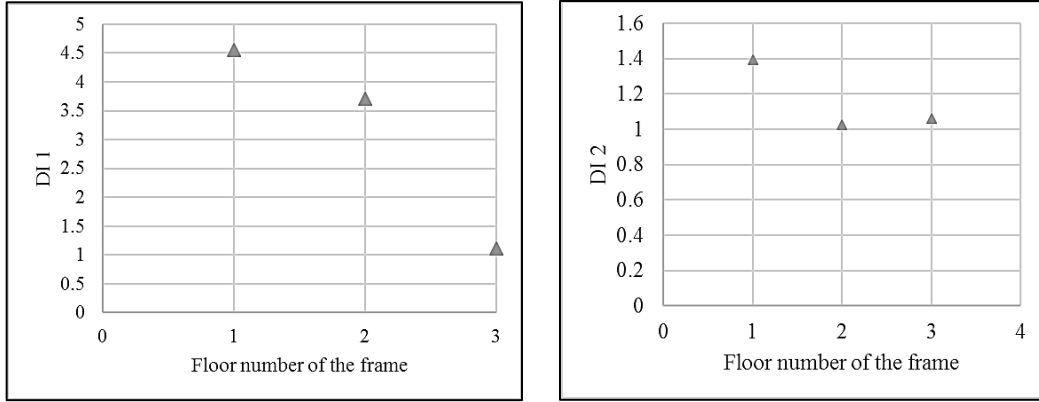


Figure 5. 23: Damage indices plots for damage in top floor of bookshelf

The top floor damage of the frame and the node 3 proximity damage in the beam is correctly localized by the first 2 DIs from normalized energies of IMFs. The next curve is the Normalized Marginal Hilbert Spectrum (NMHS) and the Damage Index related to it is DI3. Its analysis is presented here. The NMHS plots for both the case studies followed with their Damage Indices results are as follows.

$$DI_3 = \frac{kurtosis(NMHS_{undamaged})}{kurtosis(NMHS_{damaged})} \quad (5-3)$$

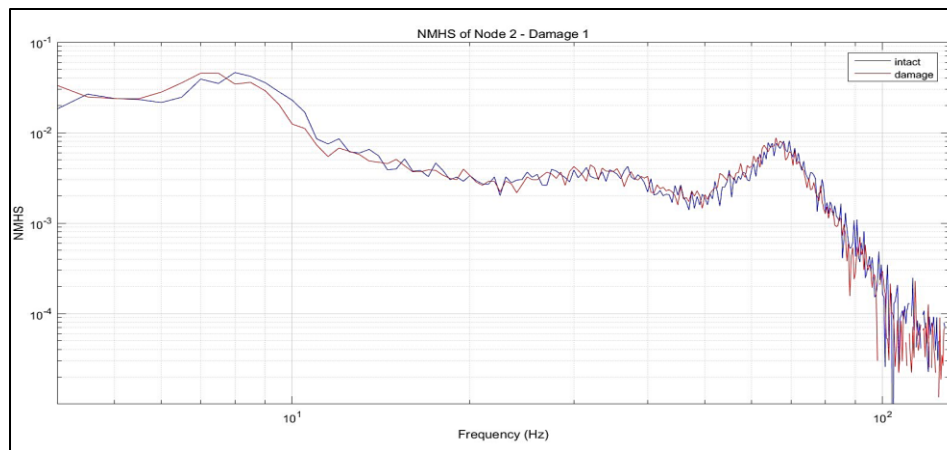
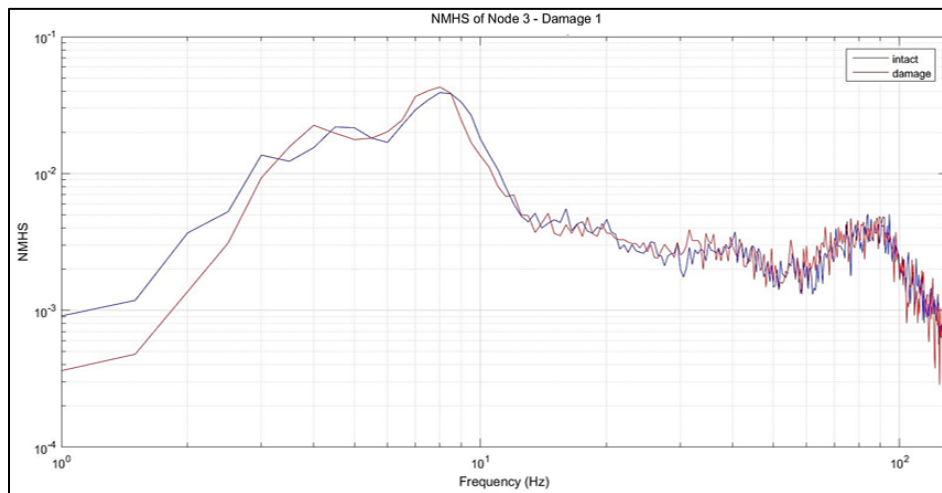
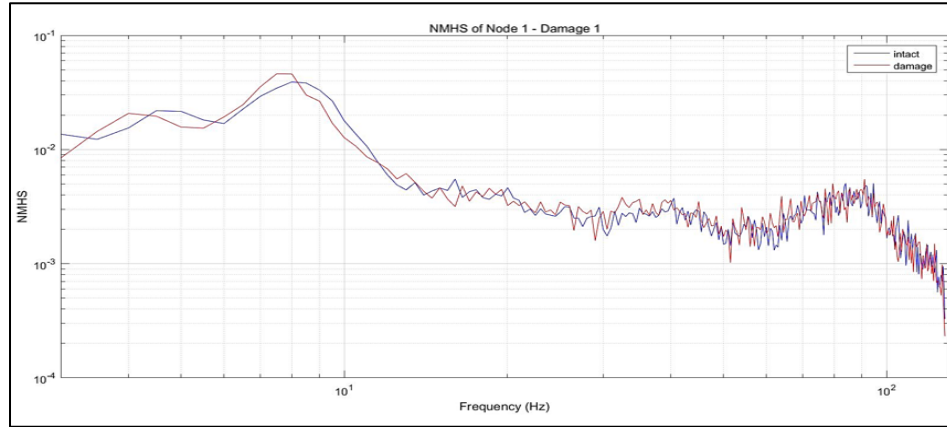


Figure 5. 24: NMHS plots for 3 sensors for damage near node 3 in the beam

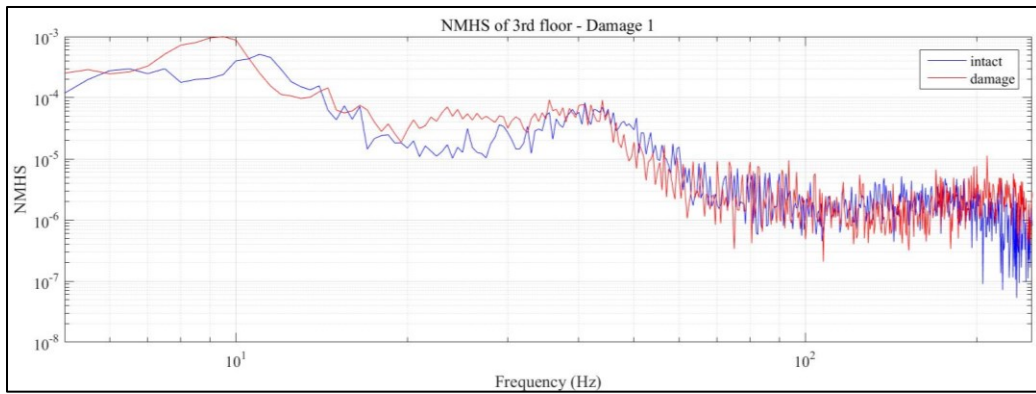
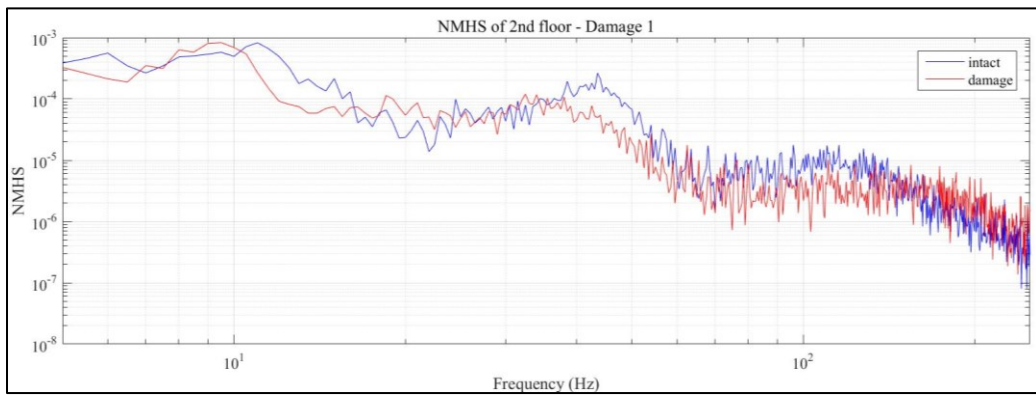
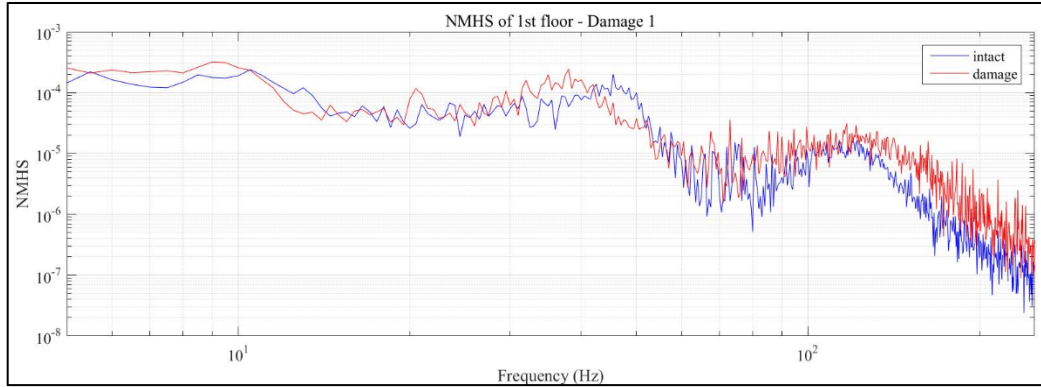


Figure 5. 25: NMHS plots for 3 sensors for damage in top floor of bookshelf structure

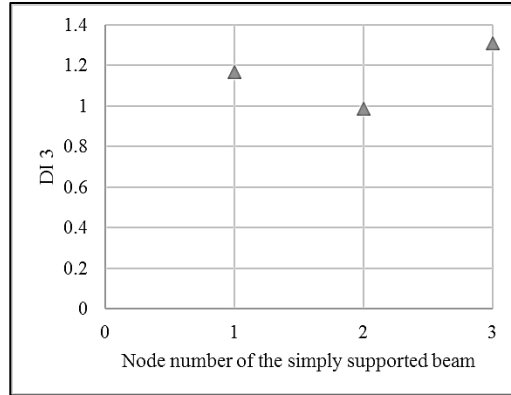


Figure 5. 26: Damage index 3 plot for damage near node 3

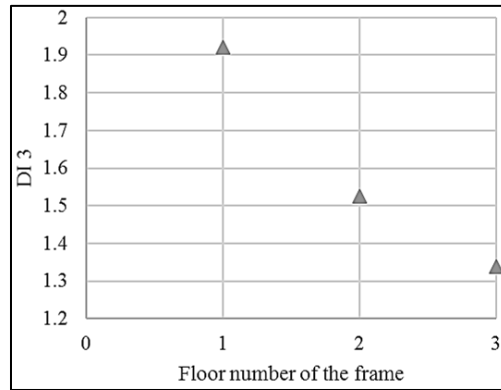


Figure 5. 27: Damage index 3 plot for damage in top floor

DI₃ also proves effective in detecting damage created in first floor of the frame. The Damage indices are in the order of extent of damage. The 3rd floor is supported by the base and hence suffers the least effect. DI₃ detects damage near node 3 as well for the software simulated damage in the beam. Next metric is DI₄ which is based on NCMHS curve. The NCMHS curves are displayed in Figure 5.28 and 5.29 for the beam and bookshelf structure respectively. The damage index for all the nodes of the beam are in Figure 5.30 and for all the floors are in Figure 5.31. It proves to be accurate for this set of data under the first damage scenario.

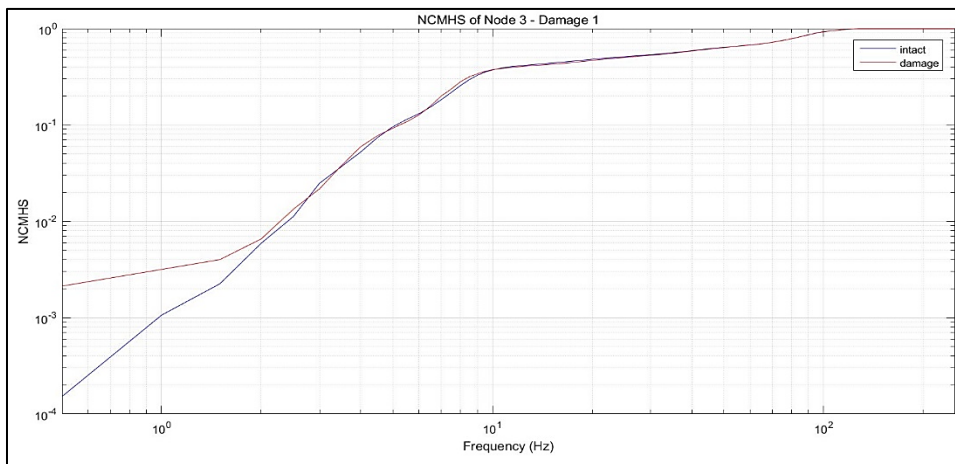
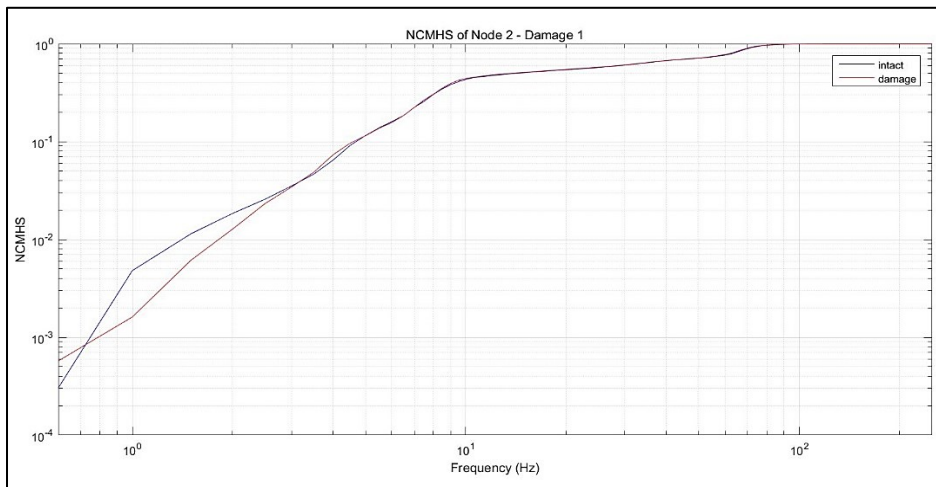
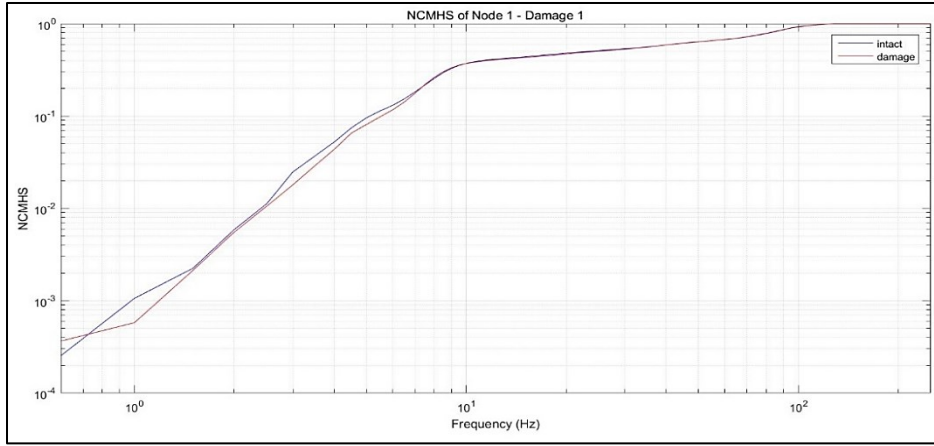


Figure 5. 28: NCMHS plots for 3 sensors for damage scenario 1 of beam

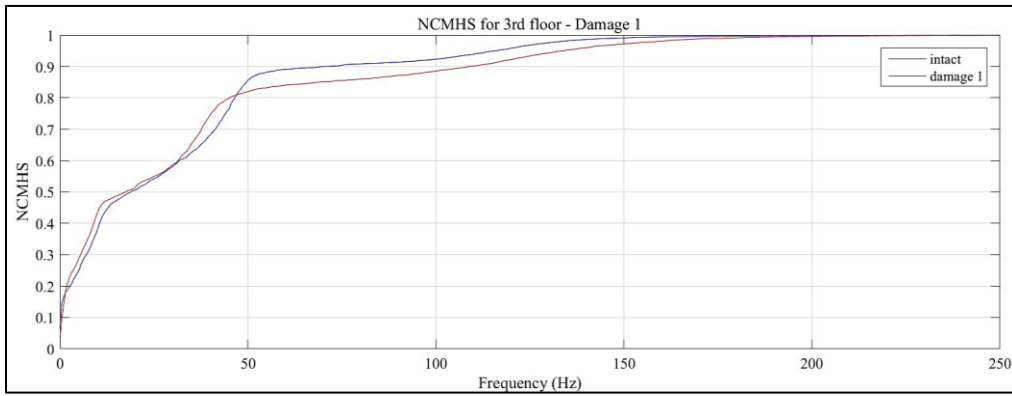
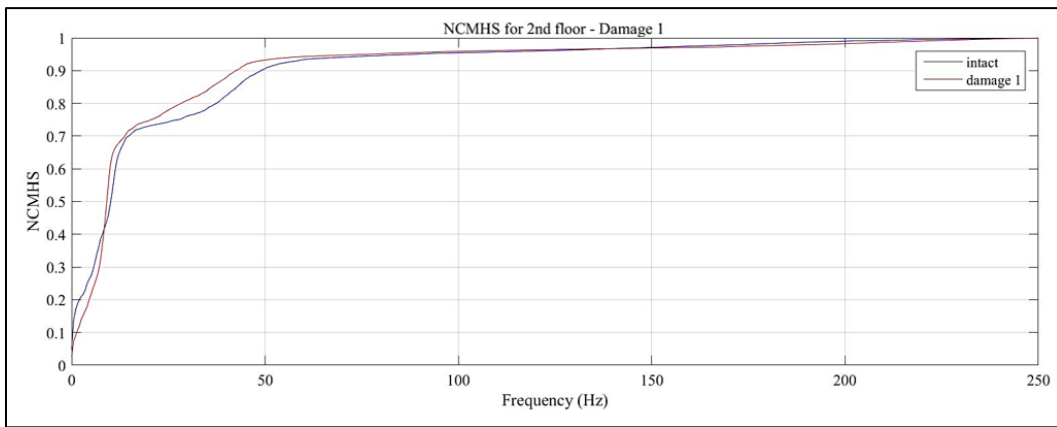
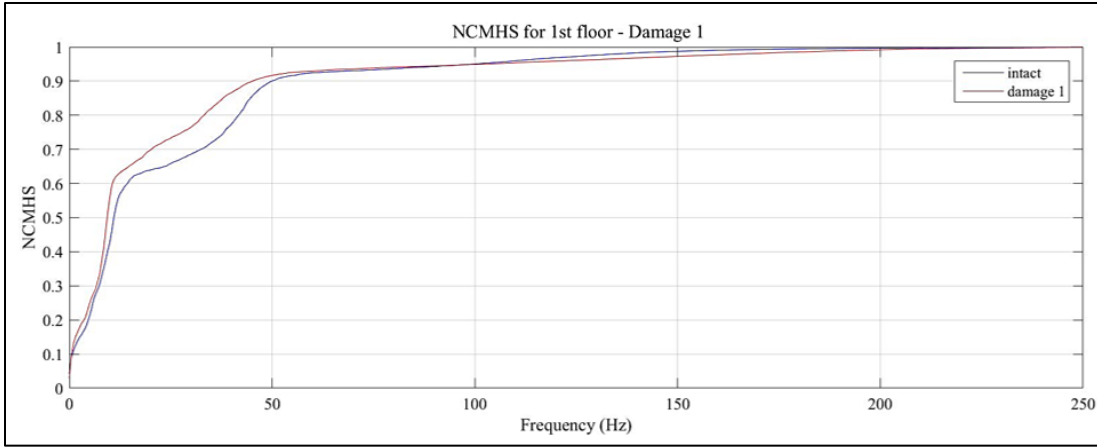


Figure 5. 29: NCMHS plots for 3 sensors for damage in top floor

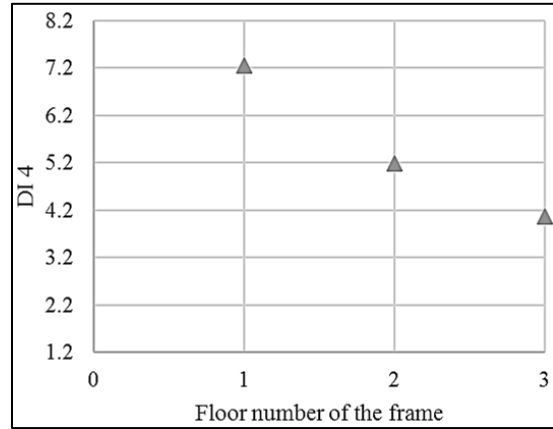


Figure 5.30: Damage index 4 plot for damage in top floor

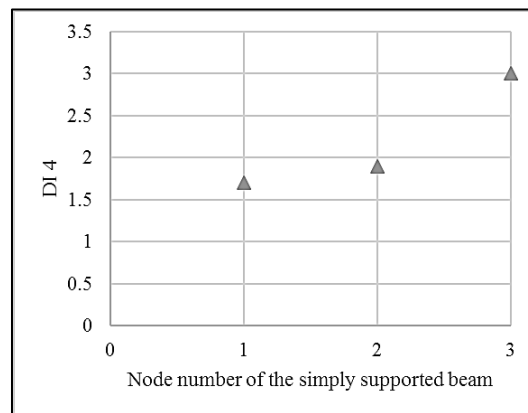


Figure 5.31: Damage index 4 plot for beam damage scenario 1

All the four proposed DIs detected the location and severity of damage accurately for first floor damage in the frame. For the simulated simply supported beam, all DIs were successful in damage localization but DI2 and DI3 showed higher damage at the other further node and not at the centre point node which is closer to the location of the damage at node 3. To further validate the robustness of all metrics for experimental data and the

simulation data, damage scenario 2 is evaluated for both the cases. Normalized energy with IMFs and the first two DIs for damage 2 are in Figure 5.32-5.35.

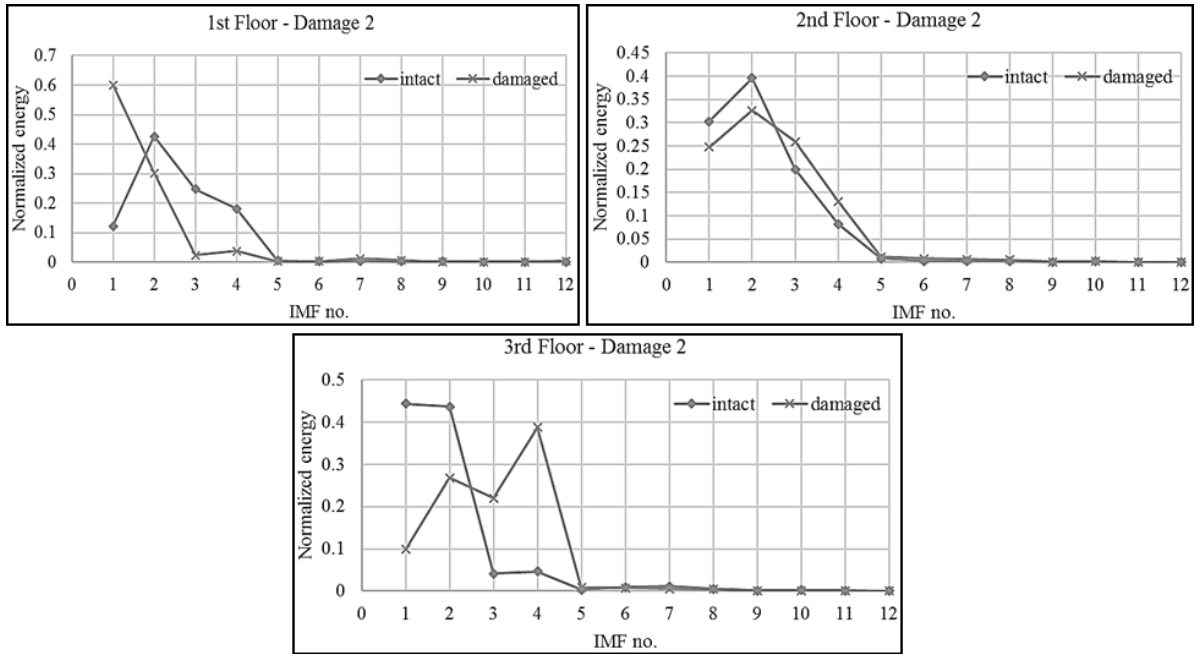


Figure 5. 32: Normalized energy vs IMF number curves for damage in middle floor

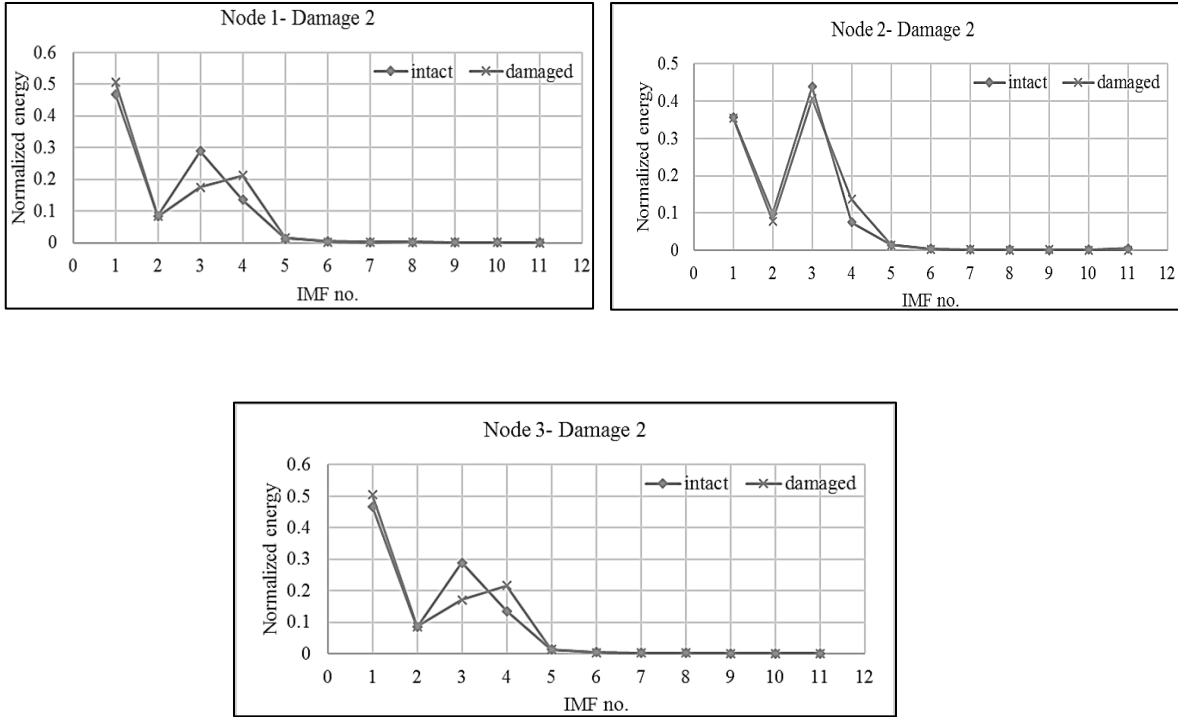


Figure 5. 33: Normalized energy vs IMF number curves for beam damage scenario 2

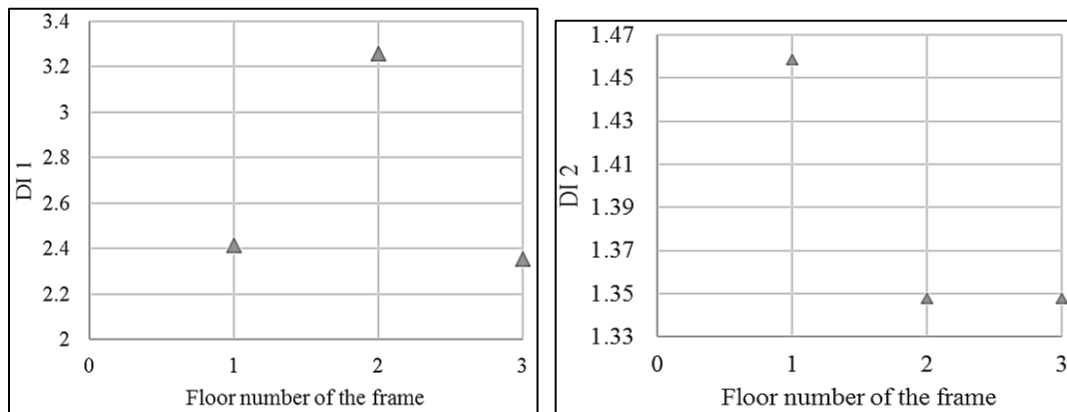


Figure 5. 34: Damage indices plots for damage in middle floor

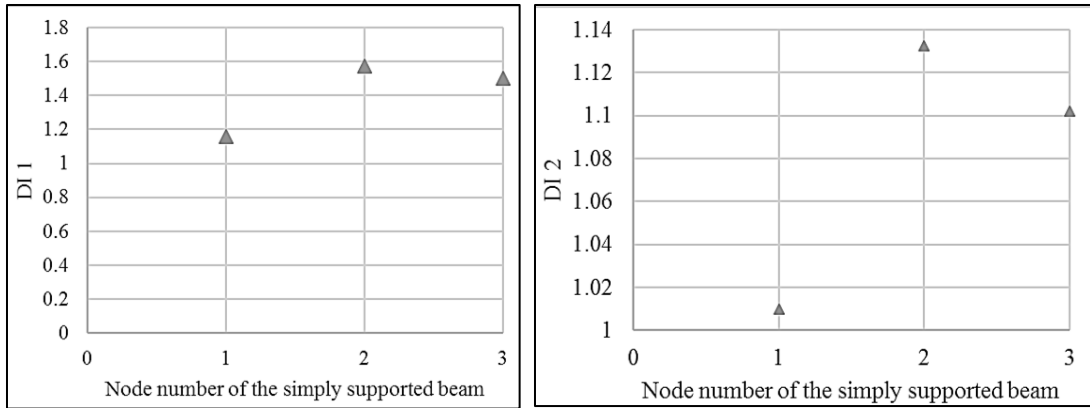


Figure 5. 35: Damage index plots for damage near node 2 in the beam

According to the results of the damage 2, DI2 which involved skewness of the distribution resulted in inaccurate damage metrics for the bookshelf structure. It points out damage in the first floor which is incorrect. Although, it should be noted that for the software simulation, both the DIs detect damage correctly. Moving on, the NMHS curves for DI₃ are plotted and assessed in Figure 5.36-5.38.

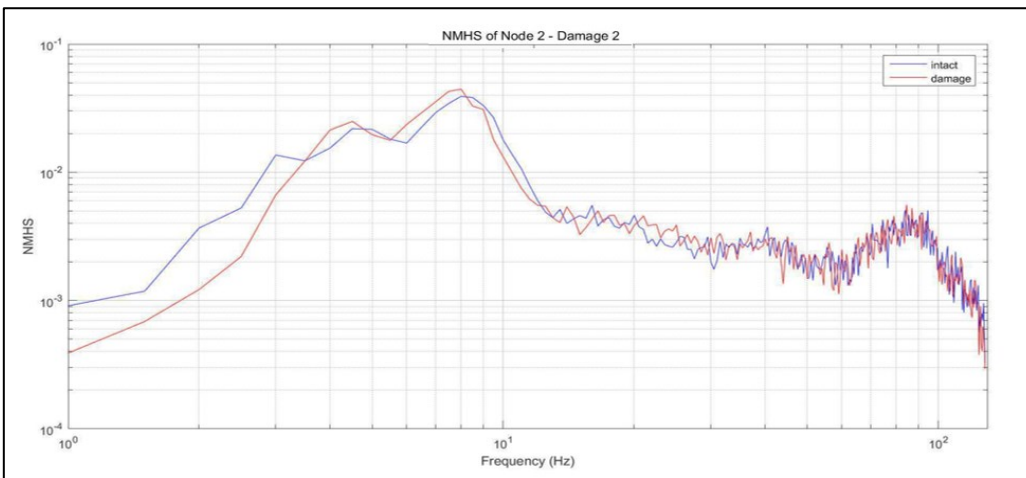
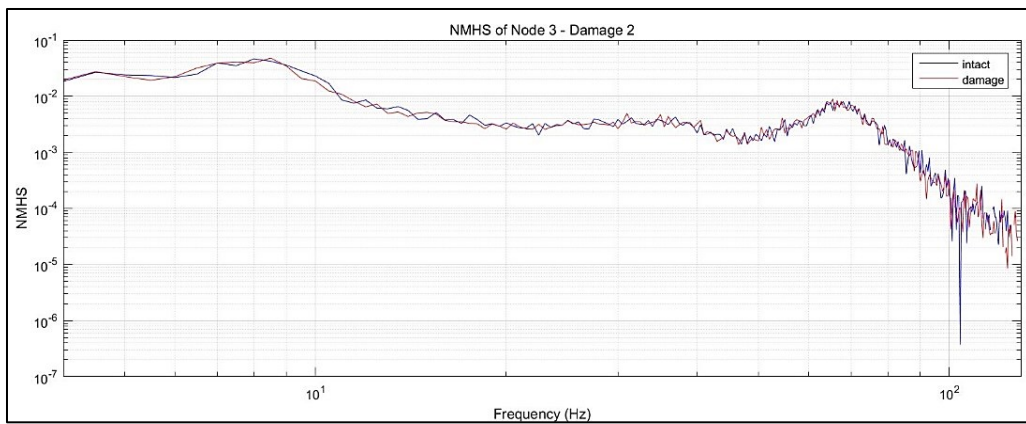
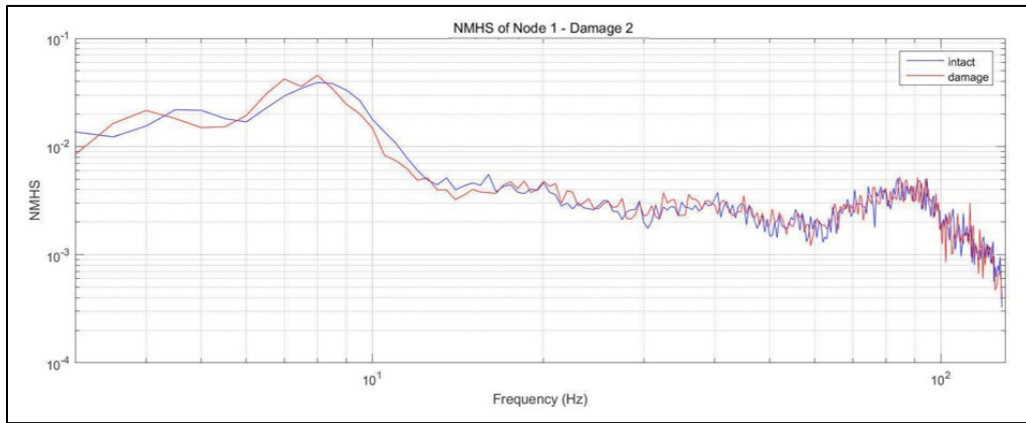


Figure 5. 36: NMHS plots for 3 sensors for damage scenario 2 in beam

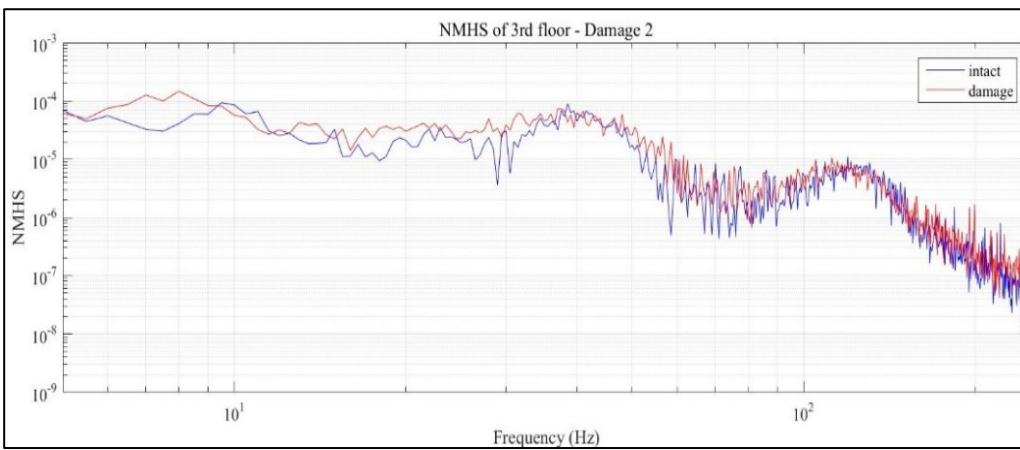
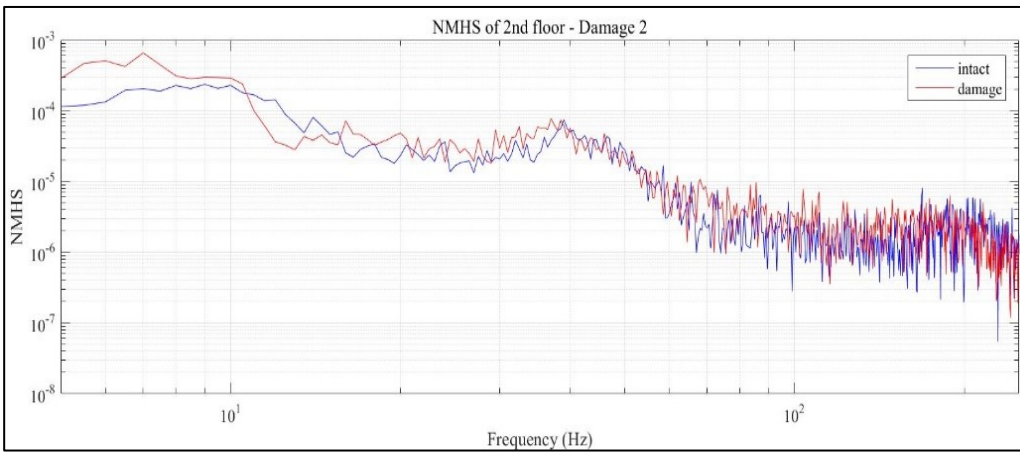
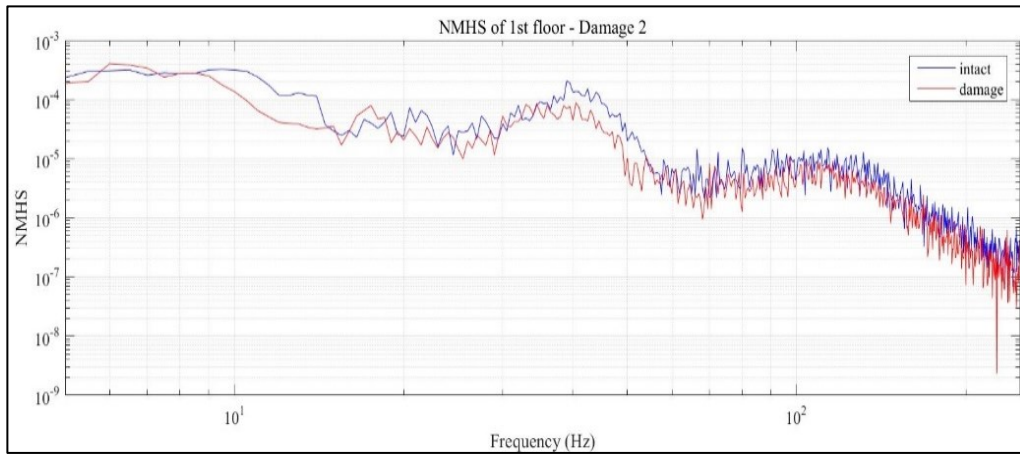


Figure 5. 37: NMHS plots for 3 sensors for damage in middle floor

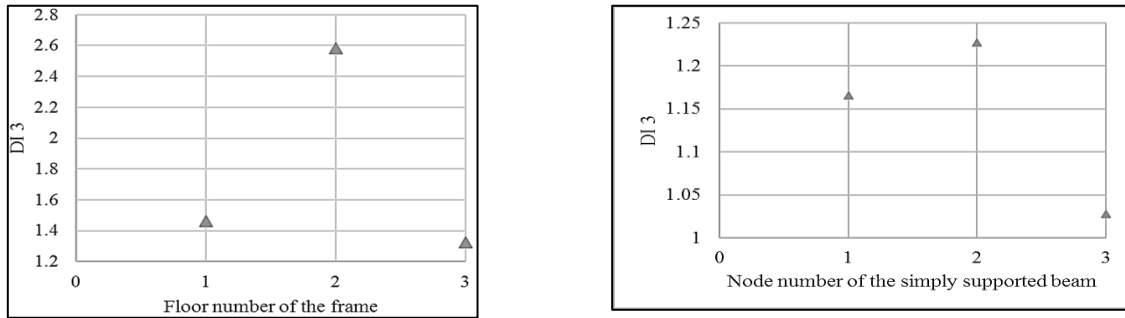


Figure 5. 38: Damage index 3 plot for both structures

DI₃ calculated using MHS of the response signal is sensitive to this damage scenario also and can distinctly detect the damage location for the frame and the beam simulation. The last metric is DI₄ based on the area curves between NCMHS of healthy and damaged states. The curves with their associated damage metric are shown in Figure 5.39-41. NCMHS also accurately detects and localizes the damage.

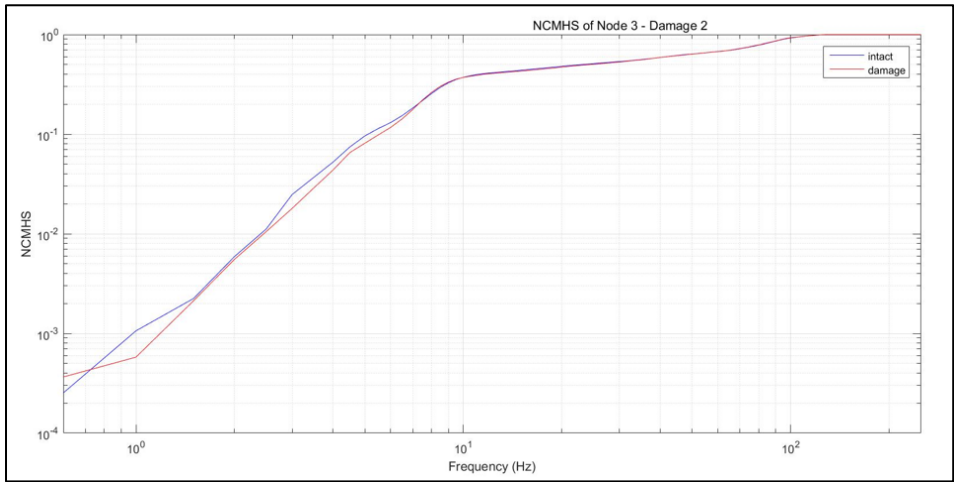
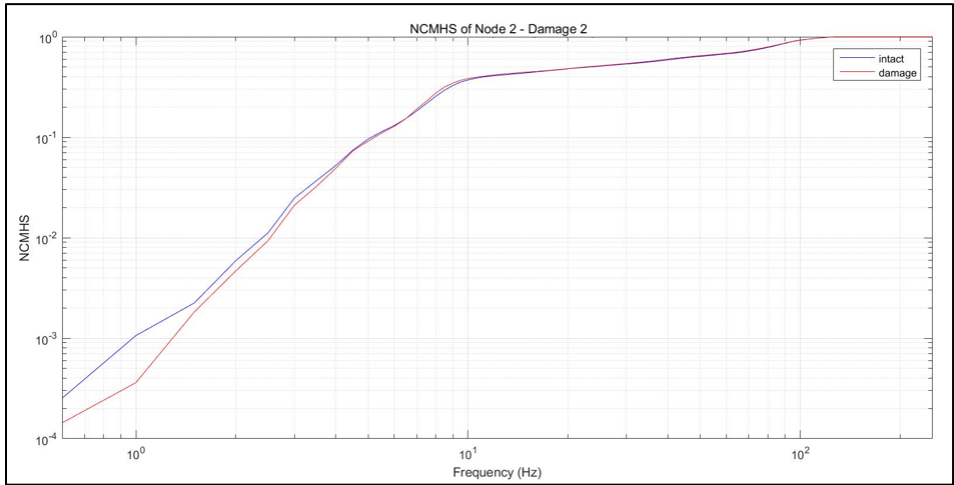
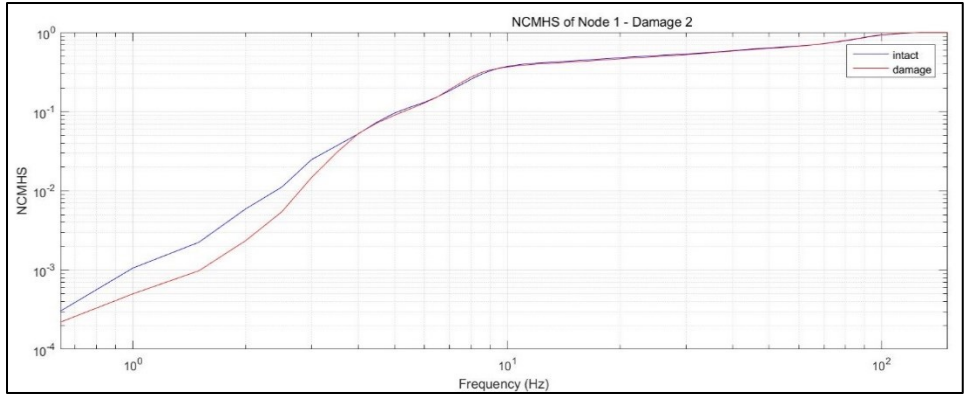


Figure 5. 39: NCMHS plots for 3 sensors for damage scenario 2 in beam

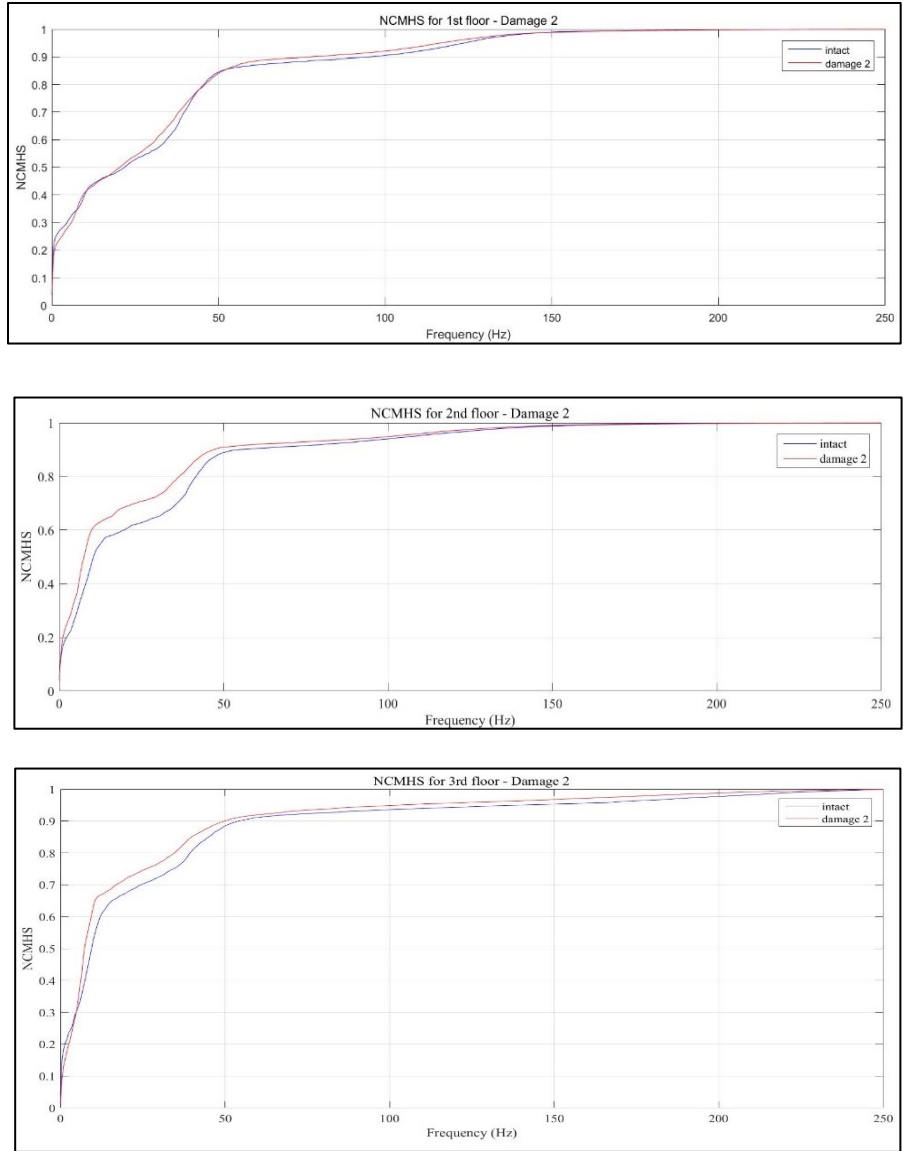


Figure 5. 40: NCMHS plots for 3 sensors for damage in middle floor of frame

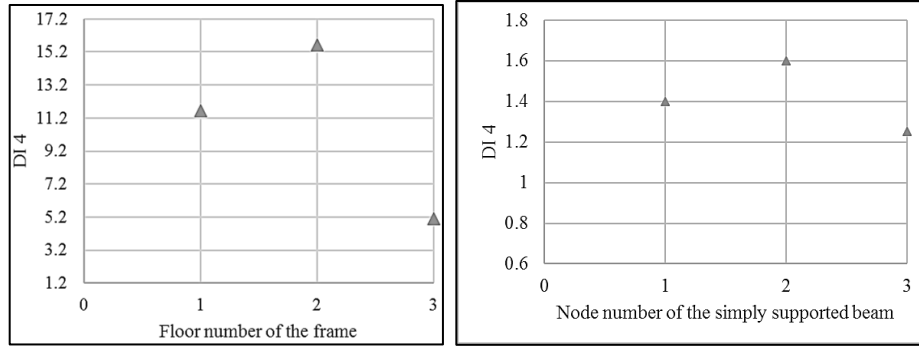


Figure 5. 41: Damage index 4 plots for the frame and beam

5.6. Discussion

In this chapter, damage detection using curves of response signals deduced by Empirical Mode Decomposition and Hilbert Huang Transform is demonstrated. Preservation of non-linear and non-stationary features increase the efficiency of this method. A simply supported beam model is created in SAP 2000 for preliminary study. Damage is created by reducing its moment of inertia at known locations. The second stage involved experiments on a steel bookshelf structure. The type of damage simulated by loosening bolts result in stiffness reduction at particular locations. The incorporated method considers same input energy in all the conditions of the structure and assesses the change in energy distribution between vibrating modes which is changed due to damage. The energy transfer between the IMFs, energy accumulation with frequencies in Marginal Hilbert Spectrum (MHS) and total energy transferred between modes by NCMHS curve are evaluated using both the case studies. The summary of results is shown in Table 5.2 and 5.3 demonstrating accuracy of the damage detection metrics.

Table 5. 2: Experimental data verification for frame

Damage Index with mathematical function	Curve used for study	Scenario-1		Scenario-2	
		Damage location	Location detected	Damage location	Location detected
1 (kurtosis)	Normalized energy-IMF	Top	Top	Middle	Middle
2 (skewness)	Normalized energy-IMF	Top	Top	Middle	Top
3 (kurtosis)	MHS	Top	Top	Middle	Middle
4 (area)	NCMHS	Top	Top	Middle	Middle

Table 5. 3: Experimental data verification for simply supported beam

Damage Index with mathematical function	Curve used for study	Scenario-1		Scenario-2	
		Damage location	Location detected	Damage location	Location detected
1 (kurtosis)	Normalized energy-IMF	Support	Support	Middle	Middle
2 (skewness)	Normalized energy-IMF	Support	Support	Middle	Middle
3 (kurtosis)	MHS	Support	Support	Middle	Middle
4 (area)	NCMHS	Support	Support	Middle	Middle

Software simulation of simply supported beam in SAP 2000 detected accurate damage locations for all the cases. The severity of damage could not be identified as predicted for

both the cases of beam simulation by all the metrics. This might be due to the low sampling rate of 256 Hz or the requirement of further data processing due to the application of WGN. Damage metric 4 utilizing NCMHS curve worked precisely for all the cases. Still, this is not an indication towards other metrics being inefficient. This is an indication of the high sensitivity of these data sets to DI 4. Next case study is the experiment on the steel frame. All the damage metrics correctly detected the damage using experimental data but one metric based on standard deviation of normalized energy distribution could not locate the damage accurately for one damage case. This is an indication of lack of sensitivity of this feature towards this dataset of damages on this structure. Skewness of this distribution highlights the nature of transfer of energy between the vibrating modes whereas kurtosis demonstrates formation or shift of modes with the peaks in the data. Nonetheless, it is a good practice to test several features for structural data as some features are sensitive to particular data set while some are not. Although, it cannot be ruled out completely as an insensitive feature and further research with multiple tests on this structure is expected to perform better feature selection for these algorithms. The higher value of DI signifies more damage content at that location. The third floor of the frame is close to the base and never damaged in this experiment which is evident from its consistent low DI.

The main aim of this research is to investigate and validate the use of HHT method for structural health monitoring for non-linear and non-stationary data. Except the aforementioned case, rest all metrics accurately determined not only the location but the severity as well. This accurate and quantifiable damage detection method is suitable for structural damage detection purposes in civil engineering.

5.7. Summary

This chapter utilizes recently proposed damage detection method based on Hilbert Spectral Analysis (HSA) on two case studies. The first case study is a software simulation of a simply supported beam in SAP 2000 and the second case study is an experiment on a three level steel bookshelf structure. Four damage metrics are evaluated for different damage locations for both the structures based on energy distribution among the Intrinsic Mode Functions of their vibration response, marginal Hilbert spectrum curve and normalized cumulative marginal Hilbert spectrum curves. NCMHS metric is found to be the most accurate in all the cases. Other metrics were able to detect and localize the damage but not all metrics were successful in severity assessment. Combination of multiple metrics, multiple tests on the structure, higher sampling rate with low noise, efficient data processing and identification of sensitive features are essential for performance boosting of damage detection by HSA.

CHAPTER 6: SUMMARY, CONCLUSIONS AND FUTURE WORK

6.1. Summary

The presented work in this thesis is built on damage detection and monitoring of structures using wireless sensors. SHM using wireless sensors has taken over conventional monitoring by wired sensors due to its several advantages of cost, flexibility and data fidelity. For a permanent and autonomous health monitoring system constituting of wireless sensors, power supply is a major concern. Energy harvesters prove to be a satisfactory solution to this problem. Solar and vibrational energy converters are the most popular ones currently.

In order to increase the robustness and accuracy of the monitoring system, sensor faults should be diagnosed and proper SHM functioning should be ensured. Adding redundant sensing points to the monitoring system is one option. In this regard, proposal of increasing deployment of energy harvesters and analyzing the data of energy harvested for damage detection of bridges is presented in Chapter-3. The advantage of this suggestion integrates dual purpose of energy harvesters. The harvester used is a linear generator working on electromagnetic induction and is proved suitable even for low frequency less volume traffic in rural areas. The harvested energy curve features vary with structural damage are energy generation is dependent on the vibration response of the bridges to ambient excitation. The case studies of a PSCB bridge and a steel truss bridge were considered to validate this

proposal. Two damage metrics were examined: one constructed on the total amount of energy harvested and the other on the statistical features of the energy harvested curve distribution. Several damage cases were simulated at different locations of the bridge span by reducing its stiffness. Both the damage metrics could localize the damage with moderate accuracy as the extent of damage was not captured effectively for some cases. The damage detection method demonstrated high effectiveness in cases where the damage was located in close proximity to the energy harvester. For cases where damage was not located near the sensors, the metrics were not very sensitive but were accurate to some extent.

The next damage detection method focuses on a relatively new method, Empirical Mode Decomposition (EMD) by Hilbert-Huang Transform (HHT) method. Chapter-4 of the thesis presents this work. The HHT method preserves the non-linear and non-stationary features of the structural response signal. The EMD process decompose the signal into Intrinsic Mode Functions (IMFs) which admit well behaved Hilbert Transform to provide instantaneous features like frequency and amplitude of the signal. The cumulative amplitude contribution of frequencies in the signal is captured by marginal Hilbert spectrum curves. The energy distribution between different vibrating modes of the structure change with damage in the structure. This concept is captured and investigated using four damage metrics: kurtosis and skewness of energy distribution of IMFS, kurtosis of marginal Hilbert spectrum curve and area between undamaged and damaged normalized cumulative marginal Hilbert curves. These metrics were used on a three story steel frame prototype experiment and tested. Prior to it, they were tested on a software simulated SAP 2000 simply supported steel beam model. The frame was struck on the top floor to simulate structural vibrations for this study. Damage was created by loosening the bolts on different

floors. The damage metrics by HHT method could capture the location and severity effectively. Only one metric was not accurate for a damage scenario, skewness of energy distribution curves with IMF. This feature of the structural response data proved to be insensitive for the generated damage scenario. The software simulation damages were accurately detected and localized by all the damage metrics. Their damage severity assessment needs some further improvement for these studied data sets. Throughout, the HHT method is very accurate in not only localizing the damage, but also providing information of the severity of damage effects in different instrumented locations of the structure.

6.2 Conclusions

- The two damage detection methods proposed and investigated in this thesis are found to be viable for damage detection of civil engineering structures.
- The energy harvesters can be used as a detector for structural damage and sensor faults improving the health monitoring system.
 - The vibration energy harvesters operating on electromagnetic induction power wireless sensors on bridges due vibration caused by passing ambient traffic, making the monitoring system autonomous. It has another application of screening the sensor faults by tapping the data of energy harvested along time and assessing it for diagnosis of structural behaviour for damages.
 - Two damage metrics were proposed using this concept taking into account the amount of energy harvested and the pattern of the energy harvested curve: ratio of total energy harvested and ratio of the energy harvested

curve's kurtosis for the damaged and healthy states. Comparison of these metrics for different damage locations were made on simulations of bridge models, and the results correspond to each other.

- The harvester-based damage detection metrics were applied to two bridges: PSCB and steel truss bridge. The bridges were subjected to White Gaussian Noise representing ambient vibration. Their vibration responses were fed into the harvester model and obtained energy harvested was analyzed using basic data processing. They proved to be most accurate when the damage is in close proximity of the harvester.
- The results of the detailed testing of the proposed method indicate that it is a promising and robust method for applications in real health monitoring systems.
- The Marginal Hilbert Spectrum (MHS) by Hilbert-Huang Transform (HHT) method is found to be very accurate not only for the cases when the vibration response of a structure is obtained from simulation using finite element software such as in the case of the beam model, but also, for experimental case study as in the case of the steel bookshelf structure.
 - The Hilbert Spectral Analysis (HSA) curves are a relatively new method for damage detection in civil engineering structures. They preserve the non-linear and non-stationary parameters of the vibration responses of structures processing them for damage detection.
 - The performance of four damage metrics related to HSA are evaluated in this thesis. The first and second metric result from kurtosis and skewness of

the energy distribution curves for Intrinsic Mode Functions (IMFs) of the response signal. The third damage metric is the kurtosis of the normalized Marginal Hilbert Spectrum curve. The area difference of the Normalized Cumulative Marginal Hilbert Spectrum (NCMHS) curves construct the fourth damage metric. All the damage metrics are compared for different locations of damaged structures with their healthy or undamaged state.

- All the four metrics are newly proposed and their investigation holds a key importance in research for them to be adopted in SHM. It is worth mentioning that the second metric was never tested before on any structure and the third metric is proposed as well as tested only in this thesis.
- This method detects and localizes damage satisfactorily preserving the non-linear and non-stationary features of the real-time response signal under structural excitation. The combination of multiple damage metrics proves to be more efficient rather than a single metric. It is more realistic to accommodate different types of structural faults by multiple damage metrics.
- The present research can benefit the infrastructure owners and managers by monitoring a structure and the damage location and magnitude. The damage localization results can be used for further investigation and for carrying out the necessary repair or rehabilitation works.
- For improvement in estimating the severity of damage by both the methods, further research can be conducted. This is discussed in the next section.

6.3. Future Work

During the course of this research, a new damage detection procedure was proposed and another relatively new damage detection method was validated experimentally. They both have lot of scope for future research since they are new and ongoing work.

- Although, the damage detection method by harvesters show correlation with damage and can be further developed; currently it faces the need of more sensitive features for damage detection at various locations. Probably, an algorithm accommodating the relation between the effects of different damages with various features of the structural response data can ensure damage detection at different locations and combination of different type of damages.
- Neural network and genetic algorithm coupled with other machine learning algorithms can improve its performance. Since, there is useful data being generated from already present or suggestive energy harvesters' deployment on structures; tapping the data and performing its analysis with data mining and machine learning tools will provide a more secure and promising wireless SHM system.
- The second method incorporating different distributions of the MHS by HHT method is very accurate but still has a lot of scope for further development. Application of HHT on full scale structures, improving signal processing details of its basic algorithm, developing its computational effort, including more damage sensitive features for multi-damage scenarios of structures, further examining other instantaneous parameters of structural response like phase and damping are some of the key areas for future research.

REFERENCES

Abbaspour, R. A practical approach to powering wireless sensor nodes by harvesting energy from heat flow in room temperature, *2010 Int. Congress on Ultra Modern Telecommunications and Control Systems and Workshops (ICUMT)*, Moscow, Russia, pp. 178 – 181, 2010.

American Association of State Highway and Transportation Officials. *Bridging the Gap: Restoring and Rebuilding the Nation's Bridges*. 2008.

Balsamo, L., Betti, R., and Beigi, H., “A structural health monitoring strategy using cepstral features,” *Journal of Sound and Vibration*, 333(19): 4526–4542, 2014.

Boller. C., Structural health monitoring – Its association and use., *New Trends in Structural Health Monitoring*, volume 542 of *CISM International Centre for Mechanical Sciences*, Chapter 1: 1–79. Springer Vienna, 2013.

Brigham, E. *The Fast Fourier Transform and its Applications*, Prentice Hall, Englewood Cliffs, NJ, 1988.

Cahill, P., O’Keeffe, R., Jackson, N., Mathewson, A. and Pakrashi, V. Structural Health Monitoring of Reinforced Concrete Beam Using Piezoelectric Energy Harvesting System, *EWSHM - 7th European Workshop on Structural Health Monitoring*, La Cité, Nantes, France, 190-196, 2014.

Callaway, E., Gorday, P., Hester, L. et al. Home networking with IEEE 802.15.4: A developing standard for low-rate wireless personal area networks, *IEEE Commun. Mag.*, 40(8): 70-77, 2002.

Cardei, M. and Du, D.Z. Improving wireless sensor network lifetime through power aware organization, *ACM Wireless Networks*, 11(3), 2005.

Chae, M., Yoo, H., Kim J. and Cho, M. Development of a wireless sensor network system for suspension bridge health monitoring, *Automation in Construction*, 21 (1): 237–252, 2012.

Cohen, L. Time-frequency analysis, *Prentice-Hall*, Englewood Cliffs, NJ, 1995.

Doebbling, S.W., Farrar, C.R. and Prime, M.B. A Summary Review of Vibration Based Damage Identification Methods, *The Shock and Vibration Digest*, 30(2): 91– 105, 1998.

Fan, W. and Qiao, P. Vibration-based damage identification methods: a review and comparative study. *Structural Health Monitoring- An International Journal*, 10(1):83–111, 2011.

Farinholt, K. M., Miller, M., Sifuentes, W., MacDonald, J., Park G. and Farrar, C. Energy Harvesting and Wireless Energy Transmission for Embedded SHM Sensor Nodes, *Structural Health Monitoring - An International Journal*, 9(3): pp. 269-280, 2010.

Farrar, C.R. and Worden, K. An introduction to structural health monitoring, *Philosophical Transactions of the Royal Society A: Mathematical, Physical and Engineering Sciences*, 365, 1851: 303–315, 2007.

Farshchin, M. Frequency Domain Decomposition (FDD) MATLAB code, <https://www.mathworks.com/matlabcentral/fileexchange/50988-frequency-domain-decomposition--fdd->, December, 2015.

Favai, P., Brien, E. O., Žnidarič, A., Loo, H. V., Kolakowski, P. and Corbally, R. BridgeMon: Improved Monitoring Techniques for Bridges, *Civil Engineering Research in Ireland*, Belfast, UK, 28- 29 August, 2014.

Ghazi, R.M. and Büyüköztürk, O. Damage detection with small data set using energy-based nonlinear features, *Struct. Control Health Monit.* (2015): 23(2):333–348, 2015.

Ghazi, R.M. and Büyüköztürk, O. Assessment and Localization of Active Discontinuities Using Energy Distribution Between Intrinsic Modes, A. Wicks (ed.), *Structural Health Monitoring, Volume 5: Proceedings of the 32nd IMAC, A Conference and Exposition on Structural Dynamics*, 2014.

Hassan, M., Man, S.-H., Ng, C.Z., Bermak, A. and Chang, C.C. Development of Energy Harvested Wireless Sensing Node for Structural Health Monitoring, *Proceedings of the 18th IEEE International Mixed-Signals, Sensors and Systems Test Workshop*, IEEE, Taipei, Taiwan, IMS3TW '12: 22–27, 2012.

Ho, D., Nguyen, K., Lee, P., Hong, D., Lee, S. et al. Wireless structural health monitoring of cable-stayed bridge using Imote2-platformed smart sensor, *Proc. SPIE Sensors and Smart Structures Technologies for Civil, Mechanical, and Aerospace Systems 2012*, SPIE, San Diego, California, USA, SPIE 8345 (83450T), 2012.

Hsu, W. K., Chiou, D. J., Chen, C.W., Liu, M. Y., Chiang, W. L. and Huang, P.C. Sensitivity of initial damage detection for steel structures using the Hilbert-Huang transform method, *Journal of Vibration and Control*, 19(6): 857–878, 2015.

Huang, N. E., Shen, Z., Long, S. R., Wu, M. C, Shih, H. H., Zheng, Q., Yen, N., Tung, C. C., Liu, H. H. The empirical mode decomposition and the Hilbert spectrum for nonlinear and non-stationary time series analysis, *Proceedings. Royal Society of London*, 454:903–995, 1998.

Humar, J., Bagchi, A. and Xu, H. Performance of Vibration-based Techniques for the Identification of Structural Damage, *Structural Health Monitoring - An International Journal*, 5(3):215-227, 2006.

Inamdar, S. M.S. thesis: Design of a solar energy harvesting system for structural health monitoring systems, *Department of Mechanical Engineering*, The University of Texas, Austin, Tex, USA, 2012.

Inman, D.J. and Grisso, B.L. Towards autonomous sensing, *Proceedings of the SPIE: Smart Structures and Materials 2006: Sensors and Smart Structures Technologies for Civil, Mechanical, and Aerospace Systems*, SPIE 6174, San Diego, CA, USA, Volume 6174, pp. 248-254, 2006.

Kim, S., Pakzad, S. and Culler D., Health monitoring of civil infrastructures using wireless sensor networks, in *Proceedings of the 6th International Symposium on Information Processing in Sensor Networks (IPSN '07)*: 254–263, 2007.

Kolakowski, P., Szelazek, J., Sekula, K., Swiercz, A., Mizerski, K. and Gutkiewicz, P. Structural health monitoring of a railway truss bridge using vibration-based and ultrasonic methods, *Smart Materials and Structures*, 20 (3): 035016, 2011.

Kunwar, A., Jha, R., Whelan, M. and Janoyan, K. Damage detection in an experimental bridge model using Hilbert-Huang transform of transient vibrations, *Structural Control and Health Monitoring*, 20(1): 1–15, 2013.

Kurata, M., Kim, J., Lynch J. P. et al., Internet-enabled wireless structural monitoring systems: development and permanent deployment at the new Carquinez suspension bridge, *Journal of Structural Engineering*, 39(10):1688–1702, 2013.

Kurata, M., Kim, J., Zhang, Y. et al., Long-term assessment of an autonomous wireless structural health monitoring system at the new Carquinez suspension bridge, *Smart Structures and Materials Nondestructive Evaluation and Health Monitoring, Proceedings of SPIE*, 798312-9, 2011.

Lynch, J. P. and Loh, K. J. A summary review of wireless sensors and sensor networks for structural health monitoring, *Shock and Vibration Digest*, 38(2): 91–130, 2006.

MATLAB user manual, The Mathworks Inc., Natick, MA, USA, 2008.

Microstrain User Manual, Microstrain Inc., Williston, VT, USA, 2008.

Miller, T.I. and Spencer, B. *M.S. thesis: Solar energy harvesting and software enhancements for autonomous wireless smart networks*, Dept. of Civil Engineering, U of Illinois at Urbana-Champaign, Urbana, Illinois, USA, 2009.

Musiani, D., Lin, K. and Rosing, T. Active Sensing Platform for Wireless Structural Health Monitoring, *6th Int.Symp. on Information Processing in Sensor Networks, IEEE*, Cambridge, MA, USA, IPSN 2007: 390 – 399, 2007.

Park, G., Rosing, T., Todd, M., Farrar, C., and Hodgkiss, W. Energy Harvesting for Structural Health Monitoring Sensor Networks, *Journal of Infrastructure Systems*, 14 (1): 64-79, 2008.

Peigney, M. and Siegert, D. Piezoelectric energy harvesting from traffic-induced bridge vibrations, *Smart Materials and Structures*, 22(9), Article 095019: 11 pages, 2013.

Perpetuum Ltd. Perpetuum wins contract to supply Southeastern Railways with energy harvester powered wireless sensor systems on 148 trains, *Perpetuum media release June 2013*: <http://www.perpetuum.com/news.asp>.

Pines, D. and Salvino, L. Structural health monitoring using empirical mode decomposition and the Hilbert phase, *Journal of Sound and Vibration*, 294 (2006): 97–124, 2006.

Ratcliffe, C.P. A Frequency and curvature based experimental method for locating damage in structures, *Journal of Vibration and Acoustics*, 122(3): 324-329, 2000

Rezaei, D. and Taheri, F. Health monitoring of pipeline girth weld using empirical mode decomposition, *Smart Materials and Structures*, 19(5): Article ID055016, 2010.

SAP 2000 user manual, CSI Analysis Reference Manual, CSI America, Berkeley, California, USA, 2015.

Sazonov, E., Haodong, L., Curry, D. and Pillay, P. Self-Powered Sensors for Monitoring of Highway Bridges, *IEEE Sensors Journal*, 9 (11): 1422-1429, 2009.

Shen, Y., Yang, P., Zhang, P., Luo, Y. et al. Development of a Multitype Wireless Sensor Network for the Large-Scale Structure of the National Stadium in China, *International Journal of Distributed Sensor Networks* Volume 2013, Article ID 709724, 16 pages, 2013.

Simulink user's guide, The Mathworks Inc., Natick, MA, USA, 2016.

Sohn, H., Farrar, C. R., Hemez, F. M., Shunk, D. D., Stinemates, D. W., and Nadler, B. R. A Review of Structural Health Monitoring Literature: 1996–2001, *Los Alamos National Laboratory Report*, LA-13976-MS, 2003.

Staszewski, W. J. Wavelet based compression and feature selection for vibration analysis, *Journal of Sound and Vibration*, 211(5): 736-760, .2000.

Straser, E. G. and Kiremidjian, A. S. A modular, wireless damage monitoring system for structure, *Report 128, John A. Blume Earthquake Center*, CE Department, Stanford University, Stanford, Calif, USA, 1998.

Sudevalayam, S. and Kulkarni, P. Energy Harvesting Sensor Nodes: Survey and Implications, *IEEE Communications Surveys & Tutorials*, 13 (3): 443-461, 2011.

The Associated Press, Canada overpass collapse kills five, *The Denver Post*, <http://www.denverpost.com/2006/10/01/canada-overpass-collapse-kills-five/>, October 1, 2006.

W. Ville, Theorie et applications de la notion de signal analytique, in: *Cables et Transmission*, Vol. 2a: 61–74 (Translated into English by I. Selin, *RAND Corp. Report T-92*, Santa Monica, CA, August 1958), 1948.

Wischke, M., Masur, M., Kröner, M. and Woias, P. Vibration harvesting in traffic tunnels to power wireless sensor nodes, *Smart Materials and Structures*, 20(8): 1-8, 2011.

Xie, X.D., Wang, Q. and Wang, S.J. Energy harvesting from high-rise buildings by a piezoelectric harvester device, *Energy Journal*, 93(2): 1345–1352, 2015.

Xu, Y. L. and Chen, J. Structural damage detection using empirical mode decomposition: experimental investigation, *Journal of Engineering Mechanics*, 130(11): 1279–1288, 2004.

Zimmerman, A.T. and Lynch, J.P. A Parallel Simulated Annealing Architecture for Model Updating in Wireless Sensor Networks, *IEEE Sensors Journal*, 9(11): 1503-1510, 2009.

APPENDIX: LIST OF PUBLICATIONS

Journals

1. **Banerji, S.**, Sudharshan, K.R., Bagchi, A. and Pilay, P. Energy harvesting methods for wireless sensors used in structural health monitoring applications, *Structural Health Monitoring-An International Journal*, 2016. (submitted)
2. **Banerji, S.** and Bagchi, A. Dual application of energy harvesters for structural health monitoring, *Journal of Smart Structures and Systems*, 2016. (in preparation)
3. **Banerji, S.**, Roy, T.B. and Bagchi, A. Damage detection of structures using metrics based on Hilbert Spectral Analysis, *Journal of Structural Health Monitoring and Control*, 2016. (in preparation)

Conferences

1. Khazaeli, S., Ravandi, A.G., **Banerji, S.** and Bagchi, A. The application of data mining and cloud computing techniques in data-driven models for structural health monitoring, *SPIE 9805, Health Monitoring of Structural and Biological Systems 2016*, 98052M, Las Vegas, USA, 1 April 2016.
2. **Banerji, S.**, Khazaeli, S. and Bagchi, A. Energy harvesting methods for structural health monitoring using wireless sensors: A review, *CSCE Conference*, London, Canada, June 2016.
3. **Banerji, S.**, Roy, T.B. and Bagchi, A. Experimental validation of a structural damage detection method based on Marginal Hilbert Spectrum, *ASCE Structures Congress 2017*, Denver, USA, April 2017. (Abstract submitted)

4. **Banerji, S.** and Bagchi, A. Damage detection of bridges by vibration energy harvester, 3rd International Conference on Smart Materials & Structures, Orlando, USA, March 2017. (Abstract submitted)

Posters

1. **Banerji, S.**, Sabamehr, A. and Bagchi, A. Fire resistance by nanoclay coating on fibre reinforced polymer for structural strengthening, *Poster presentation at IC-IMPACTS Summer Institute*, University of Alberta, Alberta, Canada, June 2016.
2. **Banerji, S.** and Bagchi, A. Structural Health Monitoring using wireless sensors, *Poster presentation at IC-IMPACTS AGM*, University of British Columbia, Vancouver, Canada, March 2016.
3. **Banerji, S.**, Rahmatian, A. and Bagchi, A. Performance of Traditional and Emerging Fiber Optic Sensors in Structural Health Monitoring Applications, *Poster presentation at IC-IMPACTS Summer Institute*, University Of Toronto, Toronto, Canada, June 2015.